

CHD8, a Novel ATP-dependent Chromatin Remodeling Enzyme

by

Brandi Arianne Thompson

A dissertation submitted in partial fulfillment

of the requirements for the degree of

Doctor of Philosophy

(Cellular and Molecular Biology)

in The University of Michigan

2009

Doctoral Committee:

Assistant Professor Daniel A. Bochar, Chair

Professor Diane M. Robins

Professor Jessica Schwartz

Associate Professor Jorge A. Iniguez-Lluhi

Associate Professor Mats E.D. Ljungman

© Brandi Arianne Thompson

2009

To Mom and Dad

Acknowledgements

I would like to thank Dr. Daniel Bochar for his guidance and for providing me with the tools to develop as an independent scientist. I would like to thank the past and present members of the Bochar lab for their help and support during the years I spent in the lab. Specifically, I would like to thank Veronique Tremblay, Tushar Menon, and Joel Yates for preparing some of the reagents used in the studies presented here. I would also like to thank Grace Lin, a former rotation student in the lab, who performed the experiment shown in Figure 2.12. I would like to thank the following sources which helped to fund the research I performed during my graduate studies: Rackham Merit Fellowship, Cellular and Molecular Biology Training Grant, American Physiological Society Porter Physiology Fellowship, and the American Cancer Society Research Scholar Grant (awarded to Daniel Bochar). I would like to thank my thesis committee, Dr. Daniel Bochar, Dr. Jessica Schwartz, Dr. Diane Robins, Dr. Jorge Iniguez-Lluhi, and Dr. Mats Ljungman for their guidance. I would also like to thank the CMB program for allowing me the opportunity to earn my PhD from the University of Michigan. Last but not least I would like to thank my parents Cheryl and Donald Thompson for their continued guidance and support without which I would not be where I am today. Thanks for always believing in me.

The majority of the work presented in Chapter II and a small portion of the work presented in Chapter III was previously published in the journal *Molecular and Cellular Biology*. The reference for that paper is as follows: Thompson, B. A., V. Tremblay, G. Lin, and D. A. Bochar. 2008. CHD8 is an ATP-dependent chromatin remodeling factor that regulates beta-catenin target genes. *Mol Cell Biol* 28:3894-904.

Table of Contents

Dedication.....	ii
Acknowledgements.....	iii
List of Tables.....	vii
List of Figures.....	viii
List of Abbreviations.....	xii
Abstract.....	xiv
Chapter	
I. Introduction.....	1
Chromatin Structure.....	1
Chromatin Remodeling Enzymes.....	2
Covalent Modification of Histones.....	3
ATP-dependent Chromatin Remodelers.....	4
Swi/Snf.....	4
Iswi.....	5
Ino80.....	5
CHD.....	6
CHD1-2 Subfamily.....	6

	CHD3-5 Subfamily.....	6
	CHD6-9 Subfamily.....	7
	Specific Aims.....	8
II.	CHD8 is an ATP-dependent Chromatin Remodeling Factor That Regulates β -catenin Target Genes.....	11
	Introduction.....	11
	Materials and Methods.....	16
	Results.....	26
	Discussion.....	40
III.	CHD8 is a Component of a WDR5 Containing Complex and Regulates Expression of Hox Genes.....	62
	Introduction.....	62
	Materials and Methods.....	66
	Results.....	80
	Discussion.....	94
IV.	The Double Chromodomains of CHD8 Recognize Both Modified and Unmodified H3/H4 Histones.....	117
	Introduction.....	117
	Materials and Methods.....	121
	Results.....	125
	Discussion.....	134
V.	Conclusion.....	149
	References.....	159

List of Tables

TABLE

2.1: Oligonucleotide sequences.....	46
3.1: Oligonucleotide Sequences.	100
3.2: MS/MS identified sequences.....	102

List of Figures

Figure

1.1: ATP-dependent chromatin remodeling enzymes.....	9
1.2: Domain structure of the CHD6-9 subfamily of proteins.....	10
2.1: CHD8 possesses nucleosome stimulated ATPase activity.....	49
2.2: Mutation of lysine 842 in CHD8 results in a loss of ATPase activity.....	50
2.3: CHD8 increases restriction enzyme accessibility of mononucleosomes in the presence of ATP.....	51
2.4: Increase in restriction enzyme accessibility of mononucleosomes in the presence of CHD8 approaches linear range over time.....	52
2.5: CHD8 slides mononucleosomes to two prominent positions along the DNA template.....	53
2.6: Two prominent species persist over time.....	54
2.7: CHD8 interacts with β -catenin <i>in vitro</i>	55
2.8: CHD8 interacts with β -catenin <i>in vivo</i>	56

2.9: CHD8 is bound to the 5' end of Axin2, Dkk1, and Nkd2.	57
2.10: CHD8 is specifically recruited to the proximal promoter region of the Axin2 gene.	58
2.11: Depletion of CHD8 in HCT116 cells results in increased expression of Axin2, Dkk1, and Nkd2.	59
2.12: Depletion of <i>Drosophila</i> Kismet increases expression of nkd.	60
2.13: CHD8 remodels mononucleosomes containing TCF binding sites.	61
3.1: CHD8 is a component of a large complex in HeLa nuclear extracts.	103
3.2: Conventional purification of CHD8.	104
3.3: Affinity purification of CHD8.	105
3.4: CHD8 interacts with WDR5 <i>in vivo</i>	106
3.5: CHD8 interacts with WDR5 <i>in vitro</i>	107
3.6: CHD8 directly interacts with RbBP5 and Ash2L.	108
3.7: CHD8 directly interacts with the core WDR5/RbBP5/Ash2L complex.	109
3.8: DNA does not mediate the interaction of CHD8 with the WDR5/RbBP5/Ash2L complex.	110
3.9: CHD8, WDR5, RbBP5, Ash2L, and MLL1 elute in the same fraction off a Superose 6 column.	111

3.10: The remodeling activity of CHD8 is not stimulated by WDR5.....	112
3.11: ATRA induces HoxA gene expression in NT2/D1 cells.....	113
3.12: CHD8 regulates HoxA gene expression in NT2/D1 cells.....	114
3.13: CHD8 is bound to the HoxA gene cluster in HeLa cells.....	115
3.14: CHD8 is bound to the HoxA gene cluster in NT2/D1 cells.....	116
4.1: CHD8 chromodomains bind H3/H4 tetramers.....	139
4.2: Western blot analysis of histones bound to GST-Chromos.....	140
4.3: CHD8 chromodomains bind recombinant H3/H4 tetramers.....	141
4.4: Clustalw alignment of CHD1 and CHD6-9 chromodomains.....	142
4.5: Mutation of conserved aromatic residues in the CHD8 chromodomains does not alter binding to core histones or recombinant H3/H4 tetramers.....	143
4.6: CHD8 chromodomains do not bind wild type or mutant H3 tails.....	144
4.7: CHD8 chromodomains bind both recombinant H3/H4 tetramers and tailless H3/H4 tetramers.....	145
4.8: CHD8 chromodomains bind recombinant H3 (K36C/C110A)/H4 tetramers.....	146
4.9: CHD8 chromodomains bind recombinant H3/H4 tetramers fluorescein labeled at K36.....	147

4.10: CHD8 chromodomains bind recombinant H3/H4 tetramers fluorescein
labeled at K79..... 148

List of Abbreviations

a.a.	amino acid
APC	adenomatous polyposis coli
ATP	adenosine triphosphate
BME	β -mercaptoethanol
bp	base pair
ChIP	chromatin immunoprecipitation
CV	column volume
DNA	deoxyribonucleic acid
Dvl	dishelved
GSK3 β	glycogen synthase kinase 3 β
GST	glutathione S-transferase
HP1	heterochromatin protein 1
IP	immunoprecipitation

MOI	multiplicity of infection
PAGE	polyacrylamide gel electrophoresis
PBS	phosphate buffered saline
Pc	Polycomb
PCR	polymerase chain reaction
PMSF	phenylmethylsulfonyl fluoride
Pol II	polymerase II
RNA	ribonucleic acid
SDS	sodium dodecyl sulfate

Abstract

CHD8, a Novel ATP-dependent Chromatin Remodeling Enzyme

by

Brandi Arianne Thompson

Chair: Daniel A. Bochar

ATP-dependent chromatin remodeling by the CHD family of proteins plays an important role in the regulation of gene transcription. The CHD family can be subdivided into three families; CHD1-2, CHD3-5, and CHD6-9. While the first two subfamilies have been extensively studied, very little is known about the CHD6-9 subfamily.

In this study we demonstrate that CHD8 is a nucleosome-stimulated ATPase, capable of remodeling the nucleosome structure. In addition, the tandem Chromodomains of CHD8 are capable of directly binding recombinant histones H3 and H4. We also demonstrate that CHD8 interacts directly with the transcriptional regulator β -catenin and that CHD8 is recruited specifically to the promoter regions of several genes responsive to β -catenin. Utilizing shRNA against CHD8, we demonstrate that CHD8 performs a negative role in regulating

β -catenin target gene expression. This regulation is evolutionarily conserved as RNAi against kismet, the apparent *Drosophila* ortholog of CHD8, similarly results in the activation of β -catenin target genes.

WDR5, RbBP5, and Ash2L are core components of the MLL1-WDR5 methyltransferase complex which alters chromatin structure through the covalent modification of histones. MLL1, the catalytic subunit of the complex, catalyzes the methylation of histone H3 lysine 4, a hallmark of active chromatin. We demonstrate that CHD8 exists in a multi-subunit complex with WDR5, RbBP5, and Ash2L that may also contain MLL1. Both WDR5 and MLL1 have previously been reported to regulate the expression of Hox genes, a family of genes involved in development. We demonstrate that CHD8 is recruited specifically to the promoter regions of several genes within the HoxA locus. Utilizing shRNA against CHD8, we demonstrate that CHD8 performs a negative role in regulating Hox gene expression. We show that CHD8, like WDR5 and MLL1, regulates Hox gene expression.

Taken together, these results demonstrate that CHD8 functions in the transcriptional regulation of both β -catenin target genes and Hox genes and suggest that this regulation is through the ATP-dependent modulation of chromatin structure within the 5' promoter regions of these genes. Our results suggest that through regulating the expression of β -catenin target genes and Hox genes CHD8 may play a role in both tumorigenesis and development respectively.

Chapter I

Introduction

Chromatin Structure

Inside the cell there are detailed instructions for the development, function, and characteristics of a given organism. These instructions are written in the language of DNA. It is our DNA or DNA in combination with the environment that determines things as trivial as eye color and hair color to things as significant as the development of diseases such as sickle cell anemia and cancer. The International Human Genome Sequencing Consortium estimates that the human genome consists of 20,000-25,000 genes. At present, 19,599 genes have been identified and confirmed and another 2,188 DNA segments have been identified that may also be genes (117). How does all of this information fit inside of an individual cell which is not visible to the naked eye?

In eukaryotes such as humans, the genome is packaged as chromatin inside the nucleus of each cell. The fundamental unit of chromatin is the nucleosome. The nucleosome core is an octamer composed of two of each

histone H3, H4, H2A, and H2B (69). Approximately 146 base pairs of DNA are wrapped around this histone octamer core to form each individual nucleosome. When visualized by electron microscopy, the primary chromatin structure consisting of nucleosomes assembled along DNA resembles “beads on a string”. This chromatin fiber then folds upon itself multiple times and ultimately results in the highly condensed chromatin structure observed at the level of metaphase chromosomes.

Chromatin structure determines the transcriptional activity of genes. While the formation of chromatin aids the cell in packaging the entire genome inside the nucleus, it also serves as a hindrance for cellular processes such as transcription, replication, recombination, and repair (62). Therefore, factors that can alter chromatin structure are essential for and provide additional regulatory points in these cellular processes.

Chromatin Remodeling Enzymes

Factors that can alter chromatin structure are termed chromatin remodeling enzymes. Two classes of chromatin remodeling enzymes exist. The first class is composed of enzymes that alter chromatin structure by the covalent modification of histones (36, 63, 142). The second class is composed of enzymes which use the energy of ATP hydrolysis to alter chromatin structure (7, 74, 86, 113). Both classes of remodeling enzymes regulate the accessibility of packaged DNA.

Covalent Modification of Histones

Multiple enzymes are capable of altering chromatin structure through the covalent modification of histones (10, 36, 63, 142). Histone acetyltransferases, methyltransferases, kinases, and ubiquitin ligases, as well as the enzymes that remove these modifications, are examples of this type of remodeling enzyme.

While these modifications can occur along the length of the histone protein, the majority of the documented covalent post-translational modifications occur on the non-globular N-terminal histone tail. The tail region can represent up to 30% of the mass of a given histone (35). Greater than 60 different modifications of the major core histones have been identified to date. These modifications can be grouped into eight different categories as follows: acetylation, methylation, phosphorylation, ubiquitylation, ribosylation, sumoylation, deimination, and isomerization. At this time, the known modifications are lysine acetylation, lysine and arginine methylation, serine and threonine phosphorylation, lysine ubiquitylation, glutamate poly-ADP ribosylation, lysine sumoylation, arginine deimination, and proline isomerization (131).

It is suspected that these post-translational modifications of histones produces a “histone code” which is then read by various cellular factors involved in controlling the state of chromatin (55). This code is written by enzymes known as “writers” and removed by “erasers”. The code is then read by protein “readers” that recognize these covalent modifications (131).

ATP-dependent Chromatin Remodelers

ATP-dependent chromatin remodeling enzymes possess a conserved Snf2 helicase domain. This domain is capable of binding and hydrolyzing ATP (33). This class of chromatin remodeling enzymes alters chromatin structure by disrupting DNA-histone contacts, moving histones to a new location on the same piece of DNA, moving histones to new DNA, or replacing histones with histone variants (40, 66, 134) (Figure 1.1).

ATP-dependent chromatin remodeling enzymes can be separated into families based on the presence of additional domains, and these enzymes usually fall into one of the following four main families: Swi/Snf, Iswi, Ino80, or CHD. These enzymes also typically exist in multi-subunit complexes with other proteins which regulate or aid the remodeler in functioning. These additional subunits can also help classify these remodelers into distinct families.

Swi/Snf

Drosophila brahma (BRM), mammalian BRG1 (Brahma related gene 1), and yeast SNF2 are examples of proteins which are categorized into the Swi/Snf (mating type switching/sucrose non-fermenting) family of proteins. In addition to the Snf2 helicase domain, all of these proteins possess a bromodomain which has been reported to bind acetylated histone tails (77, 132). In humans, the BAF and BRM complexes are two members of the Swi/Snf family of remodelers. Swi/Snf complexes function in various cellular processes such as DNA replication, repair, and transcription (132).

Iswi

Mammalian SNF2H and yeast Isw1 are examples of enzymes which are categorized as Iswi (imitation switch) remodeling enzymes. In addition to the Snf2 helicase domain, proteins within this family possess a SANT (SWI3, ADA2, NCOR, IFIIB) domain. This domain is reported to have the ability to bind histone tails (77, 132). The chromatin accessibility complex (CHRAC) (126), nucleosome remodeling factor (NURF) complex (122, 124), and ATP-utilizing chromatin assembly and remodeling factor complex (ACF) (53) are examples of complexes which are classified as Iswi complexes. The Iswi protein within each complex acts as the ATPase subunit of the given complex (34). While the Iswi family was initially identified in Drosophila, paralogues of the Drosophila Iswi protein have been found in complexes in yeast (79, 123, 127), xenopus (43, 76), and humans (4, 12, 13, 44, 67, 68, 95, 119, 137).

Ino80

SRCAP (SNF2-related CREB-activator protein) and p400 are examples of proteins which are categorized as Ino80 (inositol requiring 80) remodeling proteins. Members of this family of proteins have a split ATPase domain (3, 132). The Ino80 complex was first identified in yeast. This complex is reported to remodel chromatin, facilitate *in vitro* transcription, and exhibit DNA helicase activity (108). The DNA helicase activity of the complex has been attributed to the presence of RuvB proteins. The Ino80 complex is thought to be involved in both transcriptional regulation and DNA repair (3, 77, 108).

CHD

The CHD (Chromodomain helicase DNA binding) proteins are another example of an ATP-dependent chromatin remodeling family. Like all ATP-dependent remodeling enzymes, members of this family possess a conserved Snf2 helicase domain. In the CHDs, this domain is C-terminal to tandem chromodomains believed to function in histone binding. The CHD family of proteins can be further divided into subfamilies based on the presence of additional domains. These subfamilies are CHD1-2, CHD3-5, and CHD6-9.

CHD1-2 Subfamily

In addition to the double chromodomains and Snf2 helicase domain, CHD1 and CHD2 possess a DNA-binding domain near their C-terminus (77). In yeast, the CHD1 protein is reported to be involved in RNA pol II transcriptional elongation and termination (2, 64, 111). CHD1 is also reported to exhibit ATPase activity in yeast and drosophila. Mouse CHD1 may also contain histone deacetylase activity. Both human and yeast CHD1 are reported to bind histones methylated on H3 lysine 4, a hallmark of active transcription. Mutational analysis performed in mouse indicates that loss of CHD2 results in defects in both growth and viability (77).

CHD3-5 Subfamily

In addition to the tandem chromodomains and the Snf2 helicase domain, members of the CHD3-5 subfamily possess tandem PHD (plant homeo domain) Zn-finger-like domains N-terminal to the chromodomains (77). In vertebrates, the

CHD3/CHD4 (Mi2) proteins were identified as components of the NURD (Nucleosome Remodeling and Deacetylation) complex. As the name indicates, this complex has the ability to both remodel nucleosomes and deacetylate histones. A four subunit histone deacetylase core comprised of HDAC1/2 and RbAp46/48 is responsible for the deacetylase activity exhibited by the NURD complex (121, 129, 136, 141). This subfamily of proteins has been implicated in both lymphocyte differentiation and T cell development (77).

CHD6-9 Subfamily

In addition to the Snf2 helicase domain and the tandem chromodomains, the CHD6-9 subfamily of CHD proteins possess two other types of domains (Figure 1.2). C-terminal to the Snf2 helicase domain is a SANT [switching-defective protein 3 (SWI3), adaptor 2 (ADA2), nuclear repressor co-repressor (NCOR), transcription factor IIIB (IFIIB)] domain followed by two BRK (Brahma and Kismet) domains (45, 77). The function of the SANT and BRK domains is not clearly defined in the context of the CHD subfamily proteins.

While the CHD1-2 and CHD3-5 subfamilies have been extensively studied, the CHD6-9 subfamily is not well studied. ATPase activity, an indicator of potential chromatin remodeling activity, has been observed for some members of the CHD6-9 subfamily. However, actual chromatin remodeling activity has not been shown for any of the subfamily members (45, 77). Our studies attempt to elucidate the function of CHD8, a CHD6-9 subfamily member.

Specific Aims

Hypothesis: CHD8 exists in a multi-subunit complex with other factors that are required for the function of CHD8.

Aim 1: Identify the polypeptide composition of the endogenous CHD8 complex (es)

- A. Purify the CHD8 complex (es) from HeLa cells
- B. Confirm CHD8 associated polypeptides
- C. Analyze the transcriptional requirement of the CHD8 associated polypeptides

Hypothesis: CHD8 functions as an ATP-dependent chromatin remodeling enzyme.

Aim 2: Determine whether CHD8 acts as an ATP-dependent chromatin remodeling enzyme

- A. Perform *in vitro* chromatin remodeling assays of the CHD8 complex
- B. Analyze the domains and regions essential for chromatin remodeling activity of CHD8

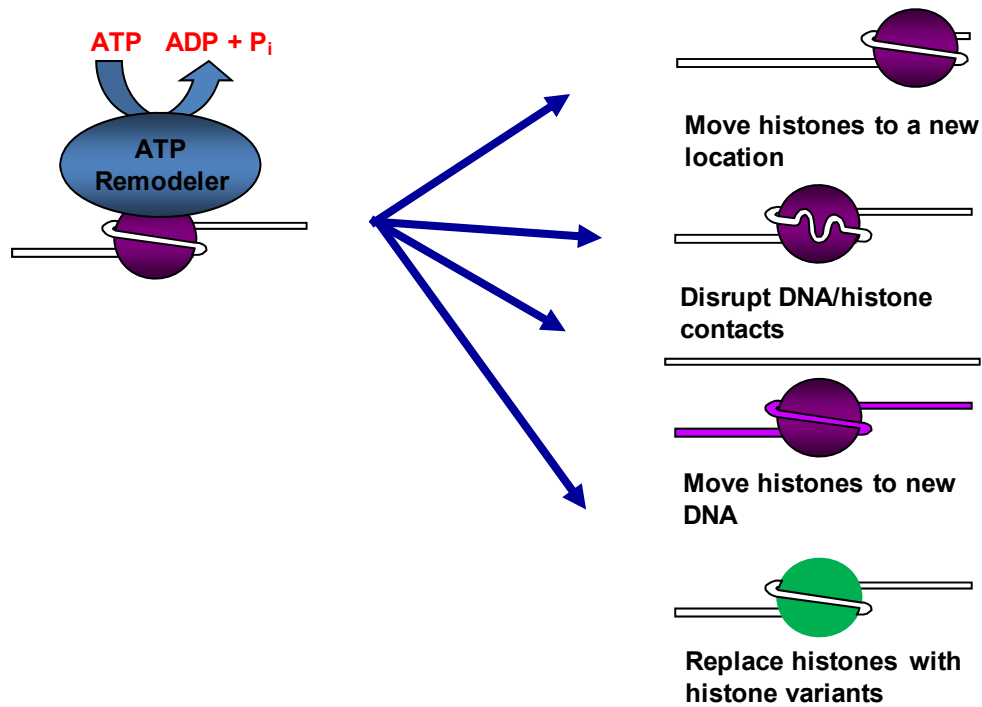


Figure 1.1: ATP-dependent chromatin remodeling enzymes. ATP-dependent chromatin remodeling enzymes alter chromatin structure by utilizing the energy of ATP hydrolysis. These enzymes can alter chromatin structure by disrupting DNA histone contacts, moving histones to a new location on the same piece of DNA, moving histones to new DNA, or replacing histones with histone variants. Members of this class of remodeling enzyme share a conserved Snf2 helicase domain capable of binding and hydrolyzing ATP.

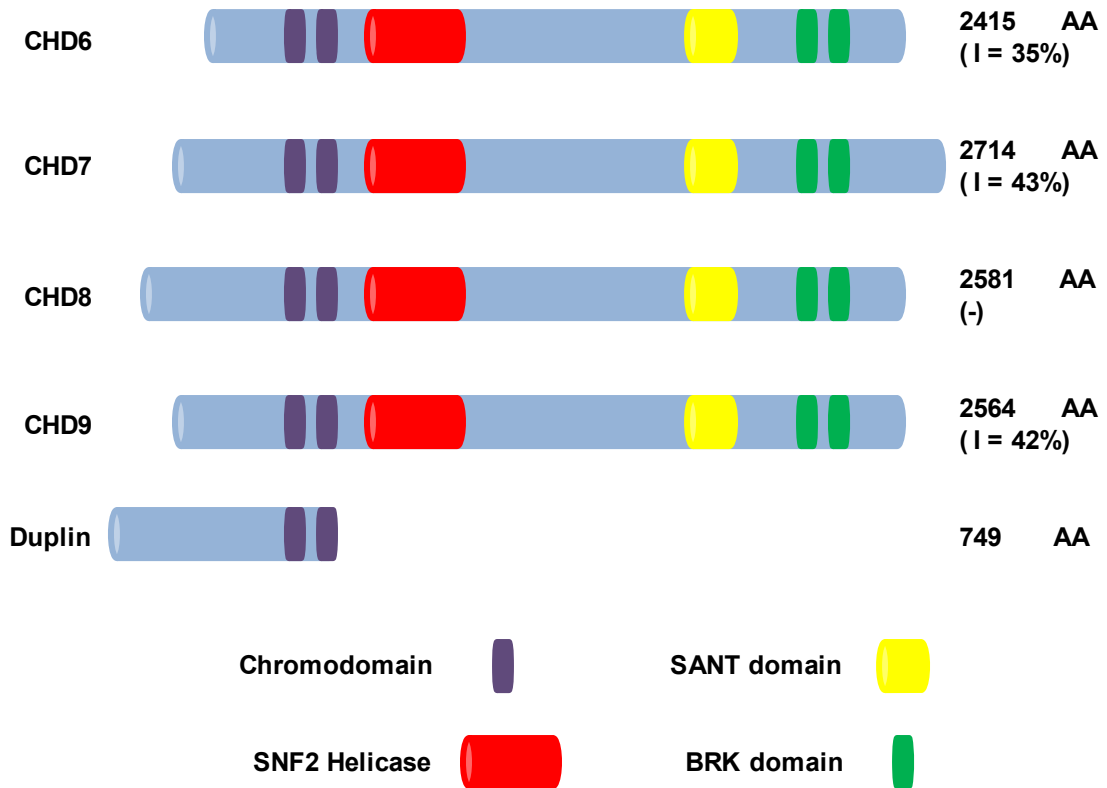


Figure 1.2: Domain structure of the CHD6-9 subfamily of proteins. The CHD (Chromodomain Helicase DNA binding) family of proteins are key regulators of chromatin structure. Members of the CHD6-9 subfamily of CHD proteins share multiple conserved domains. Included is the number of amino acids (AA) and the percent identity (I) as compared to human CHD8. Duplin, an N-terminal fragment of CHD8, was identified in rat.

Chapter II

CHD8 is an ATP-dependent Chromatin Remodeling Factor That Regulates β -catenin Target Genes

Introduction

The eukaryotic genome is packaged inside the nucleus in the form of chromatin. The fundamental unit of chromatin, the nucleosome, is formed by wrapping ~146bp of DNA around a histone octamer core composed of two of each histone H2A, H2B, H3, and H4 (69). While the formation of nucleosomes aids cells in packaging their genome inside the nucleus, it can also hinder cellular processes such as transcription, replication, and repair (62). Therefore, factors that can alter chromatin structure are important for regulation of these cellular processes. Factors that can regulate the accessibility of this packaged DNA are termed chromatin remodeling enzymes. Two classes of chromatin remodeling enzymes have been identified. One class alters chromatin structure via the covalent modification of histones (36, 63, 142). The other class of enzymes uses the energy of ATP hydrolysis to alter chromatin structure (7, 74, 86, 113).

ATP-dependent Chromatin Remodeling

All ATP-dependent chromatin remodeling enzymes share a conserved Snf2 helicase domain capable of binding and hydrolyzing ATP (33). This class of remodeling enzymes uses the energy of ATP hydrolysis to alter chromatin structure by disrupting the DNA/histone interactions, moving the histone octamers to new DNA, moving the histone octamers to a new location on the same piece of DNA, or replacing histones with histone variants (40, 66, 134). These remodeling events are essential for transcription, replication, repair, and recombination of the genome (31, 89, 110).

ATP-dependent Chromatin Remodeling and Cancer

Alterations of chromatin structure have been reported to be involved in the development of human cancers. The human SWI/SNF complex, a known ATP-dependent chromatin remodeling complex (7, 31, 74, 86, 110, 113), is one example. Alteration of this complex has been implicated in tumor formation. BRG1, the catalytic subunit of the SWI/SNF complex is mutated in multiple cancer cell lines (25, 42, 97, 98). Approximately 10% of all primary cancers exhibit a loss in expression of BRG1 (97). In mouse models, haploinsufficiency of BRG1 results in a predisposition to tumor formation (19). Ini/Snf5, a core subunit of the SWI/SNF complex, is inactivated in a variety of cancers (105, 106, 128). In mice, mutations in this subunit indicate that this protein acts as a tumor suppressor (100, 101). These data demonstrate that the SWI/SNF complex plays a role in tumor formation and highlights the importance of studying other

ATP-dependent chromatin remodeling complexes and the role they may play in carcinogenesis.

Wnt Signaling Pathway and Cancer

The Wnt signaling pathway plays a role in many developmental pathways (20), but it also is involved in tumorigenesis. The role of Wnt signaling in colorectal cancer was first discovered in patients with Familial Adenomatous Polyposis. This disorder is caused by mutations that inactivate the APC (adenomatous polyposis coli) protein (41, 87). Wnt signaling regulates β -catenin accumulation and nuclear localization (20). In the absence of Wnt ligand, β -catenin is phosphorylated by GSK3 β , a component of the APC complex (52). β -catenin is then targeted for ubiquitination and degradation by the proteasome (56, 78). In the presence of Wnt ligand, dishelved (Dvl) inhibits the APC complex preventing β -catenin phosphorylation. β -catenin is then allowed to accumulate and translocate into the nucleus. Inside the nucleus, β -catenin binds to TCF/LEF and activates transcription of β -catenin responsive genes (8, 83).

Wnt Signaling and Chromatin Remodeling

In the absence of Wnt signaling, TCF/LEF interacts with co-repressors such as groucho/TLE (17, 102) and CtBP (15, 16), creating a closed chromatin structure. Multiple proteins, such as p300/CBP (47, 82, 120) and BRG1 (5), can interact with β -catenin and play a role in opening the chromatin structure. An *in vitro* study of β -catenin mediated transcription demonstrated the need for p300 and an unidentified ATP-dependent chromatin remodeling enzyme (125). It was

determined that this unidentified remodeler is not a component of the Swi/Snf complex as purified Swi/Snf was unable to activate transcription. The identification of this unknown ATP-dependent remodeling factor is necessary to fully understand β -catenin mediated transcription.

Duplin and β -catenin

In rat, a protein termed Duplin was previously reported to bind β -catenin and inhibit Wnt or β -catenin dependent TCF activation (103). This is particularly interesting given that analysis of Duplin revealed that it is an N-terminal fragment of human CHD8, a member of the CHD (chromodomain, helicase, DNA-binding) family of proteins. The CHD family proteins are key regulators of chromatin structure (33, 39, 45, 77).

The CHD6-9 Subfamily

Remodeling enzymes can be divided into multiple families based on their domain architecture. One of these families, the CHD family of chromatin remodeling enzymes, can be further divided into 3 subfamilies: CHD1-2, CHD3-5, and CHD6-9. While the CHD1-2 and CHD3-5 subfamilies have been extensively studied, little is known about the CHD6-9 subfamily of proteins (45, 77). Members of this subfamily share multiple conserved domains. They have two chromodomains, a Snf2 helicase domain, a SANT domain, and two BRK domains. The presence of a conserved Snf2 helicase domain, the domain associated with the binding and hydrolysis of ATP, suggests that these proteins are potential ATP-dependent chromatin remodeling enzymes. ATPase activity

has been observed for CHD6 and CHD9 (75, 109), but has not previously been observed for CHD8. Chromatin remodeling activity has also not previously been shown for any of the CHD6-9 subfamily members.

Hypothesis and Summary of Results

As previously stated, *in vitro* studies of β -catenin mediated transcription suggested a need for an unidentified ATP-dependent chromatin remodeling enzyme (125). We hypothesized that CHD8 was this unidentified enzyme involved in regulating β -catenin mediated transcription. Here we demonstrate that full length human CHD8 binds β -catenin both *in vitro* and *in vivo*. We show that this binding requires the armadillo repeats of β -catenin. Our studies performed in HCT116 cells demonstrate that CHD8 binds to the region proximal to the promoter of the β -catenin responsive genes Axin2, Dkk1, and Nkd2. We show that RNAi of human CHD8 increases the expression of Axin2, Dkk1, and Nkd2. In *Drosophila* S2 cells, RNAi experiments targeting the CHD8 ortholog, *kismet*, resulted in increased expression of *nkd*, a β -catenin responsive gene. We performed ATPase assays using CHD8 which indicate that CHD8 possesses nucleosome stimulated ATPase activity. Restriction enzyme accessibility assays and nucleosome sliding assays performed with CHD8 demonstrate that CHD8 is an ATP-dependent chromatin remodeling factor that has the ability to slide nucleosomes. Collectively, our data provide evidence supporting the hypothesis that CHD8 is an ATP-dependent chromatin remodeling enzyme that functions in part by regulating the transcription of β -catenin responsive genes.

Materials and Methods

Cell Culture and Reagents

Dulbecco's modified Eagle medium (Invitrogen) with an additional 10% fetal bovine serum (Hyclone) and 1X penicillin-streptomycin-glutamine (Invitrogen) was used to culture both HeLa and HCT116 cells. Both cell lines were cultured at 37°C in 5% CO₂. HeLa Flag- β cat cells were grown under the same conditions as described above, with the exception of 5 μ g/ml of puromycin, which was added as a selection agent. HeLa nuclear extracts were prepared from cells purchased from the National Cell Culture Center (Minneapolis, MN). Schneider's *Drosophila* medium (Invitrogen) with an additional 10% fetal bovine serum and 1X penicillin-streptomycin-glutamine (Invitrogen) was used to culture *Drosophila* S2 cells at 24°C. SF9 cells were cultured at 24°C in 1X Grace's Insect medium (Invitrogen) containing an additional 10% fetal bovine serum and 1X penicillin-streptomycin-glutamine.

CHD8 rabbit polyclonal antibodies were raised against a 20 amino acid peptide (HTETVFNRVLP GPIAPESK) conjugated to keyhole limpet hemocyanin (Open Biosystems). This 20 amino acid peptide was also conjugated to Affi-Gel 10 (Bio-Rad) and used to affinity purify the CHD8 antibodies described above. Both the anti-trimethyl histone H3 Lys4 (07-473) and anti-acetyl histone H4 (06-866) antibodies were purchased from Upstate (Millipore). All oligonucleotides were synthesized by Integrated DNA Technologies (Coralville, IA). Primer sequences are listed in Table 2.1.

Recombinant Protein Production

The Bac-N-Blue baculovirus expression system (Invitrogen) was used to prepare recombinant baculoviruses containing Flag-tagged human CHD8 and Snf2H. SF9 cells at a concentration of (1×10^6 cells/ml) were infected with the recombinant baculoviruses at a multiplicity of infection (MOI) equal to 2. Cells were harvested 4 days post infection. After harvesting, cells were washed with phosphate buffered saline (PBS) and resuspended in immunoprecipitation (IP) buffer (0.2 mM EDTA, 10% glycerol, 0.2 mM phenylmethylsulfonyl fluoride [PMSF], and 20 mM Tris-HCl [pH 7.9]), with 500 mM KCl, 1% NP-40, 1 μ g/ml aprotinin, 1 μ g/ml leupeptin, and 1 μ g/ml pepstatin. A Dounce homogenizer was then used to lyse the cells. After douncing, lysates were centrifuged at ($15,806 \times g$) for 15 minutes at 4°C. Cleared lysates were dialyzed against IP buffer containing 50 mM KCl. Dialyzed lysates were then combined with 500 μ l of anti-Flag M2 conjugated agarose beads (Sigma) and rotated overnight at 4°C. Flag-IPs were washed with 10 column volumes (CV) of each of the following buffers: IP buffer with 150 mM KCl, IP buffer with 350 mM KCl, and IP buffer with 150 mM KCl. Flag-IPs were eluted with a buffer containing 400 μ g/ml Flag peptide (Sigma), 150 mM KCl, 0.2 mM EDTA, 10 mM β -mercaptoethanol (BME), 10% glycerol, 0.2 mM PMSF, 20 mM Tris-HCl (pH 7.9), 1 μ g/ml aprotinin, 1 μ g/ml leupeptin, and 1 μ g/ml pepstatin.

Glutathione S-transferase (GST)- β -catenin expression constructs were generated by polymerase chain reaction (PCR) using full length GST- β -catenin as a template or were gifts from K. A. Jones (125). *Escherichia coli* BL21 cells

were used to express GST and GST fusion proteins. After harvesting, cells were resuspended in 150 mM KCl, 0.2 mM EDTA, 10 mM BME, 10% glycerol, 0.2 mM PMSF, 20 mM Tris-HCl (pH 7.9). Resuspended cells were passed through a French pressure cell twice and lysates were then centrifuged at 105,000 X *g* for 60 minutes at 4°C. In order to remove partial fusion products, the GST-β-catenin N-terminal fragment was further purified using DEAE and Butyl Sepharose (GE Healthcare) chromatography. GST and GST fusion proteins were affinity purified on Glutathione-Sepharose (GE Healthcare). Samples were then subjected to sodium dodecyl sulfate-polyacrylamide gel electrophoresis (SDS-PAGE). The concentration of GST and GST fusion proteins in the cell lysates were determined by analysis of Coomassie stained gels compared to standards of known concentration.

Protein Interaction Studies

In vitro studies of the interaction between CHD8 and β-catenin were performed using the recombinant proteins described above. Cleared cell lysates containing 10 µg of the indicated GST fusion protein were combined with 20 µl of packed Glutathione-Sepharose beads in a 1 ml final volume of 150 mM KCl, 0.2 mM EDTA, 10 mM BME, 10% glycerol, 0.2 mM PMSF, 20 mM Tris-HCl (pH 7.9). Samples were rotated at 4°C for at least 3 hours. The samples were then washed twice for 10 minutes each with 1 ml of a buffer containing 150 mM KCl, 0.2% NP-40, 0.2 mM EDTA, 10 mM BME, 10% glycerol, 0.2 mM PMSF, and 20 mM Tris-HCl (pH 7.9). Samples were resuspended in 500 µl of the same buffer and combined with 1 µg of purified recombinant CHD8. These samples

were then rotated for at least 3 hours at 4°C. The samples were washed three times for 10 minutes each with 1 ml of buffer containing 350 mM KCl, 0.2% NP-40, 0.2 mM EDTA, 10 mM BME, 10% glycerol, 0.2 mM PMSF, and 20 mM Tris-HCl (pH 7.9). Samples were eluted by boiling in SDS-PAGE loading buffer. Eluted samples were subjected to SDS-PAGE and Western blot analysis.

Methods described by Dignam et al. (27) were used to prepare nuclear extracts for *in vivo* studies involving CHD8 and β -catenin. Nuclear extracts were prepared from approximately 1×10^7 HeLa cells or HeLa cells stably expressing Flag-tagged β -catenin. Extracts were then dialyzed against IP buffer containing 50 mM KCl. Dialyzed samples were combined with 20 μ l of packed anti-Flag M2 conjugated agarose beads (Sigma) and rotated overnight at 4°C. Flag-IPs were washed 30 minutes each with 1 ml of each of the following buffers: IP buffer with 150 mM KCl, IP buffer with 350 mM KCl, and IP buffer with 150 mM KCl. Precipitated material was eluted by boiling in SDS loading buffer. Eluted samples were subjected to SDS-PAGE and Western blot analysis.

ChIP Assays

The chromatin immunoprecipitation (ChIP) assay was adapted from the protocol described by Upstate. For each ChIP, approximately 1×10^6 cells were crosslinked by treatment with formaldehyde for 10 minutes at 37°C. The formaldehyde was added directly to the cell media at a final concentration of 1%. Cells were then washed twice with cold PBS containing 1 mM PMSF, 1 μ g/ml pepstatin, and 1 μ g/ml aprotinin. Cells were harvested by scraping after the

addition of 200 μ l of cold SDS Lysis Buffer (1% SDS, 10 mM EDTA, 50 mM Tris-HCl [pH 8.1]) containing 1 mM PMSF. DNA was sheared into ~200-1000bp fragments by sonication. Lysates were centrifuged at 20,800 X g for 10 minutes at 4°C. Cleared supernatants were diluted 10 fold in ChIP Dilution Buffer (0.01% SDS, 1.1% Triton X-100, 1.2 mM EDTA, 16.7 mM Tris-HCl, [pH 8.1], 167 mM NaCl) containing 1 mM PMSF, 1 μ g/ml pepstatin, and 1 μ g/ml aprotinin. The diluted supernatants were pre-cleared by adding 38 μ l of packed protein A agarose blocked with salmon sperm DNA. Samples were rotated at 4°C for 30 minutes. After brief centrifugation, the pre-cleared supernatants were collected and rotated overnight at 4°C with the indicated antibodies.

Chromatin/antibody complexes were collected by rotating each IP with 38 μ l of packed protein A agarose/salmon sperm DNA for 1 hour at 4° followed by centrifugation at 4°C for 1 minute at 500 X g. Protein A/antibody/chromatin complexes were washed for 30 minutes at 4°C with 1 ml of each of the following buffers: one wash with Low Salt Immune Complex Wash Buffer (0.1% SDS, 1% Triton X-100, 2 mM EDTA, 20 mM Tris-HCl [pH 8.1], 150 mM NaCl, and 1 mM PMSF), one wash with High Salt Immune Complex Wash Buffer (0.1% SDS, 1% Triton X-100, 2 mM EDTA, 20 mM Tris-HCl [pH 8.1], 500 mM NaCl, and 1 mM PMSF), one wash with LiCl Immune Complex Wash Buffer (0.25M LiCl, 1% NP-40, 1% deoxycholate, 1 mM EDTA, 10 mM Tris-HCl [pH 8.1], and 1 mM PMSF), and two washes with TE Buffer (1 mM EDTA, 10 mM Tris-HCl [pH 8], and 1 mM PMSF). After washing, samples were eluted by incubation at room temperature for 30 minutes with 500 μ l of elution buffer (1% SDS, 0.1 M

NaHCO₃). Crosslinking was reversed by adding 20 µl of 5 M NaCl to each eluate and heating at 65°C for 4 hours. Eluates were deproteinated by addition of 10 µl of 0.5 M EDTA, 20 µl of 1 M Tris-HCl (pH 6.5), and 2 µl of 10 mg/ml proteinase K and incubated at 45°C for 1 hour. Samples were purified by phenol/chloroform extraction and the DNA was recovered by ethanol precipitation.

ATPase Assays

Each ATPase reaction contained 1 mM ATP, 7.5µCi of [γ -³²P]ATP in 50 mM NaCl, 0.5 mM dithiothreitol, 5 mM MgCl₂, 25 mM Tris (pH 7.9), and 10nM of the indicated enzyme. As indicated, plasmid DNA or nucleosomes purified from HeLa cells were added to a final concentration of 5 ng/µl. The reactions were then incubated at 30°C for 1 hour. Polyethyleneimine-cellulose thin-layer chromatography plates (Sigma) were spotted with 1 µl of the reaction products. These plates were then resolved using 0.5 M LiCl in 1 M formic acid. Dry plates were imaged and quantified using a Typhoon Trio+ Imager and ImageQuant TL software (GE Healthcare).

Restriction Enzyme Accessibility Assays

The restriction enzyme accessibility assay was adapted from methods outlined by Smith and Peterson (114). A major change in the protocol was the use of fluorescently labeled DNA fragments generated by PCR using a combination of fluorescent and non-fluorescent primers. These reactions utilized pGEM3z-601 DNA from J. Widom as a template (71). Two forward primers (601 forward) were used that had the same DNA sequence, but were either unlabeled

or fluorescently labeled with 5'-Alexa Fluor 488-N-hydroxysuccinimide ester. A labeled to unlabeled primer ratio of 0.1/0.9 was used in each PCR reaction. The reverse primer (601 reverse) was unlabeled. The 277bp PCR product was verified by electrophoresis in a 2% agarose gel followed by detection using a Typhoon Trio+ Imager (GE Healthcare). The fluorescently labeled PCR products were then ethanol precipitated and used to reconstitute mononucleosomes.

Mononucleosomes were reconstituted using methods adapted from Luger et al (73). Mononucleosome reconstitution reactions were assembled using a 1:0.875 molar ratio of the 277bp fluorescently labeled DNA to core histones purified from HeLa nuclear pellets. Reconstitution reactions (100 μ l) contained 10 μ g labeled DNA, 5.16 μ g histones, and 0.1 μ g bovine serum albumin in 2 M NaCl. Mononucleosomes were formed via salt dialysis of the reconstitution reactions at 4°C. The reactions were dialyzed against a decreasing buffer gradient from a high salt buffer (1 mM EDTA, 2 M NaCl, 0.2 mM PMSF, 10 mM Tris pH 8.0) to a low salt buffer (1 mM EDTA, 0.2 mM PMSF, 10 mM Tris pH 8.0) over a 3 day period. After dialysis, reconstitutions were verified by loading reactions onto a 5% non-denaturing acrylamide/bisacrylamide (37.5:1) 0.2X Tris-borate-EDTA gel. Labeled nucleosomes were detected using a Typhoon Trio+ Imager (GE Healthcare).

Restriction enzyme accessibility assays were performed in triplicate. Each 15 μ l reaction contained 1 mM ATP or AMPPNP, 50 nM reconstituted mononucleosomes, and 20U HhaI or PmlI in remodeling buffer (3 mM MgCl₂, 50 mM NaCl, 2 mM dithiothreitol, 1 μ M ZnCl₂, 0.1 mg/ml bovine serum albumin,

20 mM Hepes [pH 8.0]). The final concentration of CHD8 was 0.009 μ M (1X) or 0.017 μ M (2X). In reactions containing CHD8 (K842R), the final concentration was 0.017 μ M. Reactions were incubated for 30 minutes at 30°C. For time course experiments, reactions contained 0.017 μ M CHD8 and were incubated at 30°C for the indicated time. Reactions were quenched by adding 15 μ l of 2X stop solution (10 mM Tris [pH 8.0], 0.6% SDS, 40 mM EDTA, 5% glycerol, 0.1mg/ml proteinase K) and incubating at 50°C for 20 minutes. Samples were analyzed on a 3% agarose gel and bands were quantified using a Typhoon Trio+ Imager and ImageQuant TL software (GE Healthcare). Data points represent the average value of each triplicate.

For remodeling experiments using mononucleosomes containing TCF binding sites, two derivatives of pGEM3z-601 were used as templates. The TCF-mid and TCF-5' templates were generated by the PCR-based overlap extension method of site-directed mutagenesis (80) using the primers 601-1, 601-2, and 601-3 in combination with the mutation containing primers 601-mut 5' or 601-mut mid. Fluorescently labeled DNA fragments using the TCF-mid and TCF-5' templates were prepared as described above. Mononucleosome reconstitution reactions were assembled as above using a (1:1) molar ratio of fluorescently labeled TCF DNA fragments to HeLa core histones.

Nucleosome Sliding Assays

For the nucleosome sliding assays, fluorescently labeled nucleosomes were prepared using the methods described above. The DNA fragment lacking

the 601 nucleosome positioning sequence was PCR amplified using the 601 downstream forward and 601 downstream reverse primers and pGEM3z-601 as the template. Two control fragments were also prepared for determining the electrophoretic mobility of mononucleosomes positioned at the end or the middle of the DNA fragment. The fragment containing the nucleosome positioning sequence at the end was prepared by PCR amplification using the 601 slid forward and 601 slid reverse primers with pGEM3z-601 as a template. The second control fragment was the standard 601 product.

Nucleosome sliding assays were prepared similar to the restriction enzyme accessibility assays but minus the restriction enzyme. Reactions were prepared on ice. Each 15 μ l reaction was composed of remodeling buffer, 1 mM ATP or AMPPNP, and 50 nM reconstituted mononucleosomes. The concentration of CHD8 was 0.017 μ M. Reactions were incubated at 30°C for the indicated times. Reactions were then quenched by adding 3 μ l of a termination solution (30% glycerol, 10 mM Tris [pH 7.8], 1 mM EDTA, 334 μ g/ml HeLa nucleosomes, and 334 μ g/ml salmon sperm DNA) and incubating at 30°C for 15 minutes. Samples were loaded on a 5% non-denaturing acrylamide/bisacrylamide (37.5:1) 0.2X Tris-borate-EDTA gel. Bands were quantified using a Typhoon Trio+ Imager and ImageQuant TL software (GE Healthcare).

RT-PCR and Quantitative PCR

Total RNA was isolated from the indicated cell lines using the RNeasy and Qiashredder kits (Qiagen) as outlined by the manufacturer. cDNA was produced using random decamers (Ambion) and Superscript II (Invitrogen) as described by the manufacturers. Real-time quantitative PCR reactions were prepared using cDNA, iQ Sybr Green Supermix (BioRad), and the indicated primers. Each reaction was performed in triplicate using the MyiQ single color real-time PCR detection system (BioRad). Quantification was performed as described by M. W. Pfaffl (94) using the levels of polymerase II (Pol II) transcribed α -tubulin (*Drosophila*) or pol III transcribed H1 (human) for normalization. For quantitative ChIP experiments, reactions were prepared with the indicated ChIP DNA, iQ Sybr Green Supermix, and the specified primers. Each reaction was performed in triplicate and analyzed using the MyiQ single color real-time PCR detection system. DNA levels were expressed relative to the level of input.

RNAi Knockdown Experiments

The RNAi experiments in HCT116 cells employed the UI2-puro SIBR shRNA vectors (21). The CHD8 RNAi experiments used a shRNA vector containing two cassettes (493 and 6410). Primers for the creation of this construct are listed in Table 2.1. A shRNA vector containing a cassette directed against luciferase, UI2-puro SIBR luc 1601, was used as a control (21). Ten micrograms of the indicated construct was transfected into HCT116 cells using Lipofectamine-2000 as described by the manufacturer (Invitrogen). Selection of

transfected cells was performed through the addition of 5 µg/ml of puromycin to the cell culture medium 24 hours post transfection. Cells were grown an additional 36 hours before being harvested for Western blot analysis and RNA isolation. Methods described by Worby *et al.* (133) were used with minor adjustments to perform RNAi experiments in *Drosophila* S2 cells. A total of 12 µg of double stranded RNA (dsRNA) was used. Four days after the addition of double stranded RNA, cells were harvested. Primers for the creation of the *kismet* and *axin* dsRNA templates are listed in Table 2.1. PCR reactions employed *Drosophila* S2 genomic DNA as a template. The control dsRNA template was created using primers directed against bacterial β-lactamase and pBSIISK as a template.

Results

CHD8 Exhibits Nucleosome Stimulated ATPase Activity

Within the CHD family of proteins, there is a high degree of identity in the catalytic Snf2 helicase domain, suggesting a similar function for these family members. While members of the CHD1-2 and CHD3-5 subfamilies have previously been shown to be involved in ATP-dependent chromatin remodeling (45, 77), members of the CHD6-9 subfamily of proteins have not been examined for this potential remodeling activity. Many ATP-dependent chromatin remodeling enzymes that have Snf2 helicase domains within their sequence exhibit ATPase activity that is stimulated by the presence of DNA and/or nucleosomes. This activity can therefore be used as an indicator of potential

remodeling activity. Both CHD6 and CHD9 have been reported to exhibit ATPase activity (75, 109), but the ATPase activity of CHD8 has not been examined.

In order to determine whether CHD8 possesses ATPase activity, assays measuring ATP hydrolysis were performed in the presence of DNA and/or nucleosomes. A baculovirus expression system was used to prepare recombinant CHD8 (rCHD8) containing an N-terminal epitope tag (Flag) for purification. Recombinant CHD8 was purified from SF9 cells and subjected to SDS-PAGE analysis to confirm the presence of expressed protein (Figure 2.1A). ATPase reactions were prepared using recombinant CHD8 or Snf2H and [γ - 32 P] ATP. Reactions were performed in the presence or absence of plasmid DNA or nucleosomes purified from HeLa cells. Snf2H is a known ATP-dependent chromatin remodeling enzyme that has previously been shown to possess nucleosome stimulated ATPase activity (12), and therefore was used as a control. The ATPase reactions were assayed for 32 P_i release using thin-layer chromatography and phosphorimaging analysis. The results of the assay are shown as % ATP hydrolyzed. In the presence of rCHD8, the % ATP hydrolyzed in the reaction containing free DNA (plasmid DNA) was comparable to the amount of ATP hydrolyzed in the no DNA control (Figure 2.1B). However, when rCHD8 was incubated in a reaction containing nucleosomal DNA there was a significant increase in the % ATP hydrolyzed when compared to the reactions with no DNA or free DNA (Figure 2.1B). This result is comparable to the results seen for reactions containing rSnf2H (Figure 2.1B), which is known to possess

nucleosomal stimulated ATPase activity. These results indicate that CHD8, like many ATP-dependent chromatin remodeling enzymes, exhibits ATPase activity which is stimulated by the presence of nucleosomal DNA.

As previously mentioned, CHD8 possesses a Snf2 helicase domain within the N-terminal portion of the protein. Within the Snf2 helicase domain there is conserved sequence (GXGKT) that is required for the hydrolysis of ATP (130). In all other ATP-dependent remodeling enzymes, mutation of the conserved lysine within this sequence to arginine results in a significant loss of ATPase activity (22, 30, 59, 123). This conserved lysine is at position 842 in CHD8. In order to test whether the observed ATPase activity of CHD8 is due to the Snf2 helicase domain, recombinant mutant CHD8 (rK842R) was prepared using a baculovirus expression system (Figure 2.1A). Purified rK842R was then tested for ATPase activity. Recombinant wild-type or mutant CHD8 was incubated with [γ -³²P] ATP in the presence of nucleosomal DNA. When the lysine at position 842 is mutated to arginine, nucleosome stimulated ATPase activity is significantly reduced as compared to wild-type CHD8 (Figure 2.2). Together, these results demonstrate that CHD8 possesses nucleosome stimulated ATPase activity which requires the Snf2 helicase domain for the hydrolysis of ATP.

CHD8 is an ATP-dependent Remodeling Factor

After determining that CHD8 possesses nucleosome stimulated ATPase activity, we then wanted to directly test whether CHD8 is an ATP-dependent chromatin remodeling enzyme. An assay commonly used to test proteins for

chromatin remodeling activity is the restriction enzyme accessibility assay (114). These accessibility assays are based on the fact that free DNA is vulnerable to cleavage by restriction endonucleases. When mononucleosomes are reconstituted through salt dialysis of core histones and DNA, restriction sites are less accessible to cleavage by restriction enzymes. However, when mononucleosomes are incubated with ATP-dependent chromatin remodeling enzymes in the presence of ATP, the DNA histone contacts can be disrupted resulting in increased accessibility of the DNA to restriction enzyme cleavage.

Restriction enzyme accessibility assays testing CHD8 utilized the 601 nucleosome positioning sequence from pGEM3z-601 (71). Fluorescently labeled primers were used to PCR amplify a 277bp DNA fragment containing the 601 sequence. When reconstituted into nucleosomes, the 601 fragment contains an HhaI restriction site near the dyad axis. The fluorescently labeled 601 fragment was reconstituted into mononucleosomes by salt dialysis with core histones purified from HeLa cells. These mononucleosomes were then used for the restriction enzyme accessibility assays. Reactions, performed in triplicate, also contained HhaI in the presence or absence of recombinant CHD8 or the CHD8 (K842R) mutant. Each reaction also included ATP or AMPPNP, the non-hydrolyzable ATP analog. In the presence of ATP and CHD8, we observed an increase in the fraction cut compared to reactions lacking CHD8 (Figure 2.3, compare lanes 1 and 2). When the concentration of CHD8 added to the reactions was doubled, we observed a further increase in the fraction cut indicating that the activity is dependent on the amount of CHD8 (Figure 2.3, lane

3). In order to test whether the remodeling activity exhibited by CHD8 requires the energy produced by ATP hydrolysis, reactions were performed substituting ATP with the non-hydrolyzable ATP analog AMPPNP. These reactions produced similar levels of cutting comparable to the basal level of cutting seen in the absence of CHD8 (Figure 2.3, compare lanes 4 and 5 to lane 1). Reactions were also performed using the recombinant CHD8 (K842R) which contains a mutation in the region of the Snf2 helicase domain that is required for the binding and hydrolysis of ATP. As with the reactions using AMPPNP, reactions that contained CHD8 (K842R) in the presence of ATP did not show an increase in restriction enzyme accessibility (Figure 2.3, lane 6). These data demonstrate that CHD8 is a chromatin remodeling enzyme and that the remodeling activity of CHD8 requires the binding and hydrolysis of ATP.

A time course of restriction enzyme accessibility was also performed. For these experiments, reactions were prepared similar to those described above. Reconstituted mononucleosomes were incubated with HhaI and ATP in the presence or absence of recombinant CHD8. Reactions, performed in triplicate, were quenched at the indicated time points (Figure 2.4). In the time course experiment, we observed an increase in the fraction cut over time when CHD8 was present. This increase in accessibility was rapid in the beginning but appeared to approach a linear range as time progressed (Figure 2.4). However, the same was not true for reactions in which CHD8 was absent. These reactions did not show a significant increase in accessibility over time (Figure 2.4). This is

similar to results observed for yeast SWI/SNF, a known ATP-dependent chromatin remodeling enzyme (114).

Another assay used to measure ATP-dependent chromatin remodeling is the nucleosome sliding assay. These assays are based on the fact that the position of a nucleosome on a DNA template affects its electrophoretic mobility through a polyacrylamide gel (32). DNA with a nucleosome positioned at the end of a template migrates faster through a polyacrylamide gel than a template with a nucleosome positioned near the center. Therefore, this assay can be used to monitor changes in the position of a nucleosome on a template.

Mononucleosomes were reconstituted by salt dialysis of HeLa purified core histones and a fluorescently labeled template lacking a nucleosome positioning sequence. The resulting nucleosomes were distributed to multiple positions on the template (Figure 2.5, lanes 3-6). Mononucleosomes were also reconstituted using DNA templates with a nucleosome positioning sequence located near the middle or end of the template as standards for approximating the position of the nucleosomes (Figure 2.5, lanes 1 and 2). Sliding reactions were prepared using reconstituted mononucleosomes in the presence or absence of CHD8, ATP, and AMPPNP. In the absence of CHD8, nucleosomes were randomly positioned along the DNA template (Figure 2.5, lane 3). The same was true for reactions in which CHD8 was present in the absence of ATP (Figure 2.5, lane 4) or in the presence of the non-hydrolysable ATP analog AMPPNP (Figure 2.5, lane 6). However, when both CHD8 and ATP were added to the reaction, nucleosomes slid to two prominent positions along the DNA template (Figure 2.5, lane 5).

These results are similar to the reported activity of both CHD1 and CHD3 which tend to slide nucleosomes towards the center of the template (99). The activity of CHD8 is similar to CHD1 in that the major product is not positioned exactly at the center, but is between the center and end of the DNA template. While CHD3 slides nucleosomes to a major position closer to the center, both CHD3 and CHD8 slide nucleosomes to a minor position near the end of a DNA template. These data suggest that members of the CHD6-9 subfamily may remodel nucleosomes in a manner similar to that of the other two CHD subfamilies.

To investigate the possibility that the major and minor species of slid nucleosomes may, over time, merge into one species, nucleosome sliding time course experiments were performed. Reactions were prepared as described above in the presence or absence of CHD8 and were quenched at the indicated time points (Figure 2.6). Consistent with the previous nucleosome sliding experiment, nucleosomes were randomly positioned along the DNA template in the absence of CHD8 (Figure 2.6, lane 3). When reactions containing CHD8 were allowed to proceed, progression into two prominent species was observed (Figure 2.6, lanes 4-10). The two species appeared simultaneously and did not merge into one species over an 80 minute time period. These results suggest that the major and minor species are the final products of CHD8 nucleosome sliding, and are not intermediates to a final single nucleosome position. Taken together with the sections above, these results demonstrate that CHD8 is, in fact, an ATP-dependent chromatin remodeling enzyme that also possesses the ability to slide nucleosomes along a DNA template.

CHD8 Directly Interacts with β -catenin

While the experiments described above demonstrate that CHD8 is an ATP-dependent chromatin remodeling enzyme, additional studies were needed in order to further define the cellular function of CHD8. Sakamoto et al. reported that an N-terminal fragment of rat CHD8, termed Duplin, binds β -catenin and inhibits Wnt or β -catenin dependent activation of TCF mediated transcription (103). Unknown to Sakamoto et al., this truncated form of Duplin resulted from a splicing event in which intron 11 of rat CHD8 was not removed. Our bioinformatic searches failed to identify any similar splicing events in either mouse or human databases (data not shown). We therefore sought to investigate whether full-length human CHD8 can also interact with β -catenin.

Several recombinant GST fusion proteins were prepared for use in the *in vitro* study of the potential interaction between human CHD8 and β -catenin. *E. coli* BL21 cells were used to express full length GST- β -catenin and four additional GST- β -catenin fusion proteins which had various regions of the β -catenin protein deleted (Figure 2.7A). Each purified GST fusion protein was bound to glutathione-Sepharose, and after washing, the samples were incubated with recombinant CHD8. Washed samples were then eluted and subjected to SDS-PAGE followed by Coomassie staining and Western blot analysis using α -CHD8 antibodies (Figure 2.7B and C). Coomassie staining of the SDS-PAGE gel confirmed the presence of GST and each GST fusion protein in the pulldown experiment (Figure 2.7B). Western blot analysis showed that CHD8 interacts with full length GST- β -cat, GST- β -cat Δ N, and GST-ARM (Figure 2.7C).

However, CHD8 did not interact with GST-N, GST-C, or GST alone (Figure 2.7C). These results indicate that CHD8 has the ability to interact with full length β -catenin (GST- β -cat), β -catenin lacking the N-terminus (GST- β -cat Δ N), and the armadillo repeats of β -catenin alone (GST-ARM). Armadillo repeats are a stretch of approximately 42 amino acids (a.a.) found in various proteins, usually as tandem repeats (93). Previous studies of β -catenin have reported that the armadillo repeats are responsible for the interaction between β -catenin and most β -catenin binding partners (49). The same appears to be true for CHD8. Our data demonstrates that CHD8 directly interacts with β -catenin *in vitro* and that this interaction requires the armadillo repeats of β -catenin.

After demonstrating that human CHD8 directly interacts with β -catenin *in vitro*, we wanted to examine whether this interaction also occurs *in vivo*. For *in vivo* experiments examining the interaction between CHD8 and β -catenin, cells were harvested from a HeLa cell line stably expressing Flag-tagged β -catenin^{active} or the parental HeLa cell line. The Flag-tagged β -catenin^{active} construct contained alanine substitutions within the glycogen synthase kinase-3 β (GSK3 β) binding region of β -catenin. These substitutions prevent the binding of the APC complex to β -catenin, allowing β -catenin to accumulate instead of being targeted for degradation by the proteasome (1, 88, 138). Nuclear extracts were prepared from the harvested cells and incubated with α -Flag M2 agarose. Flag-immunoprecipitations were washed, eluted, and subjected to SDS-PAGE followed by Western blot analysis using the indicated antibodies (Figure 2.8). Flag- β -catenin and CHD8 were immunoprecipitated from the nuclear extracts of

cells stably expressing Flag- β -cat^{active}, but CHD8 did not immunoprecipitate from nuclear extracts of the parental control (Figure 2.8). These data demonstrate that human CHD8 directly interacts with β -catenin both *in vitro* and *in vivo*, and suggest that this association may serve to target CHD8 to β -catenin responsive promoters *in vivo*.

CHD8 Localizes to Promoter Regions of β -catenin Responsive Genes

After establishing that human CHD8 directly binds β -catenin, we wanted to test whether this association localizes CHD8 to the promoters of β -catenin responsive genes. For this study, we chose to examine the binding of CHD8 to the promoters of Axin2, Dkk1, and Nkd2, as these are three well studied β -catenin responsive genes (48). The PS2 gene, an estrogen responsive gene, was used as a control. Chromatin immunoprecipitation (ChIP) experiments were performed in order to examine the *in vivo* binding of CHD8 to these genes. HCT116 cells, a colorectal carcinoma line with an activated Wnt signaling pathway (61, 84), were used in the ChIP experiments. The cells were treated with formaldehyde to crosslink the chromatin inside the cell. Lysates were sonicated and pre-cleared before incubation with α -CHD8, α -ACh4, and α -MeH3K4 antibodies. Antibody-protein complexes were precipitated and washed before the crosslinking was reversed. Recovered DNA was amplified using primers designed to amplify locations within the 5' and 3' regions of each gene (Figure 2.9A). Reactions were analyzed using a real-time PCR detection system. CHD8 was present at the 5' region, and not the 3' region, of all three β -catenin responsive genes (Figure 2.9B). CHD8 was not present at the 5' or 3' region of

the control gene, PS2. ChIPs for acetyl histone H4 (α -AcH4) and tri-methyl histone H3 Lys4 (α -MeH3K4), two marks of active chromatin (9), were also performed. The pattern of CHD8 binding did not seem to correlate with levels of acetyl histone H4, however there was similarity between CHD8 and levels tri-methyl histone H3 Lys4. This methyl mark is typically enriched at regions near transcription start sites (6, 11, 60, 104). These results suggest that CHD8 is binding the promoter regions, near the transcription start site, of these β -catenin responsive genes.

In order to further define the precise region where CHD8 binds to these β -catenin responsive genes, we performed additional ChIP experiments. Primers were designed to amplify sections within the proximal promoter region, coding sequence, and 3' UTR of the Axin2 gene (Figure 2.10A). ChIPs were performed as described above using α -CHD8 and α -AcH4 antibodies. Our results demonstrate that CHD8 binds specifically to the proximal promoter region of the Axin2 gene and possibly the 5' coding sequence but not the remaining coding sequence or the 3' UTR. The results of the AcH4 ChIP again do not correlate with the CHD8 ChIP, but the results do eliminate any questions regarding the ability of the primers to amplify the regions examined. Taken together our results indicate that CHD8 localizes to the promoter regions of β -catenin responsive genes. We therefore hypothesize that the interaction of CHD8 with β -catenin serves to localize CHD8 to β -catenin responsive promoters where CHD8 functions in the regulation of β -catenin responsive genes.

CHD8 Regulates β -catenin Mediated Transcription

After demonstrating that human CHD8 directly interacts with β -catenin and binds to the promoter region of β -catenin responsive genes, we wanted to test the hypothesis that CHD8 affects the transcription of β -catenin responsive genes. In order to examine the role that CHD8 plays in the transcription of β -catenin responsive genes, RNAi experiments were performed. HCT116 cells were transfected with shRNA vectors containing hairpin cassettes directed against CHD8 or the control luciferase. The shRNA vectors contained a puromycin resistance marker (21) which allowed the transfected cells to be selected by treatment with puromycin 24 hours post transfection. Cells were harvested for RNA isolation and western blot analysis 36 hours post puromycin treatment. cDNA prepared from the isolated RNA was analyzed by real-time quantitative PCR using primers targeting the Axin2, Dkk1, and Nkd2 genes. Western blot analysis of lysates from the transfected cells was also performed to confirm that CHD8 was indeed knocked down in these cells compared to control cells (Figure 2.11B). Westerns were probed with α -actin as a loading control. The results showed that CHD8 was significantly depleted in the cells treated with shRNA directed against CHD8.

Given the association of CHD8 with β -catenin and the localization of CHD8 to several endogenous β -catenin targets in a colorectal cell line harboring an activated Wnt signaling pathway, we predicted that depletion of CHD8 would have a negative impact on transcription. Unexpectedly, depletion of CHD8 results in a modest but reproducible induction of all three target genes (Figure

2.11A). These results clearly demonstrate that CHD8 does participate in regulation of endogenous β -catenin target genes. However, these results suggest that the normal function of CHD8 may be to negatively regulate the transcription of these target genes.

In addition to CHD8, there are 3 other members within the CHD6-9 subfamily of CHD proteins, and in HCT116 cells, transcripts are detectable for all four proteins (Data not shown). Therefore it is possible that our results were complicated by the presence of the other members of this subfamily. In order to rule out this possibility and further confirm our results, we turned to *Drosophila*. *kismet* is the only CHD8 ortholog in *Drosophila*, and the use of a *Drosophila* system would eliminate possible complications of having multiple protein family members present during the RNAi experiments. *Drosophila* S2 cells were treated with double stranded RNA directed against *kismet*, *axin*, or both *axin* and *kismet*. RNAi directed against *axin* was used to activate the Wnt signaling pathway. Axin is a negative regulator of the Wnt signaling pathway, and therefore, loss of Axin by RNAi would result in an increase in Wnt signaling. In *Drosophila*, the *nkd* gene, like its mammalian ortholog, is activated upon Wnt signaling (85). In cells where Axin was knocked down, RNAi of *kismet* resulted in a 5 fold increase in expression of the *nkd* gene when compared to the control, further confirming the results seen in human cells (Figure 2.12). There were two additional observations of interest. First, the fold activation of *nkd* was greater than seen in human cells, suggesting that the other CHD8 paralogs may indeed compensate for loss of CHD8. Second, the depletion of Kismet also resulted in a

5 fold activation of *nkd*, even in the uninduced state. This suggests that Kismet/CHD8 is involved in regulating Wnt target genes, even in the absence of pathway activation. The results in both *Drosophila* and human cells demonstrate that CHD8 does play a role in regulating transcription of β -catenin responsive genes and that CHD8 functions as a negative regulator of these targets.

CHD8 Remodels Mononucleosomes Containing TCF Binding Sites

Our data demonstrates that CHD8 is an ATP-dependent chromatin remodeling enzyme that possesses both nucleosome stimulated ATPase activity and the ability to slide nucleosomes. In addition, CHD8 directly binds β -catenin and is present at the promoter region of β -catenin responsive genes. After demonstrating that CHD8 regulates transcription of β -catenin responsive genes, we wanted to determine whether CHD8 could remodel DNA containing TCF binding sites, and to ultimately test whether recombinant TCF and β -catenin can modulate the chromatin remodeling activity of CHD8. The downstream targets of the Wnt signaling pathway are members of the T-cell factor (TCF) family of sequence specific transcription factors. During activation of the Wnt signaling pathway, β -catenin interacts with TCF bound to specific sites at β -catenin responsive genes (8, 83). In order to determine whether CHD8 could remodel DNA containing TCF binding sites, fluorescently labeled DNA templates were prepared which were derivatives of the pGEM3z-601 template (71). One template, TCF-mid, had a single TCF binding site near the middle of the sequence. The other template, TCF-5', had a TCF binding site located at the 5' end of the sequence. Mononucleosomes were reconstituted by salt dialysis of

HeLa core histones and the two fluorescently labeled 601 TCF binding site DNA templates. Reactions, performed in triplicate, were prepared using reconstituted mononucleosomes, ATP, and PmlI in the presence or absence of wt recombinant CHD8. In the presence of CHD8, an increase in the fraction cut was observed for mononucleosomes reconstituted from both the 5' and middle mutant templates (Figure 2.13). These data demonstrate that CHD8 can indeed remodel DNA which contains TCF binding sites. This, therefore, provides a valuable system to look at the effects of TCF and β -catenin on the *in vitro* chromatin remodeling activity of CHD8.

Discussion

The CHD family of proteins are critical regulators of chromatin structure. While members of the CHD1-2 and CHD3-5 subfamilies have been extensively studied, further studies are needed to elucidate the function of the CHD6-9 subfamily of proteins. Members of the CHD6-9 subfamily share a conserved Snf2 helicase domain C-terminal to their double chromodomains (45, 77). The Snf2 helicase domain of known ATP-dependent remodeling enzymes has been shown to be responsible for the binding and hydrolysis of ATP (33). The presence of this domain within the sequence of the CHD6-9 proteins suggests that members of this subfamily may function as ATP-dependent chromatin remodeling enzymes. While ATPase activity has been reported for CHD6 and CHD9, ATP-dependent chromatin remodeling activity has not previously been shown for a member of the CHD6-9 subfamily (75, 109). We chose to focus our studies on CHD8 because an N-terminal fragment of rat CHD8, termed Duplin,

was previously reported to bind β -catenin and inhibit Wnt or β -catenin dependent TCF activation (103). Multiple proteins such as p300/CBP (47, 82, 120) and BRG1 (5) have been reported to interact with β -catenin and alter chromatin structure. However, an *in vitro* study of β -catenin mediated transcription demonstrated the requirement of an unidentified ATP-dependent chromatin remodeling enzyme (125). We hypothesized that CHD8 is this ATP-dependent chromatin remodeling enzyme which functions in part by regulating β -catenin mediated transcription.

Unlike in rat, there is no evidence of a truncated form of CHD8 in humans. Therefore, we first wanted to examine whether full length human CHD8 interacts with β -catenin. Using GST-pulldown experiment with recombinant proteins, we demonstrate that CHD8 binds directly to β -catenin *in vitro*. Data obtained from these experiments also indicate that CHD8 binds to the armadillo repeats within the β -catenin protein. Immunoprecipitation experiments performed with HeLa cells stably transfected with a Flag- β -cat^{active} construct demonstrated that full length human CHD8 also can bind to β -catenin *in vivo*.

After confirming that full length CHD8, like Duplin, binds β -catenin, we examined whether human CHD8 can regulate the transcription of β -catenin responsive genes, by binding to the promoters of β -catenin target genes. β -catenin is a component of the canonical Wnt signaling pathway (20). In the absence of Wnt ligand, β -catenin is phosphorylated by the APC complex (52). This phosphorylation event targets β -catenin for ubiquitination and degradation by the proteasome (56, 78). In the presence of Wnt ligand, disheveled inhibits

the APC complex preventing phosphorylation of β -catenin. β -catenin is then allowed to accumulate and translocate into the nucleus where it binds to TCF and mediates transcription of β -catenin target genes such as Axin2, Dkk1, and Nkd2 (8, 48, 83). Using CHIP experiments, we examined whether CHD8 binds to the promoter regions of these β -catenin responsive genes. Data from our experiments demonstrates that CHD8 binds to the 5' and not the 3' end of Axin2, Dkk1, and Nkd2. Additional analysis of CHD8 binding to the Axin2 gene utilized primers that amplified locations along the length of the gene. This data demonstrates that CHD8 binds to the proximal promoter region and not the remaining coding or 3' UTR sequences of Axin2.

To directly test whether CHD8 regulates transcription of β -catenin responsive genes, RNAi experiments were performed in HCT116 cells. This colorectal carcinoma cell line has an activated Wnt signaling pathway (61, 84). We observed that when CHD8 is depleted by RNAi, expression of the Axin2, Dkk1, and Nkd2 genes increases. Although our initial hypothesis was that CHD8 should function in the transcriptional activation of these β -catenin responsive genes, our results clearly demonstrate that CHD8 performs a negative role in their regulation.

Since there are other members of the CHD6-9 family that are expressed in the HCT116 cell line, we wanted to rule out any possible complications resulting from the presence of these other proteins. We chose to address this by performing RNAi experiments in *Drosophila* cells. Kismet is the only CHD8 ortholog in *Drosophila*, and therefore by targeting Kismet for depletion, we would

be able to avoid any complications resulting from the other human paralogs. Our RNAi experiments in *Drosophila* S2 cells demonstrated that when Kismet and Axin are depleted, expression of the Wnt target gene *nkd* is increased to a level higher than seen in human cells. These results confirm the observations we made in HCT116 cells, and suggest that the other human paralogs of CHD8 may also regulate these target genes. Together, the results in human and *Drosophila* cells demonstrate that CHD8 plays a negative role in regulating transcription of β -catenin responsive genes.

Although the presence of a Snf2 helicase domain suggests that members of the CHD6-9 family are ATP-dependent remodeling enzymes, this activity has not been reported. ATPase activity has, however, been previously shown for CHD6 and CHD9 (75, 109). Here we demonstrate that CHD8 possesses ATPase activity that is stimulated by the presence of nucleosomes. This ATPase activity requires an intact Snf2 helicase domain as a lysine to arginine mutation in the conserved GXGKT sequence within this domain results in loss of ATPase activity. This conserved sequence was previously identified as a region responsible for the binding and hydrolysis of ATP in other Snf2 helicase domain containing proteins (22, 30, 59, 123, 130). These results suggest that CHD8 may indeed function as an ATP-dependent chromatin remodeling enzyme.

To directly test our hypothesis that CHD8 is an ATP-dependent chromatin remodeling enzyme, we performed restriction enzyme accessibility assays (75, 109). This assay is commonly employed to measure chromatin remodeling activity and relies on the fact that ATP-dependent remodeling enzymes increase

the access of restriction enzymes to nucleosomal DNA. When CHD8 was used in this assay, we observed an increase in restriction enzyme accessibility, consistent with CHD8 being an ATP-dependent remodeler. Substitution of wild type CHD8 with mutant CHD8 (K842R) or ATP with AMPPNP, the non-hydrolysable form of ATP, resulted in the loss of this increased accessibility; confirming that this activity resides in CHD8 and requires the hydrolysis of ATP. Collectively, the results from the ATPase and restriction enzyme accessibility experiments demonstrate that CHD8 is a *bona fide* ATP-dependent chromatin remodeling enzyme. Our results provide the first evidence of chromatin remodeling activity for a CHD6-9 subfamily member. Our data suggests that CHD6, 7, and 9 may also possess ATP-dependent chromatin remodeling activity, given that the members of this subfamily share a conserved Snf2 helicase domain.

In the studies presented here, we demonstrate that CHD8 is an ATP-dependent chromatin remodeling enzyme. We show that CHD8 binds both β -catenin and the promoter proximal region of β -catenin responsive genes. We demonstrate that CHD8 can play a negative role in the transcription of these genes. Together, these results suggest that CHD8 may regulate transcription of β -catenin responsive genes by remodeling chromatin in the promoter proximal regions of these genes. Through regulating the localization of β -catenin, the Wnt signaling pathway is intimately involved in tumorigenesis. The data we present here is further evidence of a connection between the modification of chromatin

structure and disease states such as cancer, and suggest that CHD8 may be a future therapeutic target in the treatment of human cancer.

TABLE 2.1: Oligonucleotide sequences.

Name	Sequence (5'→ 3')
601 forward	CGGGATCCTAATGACCAAGGAAAGCA
601 reverse	CTCGGAACACTATCCGACTGGCA
601 slid forward	GTGATGGACCCTATACGCG
601 slid reverse	ACTCACTATAGGGCGAATTC
601 downstream forward	GCAGGCATGCAAGCTTGAG
601 downstream reverse	AGCGCCCAATACGCAAACC
601-1	CGGGATCCTAATGACCAAGGAAAGCA
601-2	CTCGGAACACTATCCGACTGGCA
601-3	GTTCCACGCTGTTCAATACATGC
601-mut 5'	GCCGAGGCCGCTCAGATCAAAGGAGACAGCTC TAGC
601-mut mid	GCACCGCTTAAACAGATCAAAGGGCTGTCCCC CGCG
β-catenin GST-N forward	CGTGGATCCATGGCTACTCAAGCTGATTTG
β-catenin GST-N reverse	ATGACGTCATGCATGTTTCAGCATCTGTG
β-catenin GST-C forward	CGTGGATCCAATGAGACTGCTGATCTTGG
β-catenin GST-C reverse	ATGACGTCATTACAGGTCAGTATCAAACC
Axin2 ChIP 5' forward	GGACTCCCAGATTCAGCACG
Axin2 ChIP 5' reverse	GGTGTGACTGAGCTGGATTCTT
Axin2 ChIP 3' forward	GGTGCCCTACCATTGACACAT
Axin2 ChIP 3' reverse	CGCAACATGGTCAACCCTC
PS2 ChIP 5' forward	CCTGGATTAAGGTCAGGTTGGA
PS2 ChIP 5' reverse	GCTACATGGAAGGATTTGCTGAT
PS2 ChIP 3' forward	CCAGCGACCAAGTGACACAA
PS2 ChIP 3' reverse	GGTTTCATCTCCTACGCCAATTT
DKK1 ChIP 5' forward	ATTCAACCCTTACTGCCAGGC
DKK1 ChIP 5' reverse	AAGGCTACCAGCGAGCGTTAT
DKK1 ChIP 3' forward	AACTGGCAGGATGTCTGCTGT

DKK1 ChIP 3' reverse	GCACTTCAGAAAACAAGCGCA
NKD2 ChIP 5' forward	AAGCCACTGAGTTGGACACGT
NKD2 ChIP 5' reverse	TTTGCCTTGGTTTGAGCAGG
NKD2 ChIP 3' forward	AGCAAACAGCAACTGACTGCA
NKD2 ChIP 3' reverse	GGCATCGAGGGCAGAAGAG
Axin2 ChIP -1050 forward	GCCCCTACCCTTCTTAGTTTGA
Axin2 ChIP -1050 reverse	TGTGCCAAGAATCCCAAACCTC
Axin2 ChIP +2358 forward	CGCCCCATTATGAGACCATT
Axin2 ChIP +2358 reverse	GCCTTTACCACGGCTCTTAAGT
Axin2 ChIP +6614 forward	TTCCGGATTGAGGACACATG
Axin2 ChIP +6614 reverse	AAGAAGTCTCACGACCTCCTGG
Axin2 ChIP +12005 forward	TGTGCCCTCTCCCAATCAA
Axin2 ChIP +12005 reverse	ACATGGATGCCAAATGCACT
Axin2 ChIP +16687 forward	TGCCTGATTTAGCCCTCTGTAG
Axin2 ChIP +16687 reverse	TGTTCCCACTGCTTCAAACC
Axin2 ChIP +21929 forward	TGGCTGTTTTTGCAGTCCG
Axin2 ChIP +21929 reverse	GGTCAGTGCCAAAACATGACAT
Axin2 ChIP +27113 forward	GCTCAGACATGCTGTGAAAGC
Axin2 ChIP +27113 reverse	AAGAGGCTCAAATCCCAACG
Axin2 ChIP +29519 forward	CCAGGTTGATCCTGTGACTGA
Axin2 ChIP +29519 reverse	CATTTCCACGAAAGCACAGC
CHD8 shRNA 493 top	GCTGTTAAGGATAACAATCTTAGGGGTTTTGGC CTCTGACTGACTCCTAGAAGTTATCCTAAC
CHD8 shRNA 493 bottom	TCCTGTTAAGGATAACTTCTAGGAGTCAGTCAG AGGCCAAAACCCCTAAGATTGTTATCCTTAA
CHD8 shRNA 6410 top	GCTGTTGTTCTCCATCTTCATTTGGGTTTTGGC CTCTGACTGACTCAAAGAGATGGAGAACAAC
CHD8 shRNA 6410 bottom	TCCTGTTGTTCTCCATCTCTTTGAGTCAGTCAG AGGCCAAAACCCAAATGAAGATGGAGAACAAC
DKK1 RT forward	TGGAATATGTGTGTCTTCTGATCAAA
DKK1 RT reverse	AAGACAAGGTGGTTCTTCTGGAAT
NKD2 RT forward	TGGACGAGAACACGGAGC

NKD2 RT reverse	GGACCCAGGGCCGAAT
Axin2 RT forward	ACAGTGGATACAGGTCCTTCAAGAG
Axin2 RT reverse	CGTCAGCGCATCACTGGAT
H1 RT forward	ACTCCACTCCCATGTCCCTTG
H1 RT reverse	CCGTTCTCTGGGAACTCACCT
dControl RNAi forward (β -lactamase)	TAATACGACTCACTATAGGGAGATATGGCTTCA TTCAGCTCCGG
dControl RNAi reverse (β -lactamase)	AATTAACCCTCACTAAAGGGAGACATTTCCGTG TCGCCCTTAT
dKismet RNAi forward	TAATACGACTCACTATAGGGAGATGTTACCACA GTGCCTGGAAGTGA
dKismet RNAi reverse	AATTAACCCTCACTAAAGGGAGAATTGTTGTGA GTTCCCTGCTGGC
dAxin RNAi forward	TAATACGACTCACTATAGGGAGACTCTACATCC AGCAGATGTC
dAxin RNAi reverse	AATTAACCCTCACTAAAGGGAGATCGGATTTCC AGTCTTCTTTT
dNkd RT forward	TAAAATTCTCGGCGGCTACAA
dNkd RT reverse	CGCACCTGGTGGTACATCAG
d β -tubulin RT forward	AGACCTACTGCATCGACAAC
d β -tubulin RT reverse	GACAAGATGGTTCAGGTCAC

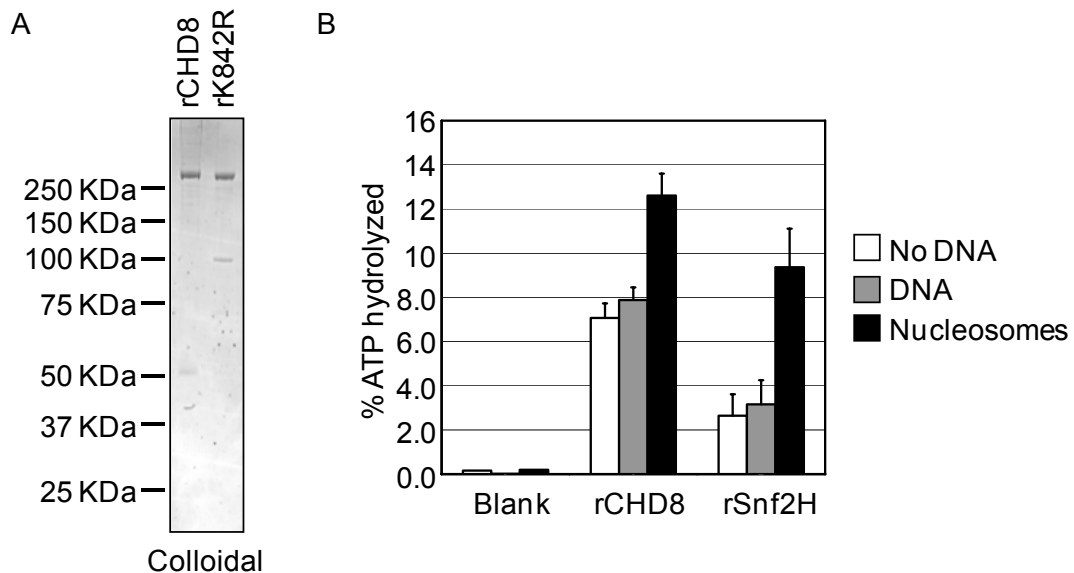


Figure 2.1: CHD8 possesses nucleosome stimulated ATPase activity. (A) SDS-PAGE of recombinant wt CHD8 (rCHD8) and recombinant mutant CHD8 (rK842R) purified from SF9 cells. (B) ATPase assays performed to detect the potential ATPase activity of CHD8. Recombinant CHD8 or Snf2H was incubated with $[\gamma\text{-}^{32}\text{P}]\text{ATP}$ in the presence or absence of plasmid DNA or nucleosomes purified from HeLa cells. ATPase reactions were analyzed by thin layer chromatography and phosphorimaging to detect the release of $^{32}\text{P}_i$. Reactions prepared in the absence of enzyme or in the absence of DNA or nucleosomes were used as controls.

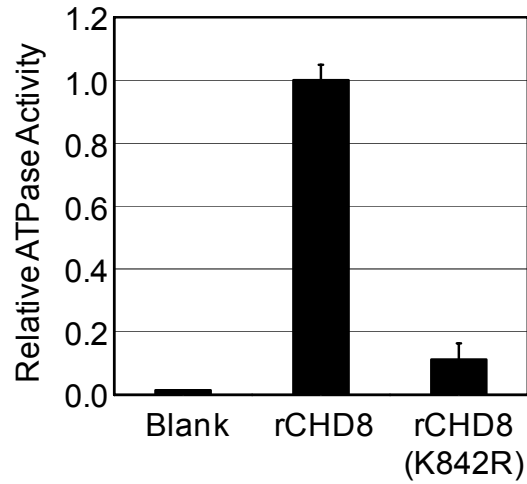


Figure 2.2: Mutation of lysine 842 in CHD8 results in a loss of ATPase activity. ATPase assays performed to compare the ATPase activity of recombinant wt CHD8 (rCHD8) and recombinant mutant CHD8 (rK842R). Recombinant wt or mutant CHD8 was incubated with [γ - 32 P] ATP and nucleosomes purified from HeLa cells. ATPase reactions were analyzed by thin layer chromatography and phosphorimaging to detect the release of 32 P_i. A reaction prepared in the absence of enzyme was used as a control.

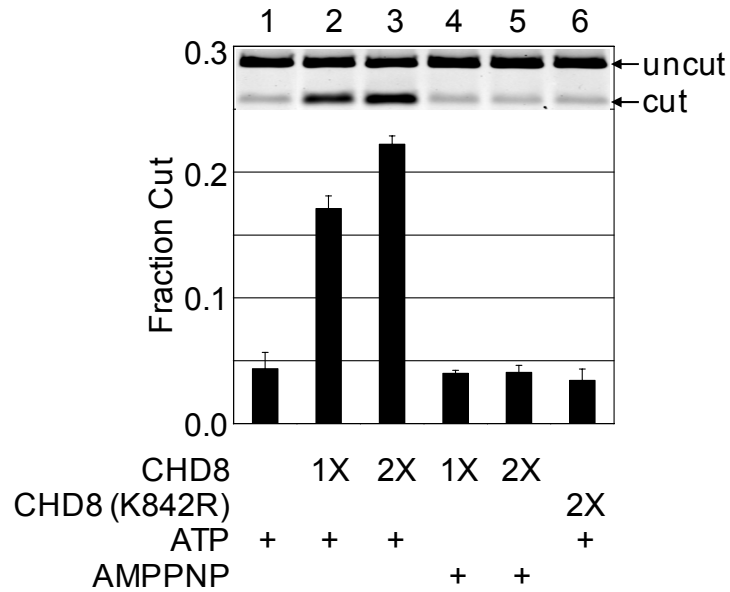


Figure 2.3: CHD8 increases restriction enzyme accessibility of mononucleosomes in the presence of ATP. Restriction enzyme accessibility assays were performed to detect increased restriction enzyme accessibility of mononucleosomes in the presence of CHD8. Recombinant CHD8 or CHD8 (K842R) was incubated with mononucleosomes, restriction enzyme HhaI, and ATP or AMPPNP. Reactions were performed in triplicate and the average plotted on the graph. A representative gel is shown in the inset. Arrows indicate the position of both uncut and cut template migration in the gel.

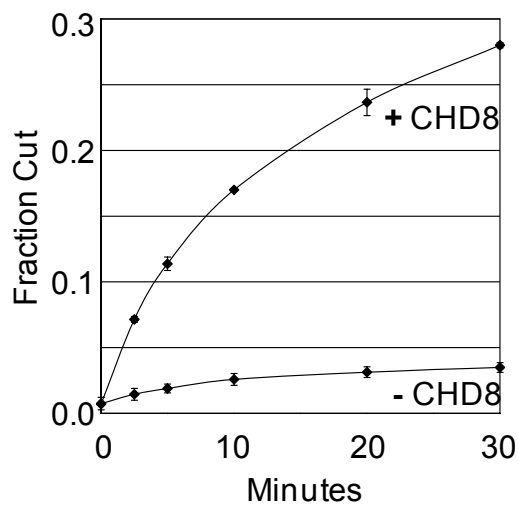


Figure 2.4: Increase in restriction enzyme accessibility of mononucleosomes in the presence of CHD8 approaches linear range over time. Restriction enzyme accessibility assays were performed over a 30 minute time period. Mononucleosomes were incubated with HhaI and ATP in the presence or absence of CHD8. Reactions were performed in triplicate and quenched at the indicated time points. Each point on the graph represents the average of the triplicate for that given time point.

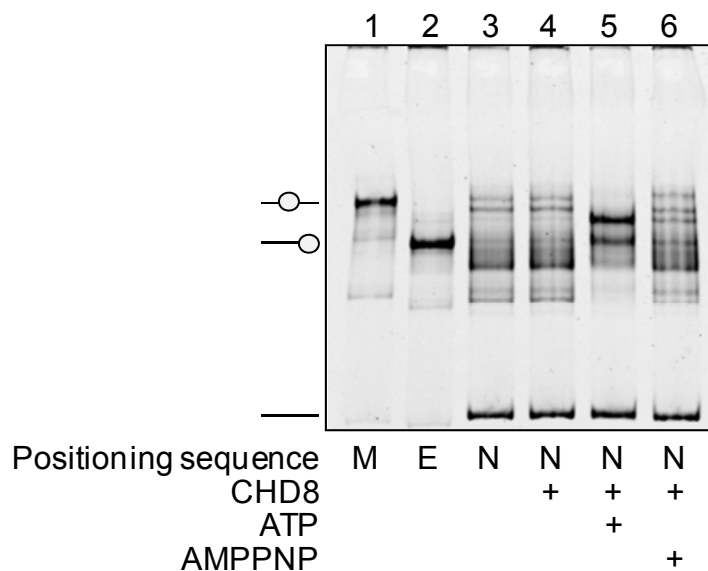


Figure 2.5: CHD8 slides mononucleosomes to two prominent positions along the DNA template. Nucleosome sliding assays were performed using reconstituted mononucleosomes prepared from a fluorescently labeled DNA template lacking a nucleosome positioning sequence (lanes 3-6). DNA templates with a nucleosome positioning sequence located at the end (lane 2) or middle (lane 1) of the template were used as controls for approximating the position of the slid nucleosomes along the test template. DNA templates with middle, end, or no nucleosome position sequence are labeled M, E, or N respectively. Reactions were prepared in the presence or absence of CHD8, ATP, or AMPPNP as indicated.

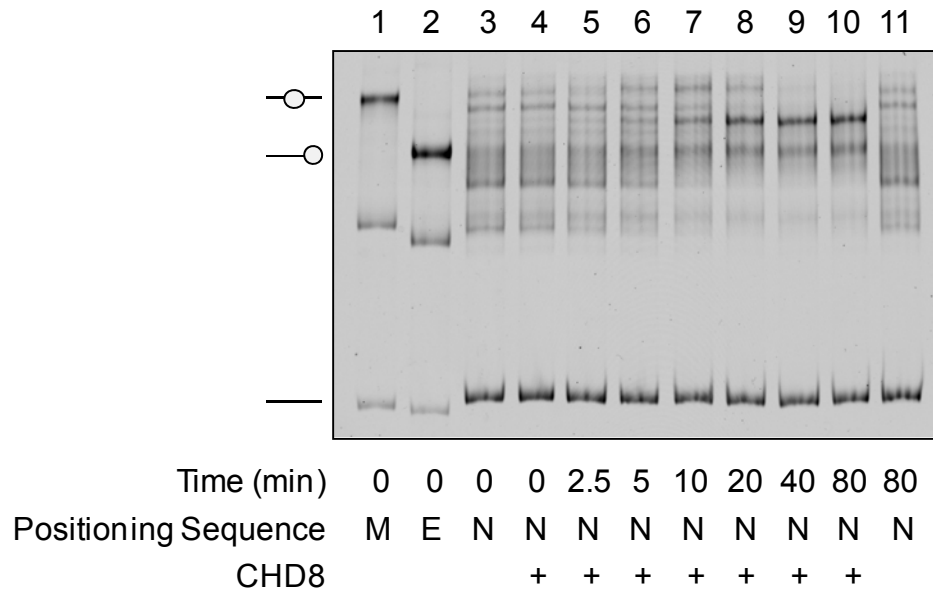


Figure 2.6: Two prominent species persist over time. Nucleosome sliding assays were performed over an 80 minute time period. Fluorescently labeled DNA templates without a nucleosome positioning sequence were reconstituted into mononucleosomes (lanes 3-11) for use in the assay. DNA templates with a nucleosome positioning sequence located at the middle (lane 1) or end (lane 2) of the template were used as controls for approximating the position of the slid nucleosomes along the template. DNA templates with middle, end, or no nucleosome position sequence are labeled M, E, or N respectively. Reactions were prepared with ATP in the presence or absence of CHD8.

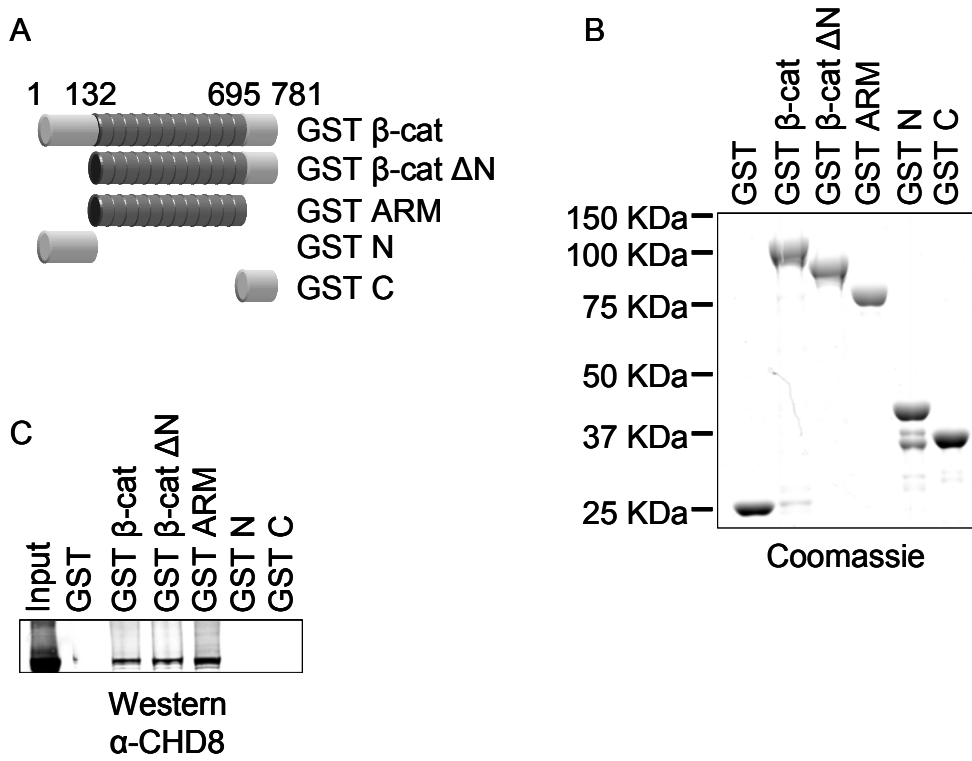


Figure 2.7: CHD8 interacts with β -catenin *in vitro*. (A) A diagram of the recombinant GST and GST- β -catenin fusion proteins used in B and C. (B) Cleared lysates containing 10 μ g of the indicated GST or GST fusion protein were incubated with glutathione-sepharose. After washing, samples were resuspended and incubated in a buffer containing 1 μ g of recombinant CHD8. Washed samples were then eluted in SDS loading buffer and subjected to SDS-PAGE. The bottom portion of the gel was Coomassie stained. (C) The top portion of the SDS-PAGE gel prepared in B was subjected to Western blot analysis using α -CHD8 antibody.

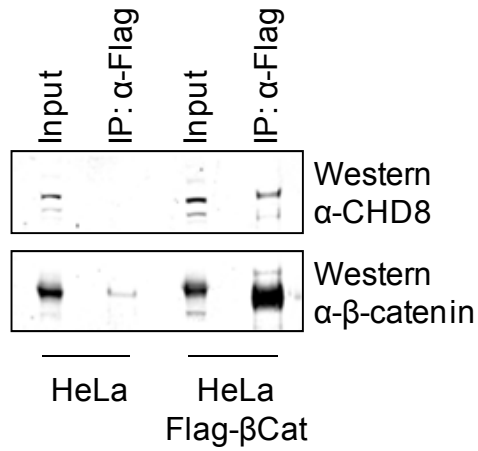


Figure 2.8: CHD8 interacts with β-catenin *in vivo*. Cells were harvested from a HeLa cell line stably expressing Flag-tagged β-catenin or the parental HeLa cell line. Nuclear extracts were prepared and incubated with α-Flag M2 conjugated agarose beads. Flag-IPs were washed and then eluted with SDS loading buffer. Eluted samples were subjected to SDS-PAGE and Western blot analysis using α-CHD8 and α-β-catenin antibodies.

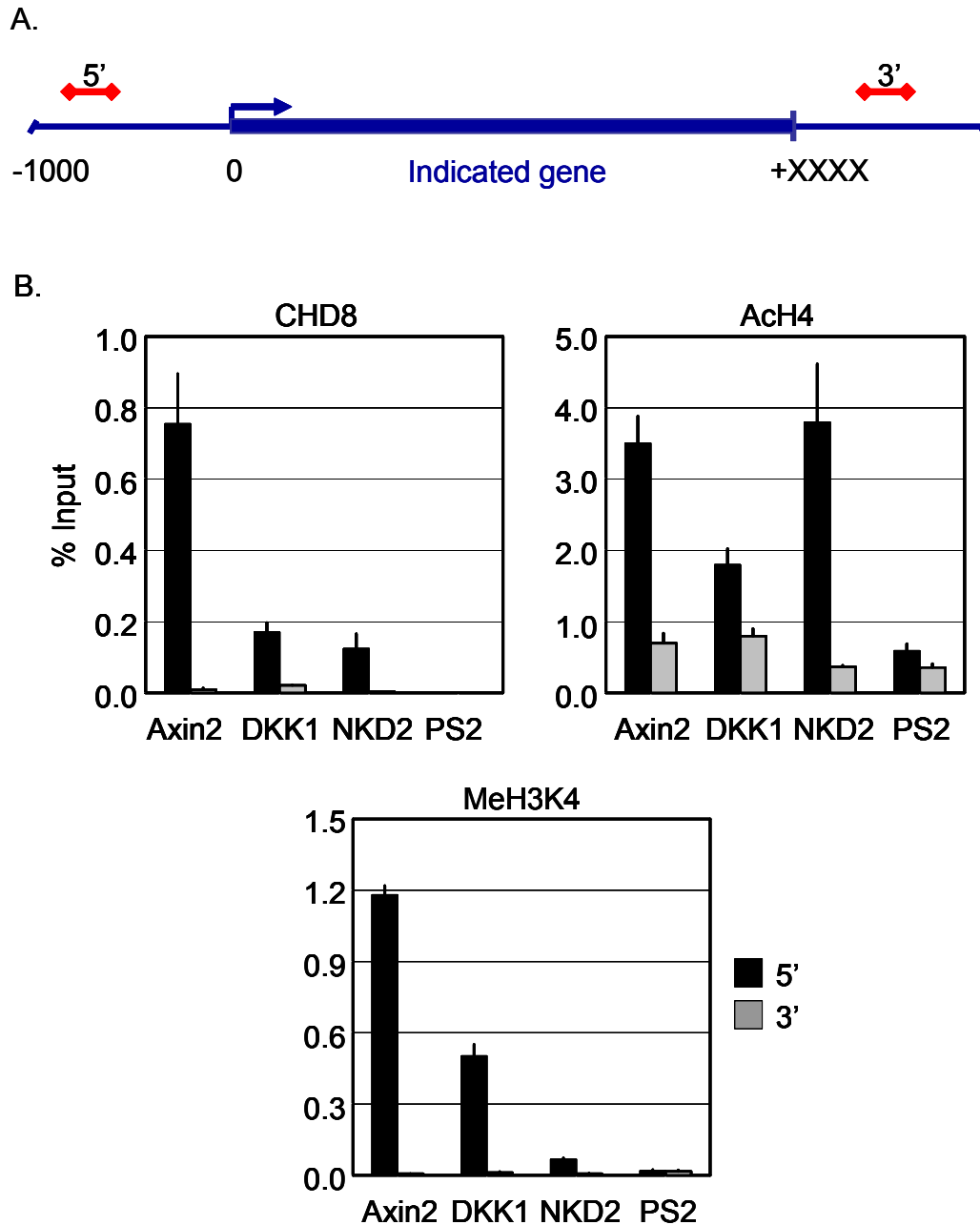


Figure 2.9: CHD8 is bound to the 5' end of Axin2, Dkk1, and Nkd2. (A) ChIP primers were designed to amplify the 5' and 3' regions of each gene of interest. (B) HCT116 cells were treated with formaldehyde to crosslink histones and DNA during the ChIP protocol. After sonication and pre-clearing, cell lysates were incubated with α -CHD8, α -acetyl histone H4, and α -trimethyl histone H3 Lys4 antibodies to form chromatin-antibody complexes. Complexes were precipitated and washed before crosslinking was reversed. Quantitative PCR reactions were performed in triplicate using DNA recovered from the ChIP protocol and primers designed to the Axin2, Dkk1, Nkd2, and PS2 genes. DNA levels were expressed relative to the level of input for the ChIP experiments. Samples precipitated using IgG served as a control and were less than 0.001% for all experiments (not shown).

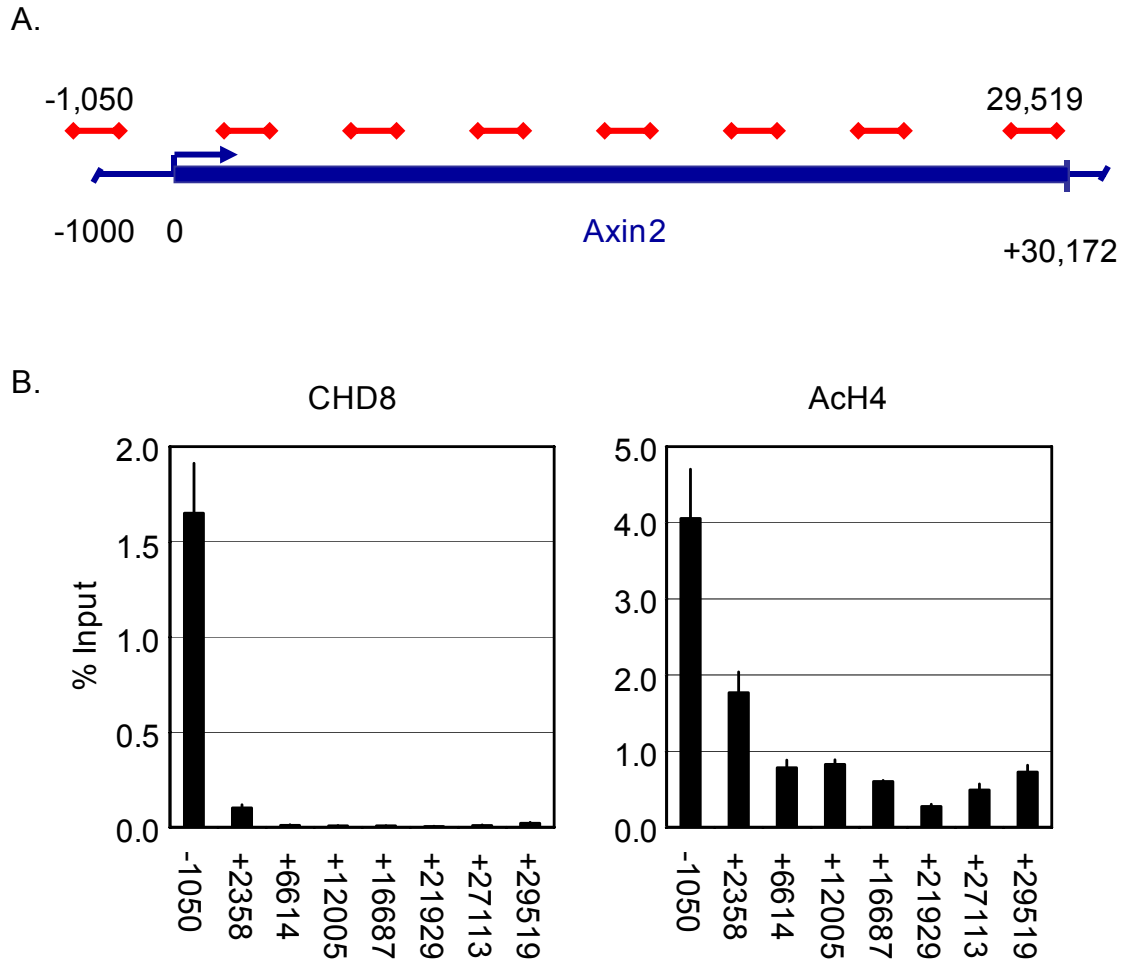


Figure 2.10: CHD8 is specifically recruited to the proximal promoter region of the Axin2 gene. (A) Primers were designed to amplify various regions spanning the length of the Axin2 gene. (B) HCT116 cells were treated with formaldehyde to crosslink histones and DNA for the ChIP protocol that followed. After sonication and pre-clearing, cell lysates were incubated with α -CHD8 and α -acetyl histone H4 antibodies to form chromatin-antibody complexes. Complexes were precipitated and washed before crosslinking was reversed. Quantitative PCR reactions were performed in triplicate using primers designed to the indicated regions of Axin2 and DNA recovered from the ChIP protocol. DNA levels were expressed relative to the level of input for the ChIP experiments. Samples precipitated using IgG served as a control and were less than 0.001% for all experiments (not shown).

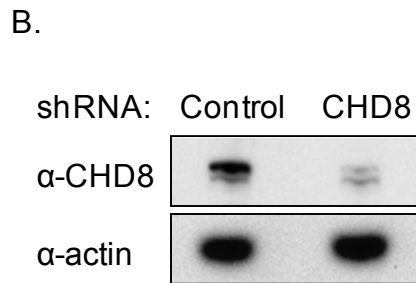
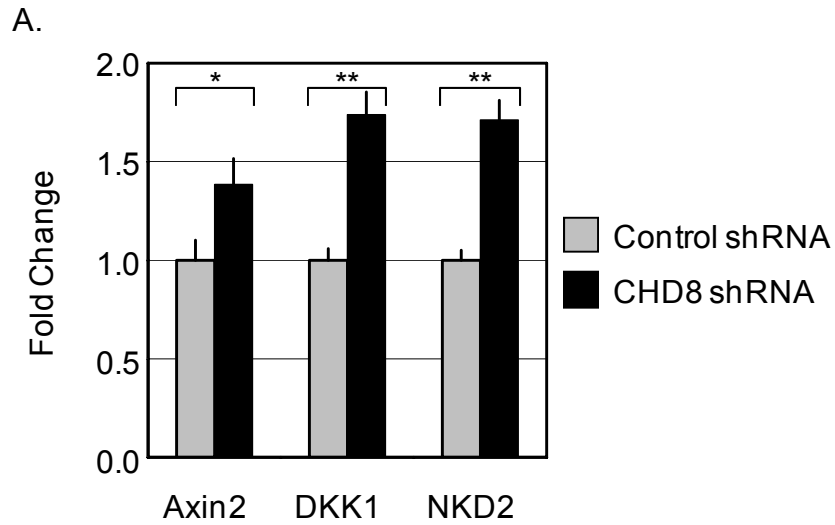


Figure 2.11: Depletion of CHD8 in HCT116 cells results in increased expression of Axin2, Dkk1, and Nkd2. (A) HCT116 cells were transfected with shRNAs directed against CHD8 or the luciferase control. Puromycin treatment was used to select for transfected cells. Post puromycin treatment, cells were harvested for RNA isolation and western blot analysis. Expression of the Axin2, Dkk1, and Nkd2 genes was analyzed by RT-PCR. Multiple experiments were performed. The data shown is a representative experiment. (*= $P < 0.05$ by Student's t test, **= $P < 0.001$ by Student's t test) (B) Cell lysates prepared from the shRNA transfected HCT116 cells were subjected to SDS-PAGE followed by Western blot analysis with the indicated antibodies. The α -actin blot was used as a loading control.

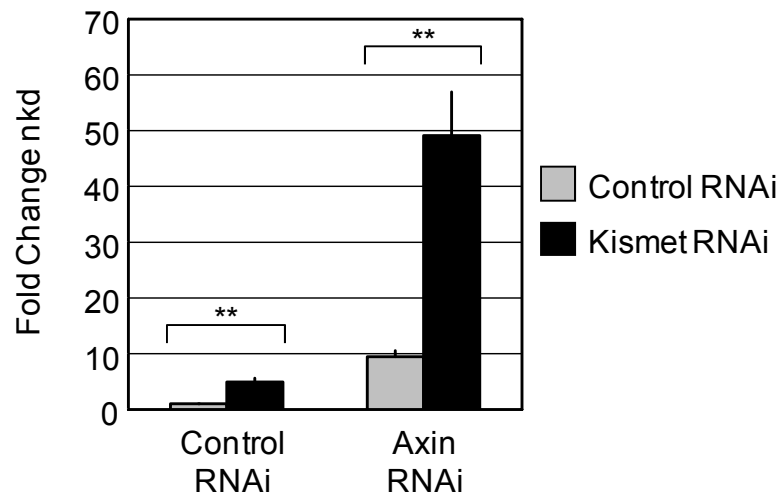


Figure 2.12: Depletion of *Drosophila* Kismet increases expression of *nkd*. *Drosophila* S2 cells were transfected with control, *kismet*, *axin*, or both *axin* and *kismet* double stranded RNAs. Cells were harvested four days post RNAi treatment. Expression of the *nkd* gene was analyzed by RT-PCR. Multiple experiments were performed. The data shown is a representative experiment. (*= $P < 0.05$ by Student's t test, **= $P < 0.001$ by Student's t test).

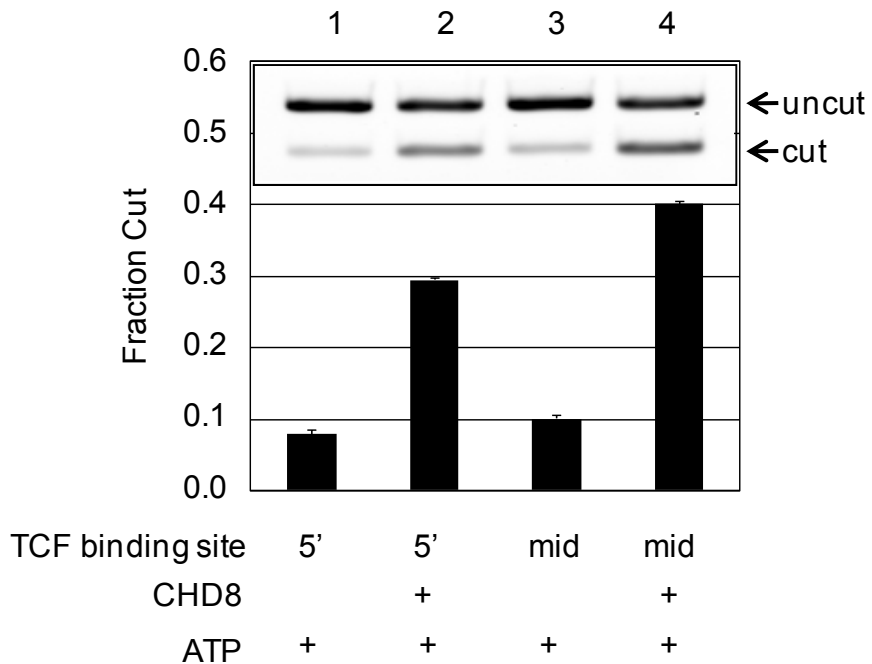


Figure 2.13: CHD8 remodels mononucleosomes containing TCF binding sites. Restriction enzyme accessibility assays were performed using reconstituted mononucleosomes prepared from fluorescently labeled DNA templates with TCF binding sites near the 5' end (lanes 1 and 2) or the middle (lanes 3 and 4) of the template. Mononucleosomes were incubated with restriction enzyme PmlI and ATP in the presence or absence of recombinant CHD8. Reactions were performed in triplicate and the average plotted on the graph. A representative gel is shown in the inset. Arrows indicate the position of both uncut and cut template migration in the gel.

Chapter III

CHD8 is a Component of a WDR5 Containing Complex and Regulates Expression of Hox Genes

Introduction

CHD8, an ATP-dependent Chromatin Remodeling Enzyme

Previously, we investigated whether CHD8, a member of the CHD family of proteins, possesses the ability to modify chromatin structure. Through the use of ATPase assays, we demonstrated that CHD8 possesses nucleosome stimulated ATPase activity and that this activity requires the Snf2 helicase domain for the hydrolysis of ATP. Many ATP-dependent chromatin remodeling enzymes that have Snf2 helicase domains within their sequence exhibit ATPase activity that is stimulated by the presence of DNA and/or nucleosomes. Therefore, the stimulated ATPase activity exhibited by CHD8 was an indication of potential remodeling activity. We then performed restriction enzyme accessibility assays to directly test CHD8 for chromatin remodeling activity. These assays

demonstrated that CHD8 possesses ATP-dependent chromatin remodeling activity. In addition, nucleosome sliding assays performed with CHD8 demonstrated that CHD8 possesses the ability to slide nucleosomes, an activity exhibited by various chromatin remodeling enzymes. Together, our data demonstrated that CHD8 is indeed an ATP-dependent chromatin remodeling enzyme.

Chromatin Remodeling Enzymes in Multi-subunit Complexes

Most known ATP-dependent chromatin remodeling enzymes exist within multi-subunit complexes with other proteins that assist the remodeling enzyme in functioning (40, 96, 132). These associated proteins may perform required activities or serve to regulate, target, or modify the specificity of the complex. The ATP-dependent chromatin remodeling complexes identified to date can be grouped into multiple families based on the domain architecture of their catalytic subunit (40, 132). Four of the well characterized families of human chromatin remodeling complexes are the SWI/SNF, ISWI, NURD/Mi-2/CHD, and INO80 families. The complexes within these families have anywhere from two to seventeen complex components (132). Identification of remodeling complex components is essential to understanding the function of a given chromatin remodeling enzyme.

The MLL-WDR5 Methyltransferase Complex

In addition to ATP-dependent chromatin remodeling, post-translational covalent histone modification such as methylation and acetylation are involved in

regulating chromatin structure. Similar to ATP-dependent chromatin remodeling enzymes, factors that establish or recognize covalent histone modifications often exist in multi-subunit complexes. Methylation of histone H3 lysine 4 (meH3K4), a hallmark of active chromatin, is catalyzed by the MLL1 complex. This complex is composed of the methyltransferase MLL1 and three additional core components, WDR5, RbBp5, and Ash2L. These core components have been reported to form a stable trimeric complex that can interact with the Set1 family of proteins which includes MLL1 (28). One of the core components, WDR5, has also been reported to recognize methylated histone H3 K4 (135).

WDR5 Regulates Expression of Hox Genes

In a search for proteins that recognize methylated histone H3 K4, a mark of active chromatin, Wysocka *et al.* identified WDR5. Through the use of RNAi targeting WDR5 and chromatin immunoprecipitation assays, they observed that WDR5 knockdown results in a decrease in histone H3 K4 trimethylation at HoxA9 and HoxC8 loci. In addition, this knockdown results in decreased expression of both HoxA9 and HoxC8 genes. In *Xenopus*, WDR5 depletion results in abnormal Hox gene expression and abnormal development (135). Identification other factors which regulate the expression of Hox genes is key to understanding vertebrate development.

Hox Genes

Hox genes are a highly conserved group of genes known to be involved in regulating patterns of development (50). In most species, Hox genes exist in

clusters and are expressed along the anterior-posterior embryonic axis where they play a role in specifying the identity of individual body segments (26, 50). Phenotypic changes termed homeotic transformations can occur when Hox gene function is disrupted. In *Drosophila*, homeotic transformation is observed when the Hox gene *ultra bithorax* is mutated. The result of this Hox gene mutation is the development of additional wings, four instead of two (50). This abnormal development demonstrates the significance of Hox genes in the normal development of body segments. It also highlights the importance of identifying and studying factors which regulate the expression of Hox genes.

Hypothesis and Summary of Results

As previously mentioned, our initial experiments demonstrate that CHD8 is a genuine ATP-dependent chromatin remodeling enzyme. Given that most ATP-dependent chromatin remodeling enzymes exist in multi-subunit complexes, we hypothesize that CHD8 also exists in a multi-subunit complex with other factors involved in or required for the function of CHD8. Here we perform a partial purification of the CHD8 complex from HeLa cells. Analysis of this partially purified complex estimated that CHD8 is a component of an approximately 900 kDa complex. Affinity purification followed by MS/MS analysis of the CHD8 complex identified multiple associated proteins which are known to be involved in altering chromatin structure. Immunoprecipitation experiments performed in HEK293 cells and GST pulldown experiments confirmed that CHD8 directly interacts with WDR5, a core component of the MLL1 methyltransferase complex. Through the use of co-infection experiments in SF9 cells, we

demonstrate that CHD8 also directly interacts with RbBp5 and Ash2L, other components of the MLL methyltransferase complex. Western blot analysis of the partially purified CHD8 complex from HeLa nuclear extract and additional co-infection experiments performed in SF9 cells suggest that CHD8 forms a complex with WDR5, RbBp5, Ash2L, and MLL1. RNAi targeting CHD8 in NT2/D1 cells demonstrates that depletion of CHD8 results in increased expression of the HoxA1-A4 genes. Chromatin immunoprecipitation experiments performed in both HeLa and NT2/D1 cells indicate that CHD8 is present at the promoter region of multiple genes of the HoxA locus. Our RNAi and ChIP experiments demonstrate that CHD8, like WDR5, plays a role in regulating Hox genes. Collectively, our data provide evidence supporting the hypothesis that CHD8 exists in a multi-subunit complex (es) with other polypeptides that are involved in the function of CHD8.

Materials and Methods

Cell Culture and Reagents

Dulbecco's modified Eagle medium (DMEM) (Invitrogen) with an additional 10% fetal bovine serum (Hyclone) and 1X penicillin-streptomycin-glutamine (Invitrogen) was used to culture HeLa, HEK293, and NTERA2 cl. D1 (NT2/D1) cells. Both HeLa and 293 cells were cultured at 37°C in 5% CO₂. NT2/D1 cells were cultured at 37°C in 10% CO₂. HeLa nuclear extracts were prepared from cells purchased from the National Cell Culture Center (Minneapolis, MN). SF9 cells were cultured at 24°C in 1X Grace's Insect medium (Invitrogen) containing

an additional 10% fetal bovine serum and 1X penicillin-streptomycin-glutamine (Invitrogen).

CHD8 rabbit polyclonal antibodies were raised against a 20 amino acid peptide (HTETVFNRVLPGPIAPESK) conjugated to keyhole limpet hemocyanin (Open Biosystems). This 20 amino acid peptide was also conjugated to Affi-Gel 10 (Bio-Rad) and used to affinity purify the CHD8 antibodies described above. The anti-acetyl histone H4 antibody (06-866) was purchased from Upstate (Millipore). The anti-Flag M2 antibody (F3165) and normal rabbit IgG (I8140) were purchased from Sigma. The anti-RbBP5 (A300-109A) and anti-Ash2L (A300-489A) antibodies were purchased from Bethyl. The anti-WDR5 antibody (22512-100) was purchased from Abcam. The anti-MLL-C antibody was received as a kind gift from Y. Dou (28). All oligonucleotides were synthesized by Integrated DNA Technologies (Coralville, IA). Primer sequences are listed in Table 3.1.

Purification of Endogenous CHD8

Methods published by Dignam *et al.* (27) were used to prepare HeLa nuclear extracts. Buffer A (20 mM Tris-HCl [pH 7.9], 0.2 mM EDTA, 10 mM β -mercaptoethanol [BME], 10% glycerol, 0.2 mM phenyl-methylsulfonyl fluoride [PMSF]) was used to perform fractionations with the indicated concentration of KCl. Size exclusion chromatography was performed with 350 mM KCl in buffer A. Columns and resins were obtained from the following manufacturers: P11

phosphocellulose (Whatman), DEAE-FF (Sigma), and Superose 6 HR 10/30 (GE Healthcare).

CHD8 was affinity purified using ~10 mg of sample obtained from the partial fractionation of HeLa nuclear extract by P11 and DEAE chromatography as described (12). The input was pre-cleared with 250 μ l of packed protein A agarose (Repligen). Anti-CHD8 antibody or normal rabbit IgG (~660 mg) was crosslinked to 500 μ l of packed protein A agarose using standard methods (46). Antibody-protein A agarose beads were incubated with the pre-cleared inputs overnight at 4°C in buffer IP (20 mM Tris-HCl [pH 7.9], 0.2 mM EDTA, 10% glycerol, 0.2 mM PMSF, 1 μ g/ml aprotinin, 1 μ g/ml leupeptin, and 1 μ g/ml pepstatin) containing 150 mM KCl. Washes were performed with 10 column volumes of buffer IP with the indicated components as follows: 2 washes with 150 mM KCl, 2 washes with 150 mM KCl and 1% NP40, 2 washes with 150 mM KCl, 4 washes with 1 M KCl, 2 washes with 150 mM KCl and 200 mM guanidine hydrochloride, and 2 washes with 150 mM KCl. Samples were eluted with 500 μ l of 100 mM glycine (pH 3.0) and neutralized with 50 μ l of 1 M Tris (pH 7.9). Peak fractions were identified by subjecting samples to SDS/PAGE followed by silver staining and western blot analysis using the α -CHD8 antibody. Peak fractions were TCA (Trichloroacetic acid) precipitated with a 1/10 volume of TCA and then subjected to SDS/PAGE followed by Colloidal Blue staining (Invitrogen). Bands were analyzed by in-gel trypsin digestion and tandem mass spectrometry (MS/MS) at the Michigan Proteome Consortium (University of Michigan).

Conventional purification was performed using ~2 g of HeLa nuclear extract followed by P11 and DEAE chromatography as described (12). The 0.5M P11/DEAE fraction was dialyzed against buffer B (20 mM HEPES [pH 7.6], 0.2 mM EDTA, 10% glycerol, 10 mM BME) containing 700 mM ammonium sulfate. Following centrifugation to remove precipitated proteins, the sample was then loaded on a 20 ml Butyl Sepharose column equilibrated with 700 mM ammonium sulfate in buffer B. The column was eluted using a gradient of 700 mM to 0 mM ammonium sulfate in buffer B. Peak fractions from the Butyl column were pooled and then dialyzed against buffer EQ (10 μ M CaCl₂, 40 mM KCl, 10% glycerol, 0.2 mM PMSF, 10 mM BME) containing 10 mM K_xPO₄ [pH 7.8]. Samples were loaded on a Hydroxyapatite column equilibrated in buffer EQ containing 10 mM K_xPO₄ (pH 7.8). The column was eluted with a gradient of 10 mM to 600 mM K_xPO₄ (pH 7.8) in buffer EQ. Peak CHD8 containing fractions were pooled and dialyzed against buffer BS (20 mM K_xPO₄ [pH 7.8], 0.2 mM EDTA, 10% glycerol, 0.2 mM PMSF, 10 mM BME) with 50 mM KCl. Samples were loaded on a MonoS 5/5 equilibrated in buffer BS containing 50 mM KCl. The column was eluted with a gradient of 50 mM to 400 mM KCl in buffer BS. Peak CHD8 containing fractions were pooled and dialyzed against buffer A with 100 mM KCl. Samples were loaded on a MonoQ 5/5 equilibrated in buffer A containing 100 mM KCl. The column was eluted with a gradient of 100 mM to 500 mM KCl in buffer A. Peak CHD8 containing fractions were pooled. Size exclusion chromatography was performed with a Superose 6 column equilibrated with buffer A (350 mM KCl). Columns and resins were obtained from the

following manufacturers: Butyl Sepharose, Mono S 5/5, Mono Q, Superose 6 (GE Healthcare) and Hydroxyapatite (BioRad). For each step of the purification, fractions were subjected to SDS/PAGE followed by silver staining and western blot analysis with α -CHD8 antibody to identify the peak CHD8 fractions.

Production of Recombinant Proteins

The Bac-N-Blue baculovirus expression system (Invitrogen) was used to prepare recombinant baculovirus containing Flag-tagged human CHD8. SF9 cells at a concentration of (1×10^6 cells/ml) were infected with the recombinant baculovirus at a multiplicity of infection (MOI) equal to 2. Cells were harvested 4 days post infection. After harvesting, cells were washed with phosphate buffered saline (PBS) and resuspended in buffer IP with 500 mM KCl, 1% NP-40, 1 μ g/ml aprotinin, 1 μ g/ml leupeptin, and 1 μ g/ml pepstatin. A Dounce homogenizer was then used to lyse the cells. After douncing, lysates were centrifuged at ($15,806 \times g$) for 15 minutes at 4°C. Cleared lysates were dialyzed against buffer IP containing 50 mM KCl. Dialyzed lysates were then combined with 500 μ l of anti-Flag M2 conjugated agarose beads (Sigma) and rotated overnight at 4°C. Flag-IPs were washed with 10 column volumes (CV) of each of the following buffers: buffer IP with 150 mM KCl, buffer IP with 350 mM KCl, and buffer IP with 150 mM KCl. Flag-IPs were eluted with buffer A containing 400 μ g/ml Flag peptide (Sigma), 150 mM KCl, 1 μ g/ml aprotinin, 1 μ g/ml leupeptin, and 1 μ g/ml pepstatin.

Escherichia coli BL21 cells were used to express GST. After harvesting, cells were resuspended in buffer BC150 (150 mM KCl, 0.2 mM EDTA, 10 mM BME, 10% glycerol, 0.2 mM PMSF, 20 mM Tris-HCl [pH 7.9]). Resuspended cells were passed through a French Pressure Cell twice and lysates were centrifuged at (105,000 X g) for 60 minutes at 4°C before collecting the supernatants. Samples were then subjected to sodium dodecyl sulfate-polyacrylamide gel electrophoresis (SDS-PAGE). The SDS-PAGE gels were Coomassie stained and used to determine the concentration of GST and GST fusion proteins in each cell lysate. GST-WDR5 was received as a kind gift from R.C. Trievel (24).

Protein Interaction Studies

In vivo experiments examining the interaction between CHD8 and WDR5 were conducted in HEK293 cells. Lipofectamine-2000 (Invitrogen) was used according to the manufacturer's instructions to transfect cells with a construct expressing Flag-tagged WDR5 or the parental Flag vector. Before harvesting, cells were washed twice with cold PBS. Cells were lysed with lysis buffer (150 mM NaCl, 1% NP-40, 0.25% sodium deoxycholate, 0.1% SDS, 50 mM Tris-HCl [pH 7.4], 1 mM EDTA, and 0.2 mM PMSF). Lysates were incubated with 20 μ l of α -Flag M2 agarose beads (Sigma) overnight at 4°C. Beads were washed with 1 ml of lysis buffer prior to elution with SDS loading buffer. Samples were subjected to SDS-PAGE and Western blot analysis using the indicated antibodies.

In vitro studies of the interaction between CHD8 and WDR5 utilized recombinant proteins. Glutathione-Sepharose beads (Sigma) were washed once with cold PBS and once with cold BC150 containing 0.2% NP-40. Beads were then resuspended in BC150 containing 0.2% NP-40 to produce a 50% slurry and divided into 40 μ l aliquots. Equal concentrations of GST and GST-WDR5 (1 μ g) were added to each tube of beads. BC150 containing 0.2% NP-40 was added to bring volumes up to 500 μ l before rotating overnight at 4°C. Beads were washed twice for 10 minutes per wash with 1 ml of BC150 containing 0.2% NP-40. After washing, beads were incubated with 1 μ g of recombinant Flag-CHD8 in 500 μ l of BC150 containing 0.2% NP-40 overnight at 4°C with rotation. Beads were washed three times with 1 ml of BC150 containing 0.2% NP-40 for 10 minutes per wash at 4°C. Bound proteins were eluted with 40 μ l of 2X SDS loading buffer. Samples were subjected to SDS-PAGE, Coomassie staining, and Western blot analysis with the indicated antibodies.

Co-infection experiments performed in SF9 cells utilized recombinant baculoviruses containing Flag-CHD8, Flag-WDR5, WDR5, Ash2L, RbBp5, and MLL-C. Flag-CHD8, Flag-WDR5, Ash2L, and RbBp5 were created using the Bac-N-Blue baculovirus expression system (Invitrogen). WDR5 and MLL-C baculoviruses were received as a kind gift from Y. Dou (28). Cells were plated at a density of 5×10^6 cells per 10 cm plate. After plating, cells were allowed to attach for 45 minutes at 24°C. Media was aspirated before adding 1 ml of each of the indicated baculoviruses. Additional media was added to bring the volume of each plate up to 5 ml. Plates were then rocked gently at room temperature for

1 hour. After incubation, media was added to each plate for a final volume of 10 ml. Plates were incubated at 24°C for 3 days before harvesting. Cells were collected and centrifuged at 500 X g for 2 minutes at room temperature. Cell pellets were washed once with cold PBS. Cells were resuspended in 500 µl of IP lysis buffer (150 mM KCl, 0.2 mM EDTA, 1% NP-40, 10% glycerol, 0.2 mM PMSF, 20 mM Tris-HCl [pH 7.9]). Lysate were centrifuged at 20,800 X g for 15 minutes at 4°C. Lysates were then incubated overnight at 4°C with 20 µl of packed anti-Flag M2 agarose beads (Sigma). Beads were washed 3 times with IP lysis buffer prior to elution with 40 µl of 2X SDS loading buffer. Samples were then subjected to Western blot analysis using the indicated antibodies.

Co-infection experiments treated with micrococcal nuclease or ethidium bromide were performed as described above with a few modifications. Instead of 1 ml, 100 µl of RbBp5 was used to infect the SF9 cells. The protocol for ethidium bromide treatment was adapted from Lai *et al.* (65). Lysates were incubated with 200 µg/ml of ethidium bromide for 30 minutes on ice. Precipitates were removed by centrifugation at 20,800 X g for 5 minutes at 4°C. Samples were then incubated with α-Flag M2 agarose as described above. All washes contained 200 µg/ml of ethidium bromide. For micrococcal nuclease treated samples, cells were harvested and treated as above. Prior to elution, beads were incubated for 1 hour at 37°C with 15 units of micrococcal nuclease (Roche) in 50 µl of digestion buffer (50 mM NaCl, 10 mM Tris, 4 mM CaCl₂, pH 7.0). Beads were then washed for 10 minutes with 1 ml of digestion buffer and eluted as above.

Purification of HeLa Core Histones

HeLa nuclear pellets were prepared using methods described by Dignam et al (27). Cells were purchased from the National Cell Culture Center (Minneapolis, MN). Nuclear pellets were homogenized by douncing in a chilled buffer containing 20 mM Tris (pH 7.9), 25% glycerol, 0.42M NaCl, 1.5 mM MgCl₂, 0.2 mM EDTA, 0.5 mM PMSF, and 0.5 mM DTT. Purification of core histones was performed using hydroxyapatite chromatography as described by Cote et al. (23) with minor changes. HAP buffer (50 mM NaPO₄ [pH 6.8], 1 mM BME, 0.5 mM PMSF) was prepared and chilled to 4°C. The DNA content of the homogenized nuclear pellet was estimated by diluting 1000 fold in 2 M NaCl in order to measure the OD₂₆₀ of the pellet. Approximately a 42 mg DNA equivalent of the homogenized pellet was added to 75 ml of HAP buffer with 0.6 M NaCl. This mixture was stirred gently at 4°C for 10 minutes. While stirring, 35 g of Hydroxyapatite Bio Gel HTP (BioRad) was added to the mixture. Additional HAP buffer containing 0.6 M NaCl was added to allow the mixture to be poured into a column. The column was washed overnight at 4°C with HAP buffer containing 0.6 M NaCl at a flow rate of ~1ml/min. Core histones were eluted with HAP buffer containing 2.5 M NaCl. The peak fractions were identified by Bradford analysis. The peak fractions were pooled and concentrated using a Centriprep YM-10 concentrator (Amicon).

Restriction Enzyme Accessibility Assay

The restriction enzyme accessibility assay was adapted from methods outlined by Smith and Peterson (114). A major change in the protocol was the use of fluorescently labeled DNA fragments generated by PCR using a combination of fluorescent and non-fluorescent primers. These reactions utilized pGEM3z-601 DNA from J. Widom as a template (71). Two forward primers (601 forward) were used that had the same DNA sequence, but were either unlabeled or fluorescently labeled with 5'-Alexa Fluor 488-N-hydroxysuccinimide ester. A labeled to unlabeled primer ratio of 0.1/0.9 was used in each PCR reaction. The reverse primer (601 reverse) was unlabeled. The 277bp PCR product was verified by electrophoresis in a 2% agarose gel followed by detection using a Typhoon Trio+ Imager (GE Healthcare). The fluorescently labeled PCR products were then ethanol precipitated and used to reconstitute mononucleosomes.

Mononucleosomes were reconstituted using methods adapted from Luger et al (73). Mononucleosome reconstitution reactions were assembled using a 1:0.875 molar ratio of the 277bp fluorescently labeled DNA to core histones purified from HeLa nuclear pellets. Reconstitution reactions (100 μ l) contained 10 μ g labeled DNA, 5.16 μ g histones, and 0.1 μ g bovine serum albumin in 2 M NaCl. Mononucleosomes were formed via salt dialysis of the reconstitution reactions at 4°C. The reactions were dialyzed against a decreasing buffer gradient from a high salt buffer (1 mM EDTA, 2 M NaCl, 0.2 mM PMSF, 10 mM Tris [pH 8.0]) to a low salt buffer (1 mM EDTA, 0.2 mM PMSF, 10 mM Tris [pH 8.0]) over a 3 day period. After dialysis, reconstitutions were verified by

loading reactions onto a 5% non-denaturing acrylamide/bisacrylamide (37.5:1) 0.2X Tris-borate-EDTA gel. Labeled nucleosomes were detected using a Typhoon Trio+ Imager (GE Healthcare).

Restriction enzyme accessibility assays were performed in triplicate. Each 15 μ l reaction contained 1 mM ATP, 50 nM reconstituted mononucleosomes, and 20U HhaI in remodeling buffer (3 mM MgCl₂, 50 mM NaCl, 2 mM dithiothreitol, 1 μ M ZnCl₂, 0.1 mg/ml bovine serum albumin, 20 mM Hepes [pH 8.0]). The final concentration of CHD8 was 0.017 μ M. In reactions containing GST, the final concentration of GST was 0.009 μ M (0.5X) or 0.017 μ M (1X). In reactions containing GST-WDR5, the final concentration of GST-WDR5 was 0.009 μ M (0.5X) or 0.017 μ M (1X). Reactions were incubated for 30 minutes at 30°C. Reactions were quenched by adding 15 μ l of 2X stop solution (10 mM Tris [pH 8.0], 0.6% SDS, 40 mM EDTA, 5% glycerol, 0.1mg/ml proteinase K) and incubating at 50°C for 20 minutes. Samples were analyzed on a 3% agarose gel and bands were quantified using a Typhoon Trio+ Imager and ImageQuant TL software (GE Healthcare). Data points represent the average value of each triplicate.

RT-PCR, Quantitative PCR, and PCR

For real-time quantitative PCR, total RNA was isolated from the indicated cell lines using the RNeasy and Qiashredder kits (Qiagen) as outlined by the manufacturer. cDNA was produced using random decamers (Ambion) and Superscript II (Invitrogen) as described by the manufacturers. Real-time

quantitative PCR reactions were prepared using cDNA, iQ Sybr Green Supermix (BioRad), and the indicated primers. Each reaction was performed in triplicate using the MyiQ single color real-time PCR detection system (BioRad).

Quantification was performed as described by M. W. Pfaffl (94) using pol III transcribed H1 (human) for normalization. For quantitative ChIP experiments, reactions were prepared with the indicated ChIP DNA, iQ Sybr Green Supermix, and the specified primers. Each reaction was performed in triplicate and analyzed using the MyiQ single color real-time PCR detection system. DNA levels were expressed relative to the level of input. For non-quantitative ChIP experiments, reactions were prepared with the indicated ChIP DNA and the specified primers. Non-quantitative ChIP experiments employed standard PCR techniques.

ATRA Induction Experiments

For the Hox gene induction experiments and chromatin immunoprecipitation experiments, $\sim 7.75 \times 10^5$ NT2/D1 cells were plated on a 10 cm dish. Cells were treated with 1×10^{-5} M all-trans retinoic acid (ATRA) dissolved in DMSO (induced) or an equivalent volume of DMSO alone (uninduced). Cells were grown ~ 38 hours before being harvested for RNA isolation.

RNAi Knockdown Experiments

The RNAi experiments in NT2/D1 cells employed the UI2-puro SIBR shRNA vectors (21). The CHD8 RNAi experiments used a shRNA vector

containing two cassettes (493 and 6410). Primers for the creation of this construct are listed in Table 3.1. A shRNA vector containing a cassette directed against luciferase, UI2-puro SIBR luc 1601, was used as a control (21). Five micrograms of the indicated construct was transfected into NT2/D1 cells ($\sim 7.75 \times 10^5$) using Lipofectamine-2000 as described by the manufacturer (Invitrogen). Selection of transfected cells was performed through the addition of 5 $\mu\text{g}/\text{ml}$ of puromycin to the cell culture medium 24 hours post transfection. Cells were treated 25 hours later with ATRA at a final concentration of 1×10^{-5} M. Cells were then grown a ~ 38 hours before being harvested for RNA isolation.

ChIP Assays

The chromatin immunoprecipitation (ChIP) assay was adapted from the protocol described by Upstate. For each ChIP, approximately 1×10^6 cells were crosslinked by treatment with formaldehyde for 10 minutes at 37°C . The formaldehyde was added directly to the cell media at a final concentration of 1%. Cells were then washed twice with cold PBS containing 1 mM PMSF, 1 $\mu\text{g}/\text{ml}$ pepstatin, and 1 $\mu\text{g}/\text{ml}$ aprotinin. Cells were harvested by scraping after the addition of 200 μl of cold ChIP Lysis Buffer (1% SDS, 10 mM EDTA, 50 mM Tris-HCl [pH 8.1], 1 mM PMSF). DNA was sheared into ~ 200 -1000bp fragments by sonication. Lysates were centrifuged at $20,800 \times g$ for 10 minutes at 4°C . Cleared supernatants were diluted 10 fold in ChIP Dilution Buffer (0.01% SDS, 1.1% Triton X-100, 1.2 mM EDTA, 16.7 mM Tris-HCl, [pH 8.1], 167 mM NaCl) containing 1 mM PMSF, 1 $\mu\text{g}/\text{ml}$ pepstatin, and 1 $\mu\text{g}/\text{ml}$ aprotinin. The diluted supernatants were pre-cleared by adding 38 μl of packed protein A agarose

blocked with salmon sperm DNA. Samples were rotated at 4°C for 30 minutes. After brief centrifugation, the pre-cleared supernatants were collected and rotated overnight at 4°C with the indicated antibodies. Chromatin/antibody complexes were collected by rotating each IP with 38 µl of packed protein A agarose/salmon sperm DNA for 1 hour at 4° followed by centrifugation at 4°C for 1 minute at 500 X *g*. Protein A/antibody/chromatin complexes were washed for 30 minutes at 4°C with 1 ml of each of the following buffers: one wash with Low Salt Immune Complex Wash Buffer (0.1% SDS, 1% Triton X-100, 2 mM EDTA, 20 mM Tris-HCl [pH 8.1], 150 mM NaCl, and 1 mM PMSF), one wash with High Salt Immune Complex Wash Buffer (0.1% SDS, 1% Triton X-100, 2 mM EDTA, 20 mM Tris-HCl [pH 8.1], 500 mM NaCl, and 1 mM PMSF), one wash with LiCl Immune Complex Wash Buffer (0.25M LiCl, 1% NP-40, 1% deoxycholate, 1 mM EDTA, 10 mM Tris-HCl [pH 8.1], and 1 mM PMSF), and two washes with TE Buffer (1 mM EDTA, 10 mM Tris-HCl [pH 8], and 1 mM PMSF). After washing, samples were eluted by incubation at room temperature for 30 minutes with 500 µl of elution buffer (1% SDS, 0.1 M NaHCO₃). Crosslinking was reversed by adding 20 µl of 5 M NaCl to each eluate and heating at 65°C for 4 hours. Eluates were deproteinated by addition of 10 µl of 0.5 M EDTA, 20 µl of 1 M Tris-HCl (pH 6.5), and 2 µl of 10 mg/ml proteinase K and incubated at 45°C for 1 hour. Samples were purified by phenol/chloroform extraction and the DNA was recovered by ethanol precipitation.

Results

CHD8 is a Component of a Large Multi-subunit Complex

In the previous chapter, we performed multiple experiments demonstrating that CHD8 is an ATP-dependent chromatin remodeling enzyme. As most ATP-dependent chromatin remodeling enzymes exist in multi-subunit complexes with other proteins that are required for targeting or regulating the remodeler, we hypothesize that CHD8 would also exist in a multi-subunit complex. The identification and characterization of these proteins is therefore key to the understanding of CHD8.

In order to determine whether CHD8 exists in a multi-subunit complex, a partial purification of CHD8 from HeLa nuclear extract was performed. HeLa nuclear extract was first fractionated using P11 phosphocellulose chromatography. P11 fractions were eluted stepwise with a buffer containing various concentrations of KCl (0.1 M, 0.3 M, 0.5 M, and 1 M). Western blot analysis using α -CHD8 antibody indicated that the fraction eluted with 0.5 M KCl was the peak CHD8 containing fraction (Figure 3.1). This fraction was purified further by DEAE-Sepharose chromatography. Fractions were eluted stepwise with a buffer containing varying concentrations of KCl (0.1 M and 0.35 M). The fraction eluted with 0.35 M KCl was further purified using a Superose 6 size exclusion column. Fractions eluted from the Superose 6 column were subjected to Western blot analysis using α -CHD8 antibodies. The elution profile of CHD8 obtained from the size exclusion column was consistent with a complex of

~900 KDa (Figure 3.1). Since the molecular weight of a CHD8 monomer is predicted to be ~290 KDa, this profile suggests that CHD8 exists in a multi-subunit complex.

In order to verify the existence of a multi-subunit CHD8 complex and identify the individual components, a conventional purification of CHD8 was performed. Nuclear extract from 200 liters of HeLa cell culture (~2 g) was chromatographed using sequential combinations of hydrophobic, ionic, affinity, and size exclusion separation columns. In the first step of the purification, HeLa nuclear extract was fractionated over P11 phosphocellulose followed by DEAE-Sepharose chromatography as described above. Figure 3.2A outlines the purification protocol. The DEAE 0.35 M KCl fraction was then further fractionated using a butyl Sepharose column eluted with a gradient of 0.7 M to 0 M ammonium sulfate. The peak CHD8 containing fractions from the butyl Sepharose column were then subjected to hydroxyapatite chromatography. Fractions were eluted from the hydroxyapatite column using a gradient of K_2PO_4 from 0.01 M to 0.6 M. The peak CHD8 containing fractions from the hydroxyapatite column were then fractionated further using Mono S and Mono Q columns. Fractions were eluted from the Mono S and Mono Q columns using a gradient of KCl from 0.05 M to 0.4 M or 0.1 M to 0.5 M, respectively. SDS-PAGE followed by silver staining and Western blot analysis of the fractions eluted from the Mono Q column identified fraction 25 as the peak CHD8 containing fraction (Figure 3.2B). In the final step of the conventional purification, the peak fraction from the Mono Q column was fractionated using a Superose 6 size exclusion

column equilibrated in 0.35 M KCl. Fractions were subjected to SDS-PAGE followed by silver staining and Western blot analysis. Fraction 24 was identified as the peak CHD8 containing fraction in this step of the conventional purification (Figure 3.2C). Unfortunately, the amount of purified product obtained from the conventional purification was insufficient for polypeptide identification by MS/MS analysis.

Given that we were unable to use a conventional purification to isolate the CHD8 complex, affinity purification was performed as an alternative approach. For this experiment, α -CHD8 antibodies were crosslinked to protein A agarose. As a control, normal rabbit IgG antibodies were also crosslinked to protein A agarose. HeLa nuclear extract partial purified by the P11 and DEAE chromatography steps described above was applied to each column (Figure 3.3). As outlined in Figure 3.3, the columns were washed several times under a variety of conditions. The glycine eluted samples were then subjected to SDS-PAGE followed by Western blot analysis using α -CHD8 antibodies. The peak CHD8 containing fraction identified by Western blot analysis was precipitated using TCA. This precipitated sample was subjected to SDS-PAGE followed by colloidal blue staining. This staining revealed multiple bands present in the fraction eluted from the α -CHD8 column and not from the control column (Figure 3.3). The predominant bands visualized by colloidal blue staining were subjected to trypsin digestion and MS/MS analysis. CHD8 was identified as the ~290 KDa protein eluted off the α -CHD8 column (Figure 3.3). MS/MS analysis also identified several proteins known to be involved in the modification of chromatin

structure (Table 3.2). These included multiple components of the Swi/Snf, NURD, CoREST, and WDR5/MLL chromatin remodeling and modifying complexes. Since the partial purification of CHD8 shown in Figure 3.1 suggested that the bulk of CHD8 is present in an ~900 KDa complex and the total molecular mass of the proteins identified by MS/MS is well over 900 kDa, our MS/MS suggests that there may be multiple CHD8 containing complexes. Additional experiments, such as repeating the conventional purification, need to be performed to explore this further.

CHD8 Forms a WDR5 Containing Complex

The affinity purification identified multiple proteins as possible components of a CHD8 complex. We therefore sought to confirm the association of each protein that was identified by MS/MS. Our first candidate for consideration was WDR5, as a previous study suggested a possible interaction. In an attempt to identify components of the MLL1 histone methyltransferase complex, Dou *et al.* performed an affinity purification of WDR5, a known MLL1 interacting protein (29). Surprisingly, over 25 different polypeptides were identified, one of which was CHD8. However, further characterization was not done to confirm this association, and therefore CHD8 may represent a contaminant in their purification. We did not identify MLL1 by MS/MS analysis of our CHD8 affinity purification and we also did not detect MLL by Western blot analysis (data not shown). As WDR5 was common to both of these affinity purifications, we speculated that CHD8 and WDR5 exist in a separate complex in the absence of MLL1.

The first step in verifying the association of CHD8 with WDR5 was to determine whether CHD8 and WDR5 interact *in vivo*. We performed experiments in HEK293 cells transfected with Flag-tagged WDR5 or the control Flag vector. Harvested cells were immunoprecipitated using α -Flag M2 agarose beads. After washing, Flag immunoprecipitations were subjected to SDS-PAGE followed by Western blot analysis with α -Flag and α -CHD8 antibodies (Figure 3.4). Western blot analysis using α -CHD8 antibodies indicated that CHD8 was present in the input samples prepared from cells transfected with either the control Flag vector or Flag-WDR5. However, when samples were immunoprecipitated with α -Flag agarose, CHD8 was only detected in samples obtained from cells transfected with Flag-WDR5 (Figure 3.4). Western blot analysis using α -Flag antibodies detected the presence of Flag-WDR5 only in cells transfected with the Flag-WDR5 vector and not the control vector (Figure 3.4). This experiment demonstrates that WDR5 interacts with CHD8 *in vivo* and provides evidence in support of our MS/MS analysis.

In order to determine whether the interaction between CHD8 and WDR5 is a direct interaction, *in vitro* GST pulldown experiments were performed. Recombinant CHD8 was incubated with GST or GST-WDR5 bound to glutathione-Sepharose beads. After multiple washes, samples were eluted and subjected to SDS-PAGE followed by Western blot analysis and Coomassie staining. Staining of the bottom portion of the SDS-PAGE gel indicated the presence of GST and GST-WDR5 in the appropriate samples (Figure 3.5). When the top portion of the gel was subjected to Western blot analysis with

α -CHD8 antibodies, recombinant CHD8 was detected when GST-WDR5 was present and not in the presence of the GST control (Figure 3.5). The results of this experiment demonstrate that CHD8 directly interacts with WDR5 and therefore further confirms the results obtained from our affinity purification.

In addition to being in a complex with MLL1, WDR5 has been reported to form a stable trimeric complex with two other components, RbBP5 and Ash2L (118). Both of these proteins were identified in our MS/MS analysis. Therefore, after confirming the interaction between WDR5 and CHD8, we wanted to verify the interaction between CHD8 and the other components of the WDR5 complex, RbBP5 and Ash2L. In order to confirm these interactions, we performed co-infection experiments in SF9 cells. We prepared recombinant baculoviruses designed to express Flag-CHD8, Ash2L, and RbBP5. SF9 cells were co-infected with Flag-CHD8 and either Ash2L or RbBP5. After harvesting, cell lysates were incubated with α -Flag M2 agarose beads. Flag immunoprecipitations (Flag-IPs) were then washed and subjected to SDS-PAGE followed by Western blot analysis with the indicated antibodies (Figure 3.6). In cells co-infected with Flag-CHD8 and RbBP5, Western blot analysis α -RbBP5 antibodies detected the presence of RbBP5 in both the input and Flag immunoprecipitated samples (Figure 3.6). In cells co-infected with Flag-CHD8 and Ash2L, Western blot analysis using α -Ash2L antibodies detected Ash2L in both the input and Flag immunoprecipitated samples (Figure 3.6). Western blot analysis using α -CHD8 antibodies detected CHD8 in all samples. Together, these results demonstrate

that CHD8 directly interacts with both RbBP5 and Ash2L and confirms the association as detected by our MS/MS analysis.

Above we demonstrate that CHD8 can directly interact with WDR5, RbBP5, and Ash2L. These three proteins not only form a stable trimeric complex, but also are the core of the MLL1 histone methyltransferase complex (28, 118). We therefore wanted to determine whether CHD8 can form a complex with all three proteins in the presence of MLL1. The presence of CHD8 in a MLL1-WDR5 complex would potentially link chromatin remodeling and modification in a single complex. Co-infection experiments were employed in order to examine this possibility. We prepared recombinant baculoviruses designed to express Flag-CHD8, Flag-WDR5, WDR5, Ash2L, RbBP5, and MLL-C. Each co-infection utilized various combinations of these baculoviruses. After harvesting, cell lysates were immunoprecipitated with α -Flag M2 agarose beads. Flag-IPs were washed and then subjected to SDS-PAGE and Western blot analysis with the indicated antibodies (Figure 3.7). In cells co-infected with Flag-WDR5, Ash2L, and RbBP5, Western blot analysis detected all three proteins in the α -Flag immunoprecipitated sample. In addition, cells co-infected with F-WDR5, Ash2L, RbBP5, and MLL-C, all four proteins were detected in the Flag-IP (Figure 3.7). These results are consistent with previously reported data demonstrating that Ash2L, WDR5, and RbBP5 can form a stable trimer in the absence of MLL-C and that when present, MLL-C can bind to this trimer (28). In cells co-infected with Flag-CHD8, Ash2L, WDR5, and RbBP5, Western blot analysis of the Flag immunoprecipitated lysates detected all four proteins

(Figure 3.7). These data suggest that, like MLL1, CHD8 can form a complex with the WDR5, Ash2L, and RbBP5 trimer. When this co-infection was performed in the presence of MLL-C, all five proteins, including MLL1, were detected in the Flag immunoprecipitation (Figure 3.7). This result indicates that while we were not able to detect MLL1 in our affinity purified material, MLL1 may interact with the CHD8/WDR5/Ash2L/RbBP5 complex.

While our data are compelling, the possibility does exist that the interactions we observed are not direct, but instead bridged through DNA. In order to examine this possibility, immunoprecipitations were performed in the presence of ethidium bromide or micrococcal nuclease. Both reagents would disrupt possible interactions bridged through DNA either by disrupting DNA-protein interactions (ethidium bromide) or by cleaving the DNA between sites of interaction (micrococcal nuclease). In these experiments, SF9 cells were co-infected with Flag-CHD8, WDR5, RbBP5, Ash2L, and MLL-C. After harvesting, the lysate was treated with 200 $\mu\text{g}/\text{ml}$ of ethidium bromide or left untreated for use in the micrococcal nuclease experiment. Both lysates were then incubated with α -Flag M2 agarose. After multiple washes were performed, the untreated sample was incubated with micrococcal nuclease and then subjected to additional washing. All immunoprecipitations were eluted and subjected to SDS-PAGE followed by Western blot analysis with the indicated antibodies (Figure 3.8). In samples treated with ethidium bromide, there was a decrease in Flag-CHD8 immunoprecipitated by the α -Flag agarose suggesting that the treatment affected the overall efficiency of the IP, however, it did not

disrupt the interaction between F-CHD8, MLL-C, RbBP5, WDR5, and Ash2L. No effect was seen upon treatment with micrococcal nuclease. The results of these experiments demonstrate that the interaction observed between these five proteins is direct and not bridge by DNA.

The results presented here clearly demonstrate the existence of a CHD8/WDR5/Ash2L/RbBP5 complex which may associate with MLL1. The MS/MS analysis identified numerous other CHD8 associated polypeptides suggesting that CHD8 exists in multiple complexes. We therefore wanted to determine if the CHD8/WDR5/Ash2L/RbBP5 complex is the major CHD8 containing complex in human cells. As size exclusion chromatography can often separate distinct complexes, we therefore subjected partially fractionated HeLa nuclear extract to Superose 6 size exclusion chromatography. Fractions obtained from the Superose 6 column were then subjected to SDS-PAGE followed by Western blot analysis with the indicated antibodies (Figure 3.9). In this analysis, all five proteins were detected in fraction 18. This experiment supports our observation that CHD8 forms a complex with RbBP5, WDR5, Ash2L and possibly MLL1. It is important to note that while fraction 18 was the peak of RbBP5, MLL1, WDR5, and Ash2L, it was not the peak CHD8 containing fraction. Fraction 24, not 18, was identified as the peak CHD8 containing fraction. Given that the bulk of CHD8 exists outside of this complex, this data supports the idea that CHD8 forms multiple complexes and that the CHD8/WDR5/Ash2L/RbBP5 complex is not the major CHD8 containing complex in HeLa cells.

WDR5 Alone Does Not Affect the Remodeling Activity of CHD8

As discussed in Chapter II, we used restriction enzyme accessibility assays to determine that CHD8 is an ATP-dependent chromatin remodeling enzyme. These assays are based on the fact that free DNA is vulnerable to cleavage by restriction endonucleases. When mononucleosomes are reconstituted through salt dialysis of core histones and DNA, restriction sites are less accessible to cleavage by restriction enzymes. However, when mononucleosomes are incubated with ATP-dependent chromatin remodeling enzymes in the presence of ATP, the DNA histone contacts can be disrupted resulting in increased accessibility of the DNA to restriction enzyme cleavage. After obtaining data demonstrating that CHD8 exists in a multi-subunit complex, we wanted to determine whether the identified proteins influence the remodeling activity of CHD8.

Restriction enzyme accessibility assays utilized the 601 nucleosome positioning sequence from pGEM3z-601 (71). Fluorescently labeled primers were used to PCR amplify a 277bp DNA fragment containing the 601 sequence. When reconstituted into nucleosomes, the 601 fragment contains an HhaI restriction site near the dyad axis. The fluorescently labeled 601 fragment was reconstituted into mononucleosomes by salt dialysis with core histones purified from HeLa cells. Restriction enzyme accessibility reactions were performed in triplicate. Each reaction contained reconstituted mononucleosomes, HhaI, and ATP in the presence or absence of recombinant CHD8. Reactions were also performed in the presence and absence of recombinant GST or GST-WDR5. As

before, when CHD8 is present we observe an increase in the fraction cut when compared to reactions without CHD8 (Figure 3.10, compare lanes 1 and 2). Since the WDR5 used in this experiment is fused to GST, we also prepared reactions in the presence of GST as a control. Addition of GST to reactions containing CHD8 did not affect the level of cutting observed (Figure 3.10, compare lanes 3 and 4 to lane 2). We also did not observe a significant change in the level of cutting when reactions were prepared in the presence of CHD8 and GST-WDR5 (Figure 3.10, compare lanes 5 and 6 to lanes 2-4). Therefore, we conclude that WDR5 alone does not affect the ATP-dependent chromatin remodeling activity of CHD8. However, as CHD8 not only interacts with WDR5, but with the WDR5/Ash2L/RbBP5 complex, a different result may be observed when other complex components are present. Future experiments will examine this possibility.

CHD8 Regulates Expression of Hox Genes

Previous studies have reported that WDR5 is recruited to Hox loci and regulates Hox gene expression (51, 135). The expression of these genes, which are involved in regulating patterns of development, is also reported to be regulated by MLL1 (81). Since our previous studies demonstrate that CHD8 directly interacts with WDR5 and suggests that CHD8 can form a complex with both WDR5 and MLL, we wanted to investigate the possibility that CHD8 also regulates Hox gene expression.

In order to examine a possible role for CHD8 in Hox gene expression, we performed experiments using NTERA2 cl. D1 (NT2/D1) cells. The NT2/D1 cell line is a human embryonal carcinoma cell line in which Hox genes can be induced upon the addition of all-trans retinoic acid (ATRA) (14, 51). We treated NT2/D1 cells with ATRA dissolved in DMSO or an equivalent volume of DMSO alone. Cells were grown for ~38 hours prior to harvesting for RNA isolation. Real time quantitative PCR was then performed using primers designed to amplify HoxA1, HoxA2, HoxA3, and HoxA4 (Table 3.1). We observed a greater than 500 fold increase in HoxA1 expression upon treatment with ATRA (Figure 3.11). We also observed an ~75 and 10 fold increase in expression of HoxA2 and HoxA3 respectively. These results demonstrate that this system is suitable for the study of HoxA gene expression.

We then performed RNAi experiments to examine the role that CHD8 plays in transcription of these Hox genes. NT2/D1 cells were transfected with shRNA vectors containing hairpin cassettes directed against CHD8 or luciferase as a control. These shRNA vectors also contained a puromycin resistance marker (21) which allows for transfected cells to be selected by treatment with puromycin 24 hours post transfection. Cells were treated with ATRA 25 hours later. Cells were harvested for RNA isolation and Western blot analysis ~38 hours post ATRA treatment. cDNA prepared from the isolated RNA was analyzed by real-time quantitative PCR using primers targeting the HoxA1, HoxA2, HoxA3, and HoxA4 genes (Figure 3.12). We observed that depletion of CHD8 results in an increase in expression of all four Hox genes. Interestingly,

the greatest effect was seen on HoxA4 expression, the gene with the lowest level of induction with ATRA. The effect due to the loss of CHD8 decreased as the level of induction by ATRA increased. The results of this experiment suggest that CHD8 negatively regulates the expression of the Hox genes studied here and indicate that the extent of negative regulation inversely correlates with the level of gene expression.

CHD8 is Recruited to the Hox Locus

After demonstrating that loss of CHD8 results in disruption of the normal Hox gene expression pattern, we wanted to determine if this regulation was direct by asking whether CHD8 associates with the promoters of these Hox genes. Chromatin immunoprecipitation (ChIP) experiments were performed to examine the *in vivo* binding of CHD8 to various genes of the HoxA locus. Given that our affinity purification was performed from HeLa nuclear extract, we first performed ChIP experiments in these cells. HeLa cells were treated with formaldehyde to crosslink the chromatin inside the cell. Lysates were sonicated and pre-cleared before incubation with α -CHD8 or α -control antibodies. Antibody-protein complexes were precipitated and washed before the crosslinking was reversed. Recovered DNA was amplified using primers designed to amplify locations within the promoter region of each HoxA gene (Figure 3.13). Reactions were analyzed using standard PCR techniques. CHD8 was present at the promoter region of multiple HoxA genes, particularly, the HoxA1, A7, A11, and A13 genes. This result demonstrates that CHD8 can indeed directly interact with various HoxA promoters, and suggests that the

changes in HoxA gene expression are due to CHD8 functioning at these promoters.

Our initial ChIP experiments in HeLa cells clearly demonstrate that CHD8 can directly bind to target HoxA promoters. Given that our Hox gene expression studies with CHD8 RNAi were performed in the inducible NT2/D1 cell line, it was important to determine whether CHD8 could also directly bind to Hox gene promoters in these cells. Therefore chromatin immunoprecipitation experiments were performed in the NT2/D1 cell line. For these ChIP experiments, NT2/D1 cells were first treated with ATRA dissolved in DMSO (induced) or an equivalent volume of DMSO alone (uninduced). Cells were grown ~38 hours before being treated with formaldehyde to crosslink the chromatin *in vivo*. α -CHD8 and α -Acetyl H4 (data not shown) antibodies were used in these ChIP experiments. Recovered DNA was amplified using primers designed to amplify locations within the promoter region of the HoxA1, A2, A3, and A4 genes (Figure 3.14). Reactions were analyzed using a real-time PCR detection system. In the uninduced state, CHD8 was bound to the HoxA1, A2, and A4 promoters, but we observed the highest percentage of CHD8 bound to the promoter region of the HoxA1 gene. Surprisingly, upon induction with ATRA, we observed a decrease in CHD8 at the HoxA1 promoter and an increase in CHD8 at the HoxA2 and HoxA4 promoters. This result shows that CHD8 clearly relocalizes upon treatment with ATRA, and that the sites of this relocalization are the promoters of genes most influenced by the activity of CHD8.

In the ChIP experiments performed with the α -Acetyl H4 antibodies (data not shown), low levels of histone H4 acetylation was detected at the HoxA1, A2, and A4 promoters prior to induction. We observed an increase in histone H4 acetylation at all three promoters when gene expression was induced with ATRA. Given that this acetyl mark is typically associated with active chromatin, this was the expected result. We did not, however, detect CHD8 or histone H4 acetylation at the HoxA3 promoter. We believe that this is due to a misidentification of the promoter region of the HoxA3 gene in several public databases. Additional experiments, such as 5'RACE, should be performed to correctly identify the promoter region of HoxA3. In total, the ChIP experiments in HeLa and NT2/D1 cells demonstrate that CHD8 does indeed bind to the promoter region of genes within the HoxA locus and suggests that CHD8 regulates the expression of these genes by binding and remodeling chromatin at these promoter regions.

Discussion

The eukaryotic genome is packaged inside the nucleus of cells in the form of chromatin. The fundamental unit of chromatin, the nucleosome, is composed of 146 base pairs of DNA wrapped around a histone octamer core. While the formation of chromatin aids the cell in packaging DNA inside the nucleus, it serves as a hindrance for cellular processes such as replication, transcription, and repair. Chromatin remodeling enzymes are crucial cellular components since they possess the ability to regulate the accessibility of this packaged DNA. Most ATP-dependent chromatin remodeling enzymes exist in multi-subunit complexes with other proteins that are involved in or required for the normal

function of the remodeler. Our previous work identified CHD8 as an ATP-dependent chromatin remodeling enzyme. In the studies presented here, we test the hypothesis that CHD8, like most other ATP-dependent chromatin remodeling enzymes, exists in a multi-subunit complex with proteins that play a role in the function of CHD8.

In order to estimate the size of the potential CHD8 complex, we performed P11, DEAE, and Superose 6 chromatography using HeLa nuclear extract as the starting material. The elution profile of CHD8 obtained from the Superose 6 size exclusion column is consistent with a CHD8 complex of ~900kDa. We then sought to identify the individual components of the CHD8 complex. Two different approaches were utilized, conventional and affinity purification. The conventional purification used a series of hydrophobic, ionic, affinity, and size exclusion columns to purify the CHD8 complex from HeLa nuclear extract. The affinity purification was performed using α -CHD8 antibodies crosslinked to protein A agarose to purify the CHD8 complex from a HeLa nuclear extract partially purified by P11/DEAE chromatography. Although the conventional purification did not yield a sufficient quantity of sample, the affinity purification was successful. MS/MS analysis of the affinity purified sample identified CHD8 and multiple factors known to be involved in altering chromatin structure. Among the factors identified were members of the MLL/WDR5, NURD, Swi/Snf, and CoREST chromatin modifying and remodeling complexes.

Following our MS/MS analysis of the affinity purified CHD8 associated proteins, we sought to verify the interaction between the associated proteins and

CHD8. Since CHD8 was previously reported to be a component of a MLL1/WDR5 methyltransferase complex purified from cells stably expressing Flag-WDR5 (29), we first focused our efforts on confirming the interaction between CHD8 and WDR5. The presence of CHD8 in a MLL/WDR5 containing complex is particularly interesting because it would potentially link chromatin remodeling and modification in a single complex. However, we did not detect MLL1 by MS/MS or Western blot analysis of our affinity purified sample. Also, the Dou *et al.* study (29) did not confirm the interaction between CHD8 and the MLL/WDR5 complex. Together, this information lead us to speculate that CHD8 exists in a WDR5 complex in which MLL is not present.

In order to confirm the CHD8/WDR5 interaction, we transfected 293 cells with Flag-WDR5 and immunoprecipitated the lysates with α -Flag agarose. CHD8 was detected in the Flag immunoprecipitated sample. The result of this experiment demonstrates that CHD8 and WDR5 interact *in vivo*. By performing GST pulldown assays with recombinant GST-WDR5 and CHD8, we confirmed this interaction *in vitro* and demonstrate that CHD8 directly interacts with WDR5.

After confirming the interaction between CHD8 and WDR5, we sought to confirm the association of CHD8 with other components of the MLL/WDR5 complex. In addition to WDR5, we identified RbBP5 and Ash2L, in our affinity purification. Both proteins are core components of the MLL/WDR5 methyltransferase complex. In an attempt to confirm these interactions, we performed co-infection experiments in SF9 cells using Flag-CHD8, Ash2L, and RbBP5. Western blot analysis of Flag immunoprecipitations performed using

lysates from the co-infected cells detected the presence of both Ash2L and RbBP5. This result confirmed the interaction between CHD8 and these two proteins.

After confirming the interaction between CHD8 and the individual core components of the MLL/WDR5 complex, we wanted to determine whether CHD8 could form a complex with RbBP5, Ash2L, and WDR5. We performed a series of co-infection experiments using SF9 cells and Flag-CHD8, Flag-WDR5, WDR5, Ash2L, RbBP5, and MLL-C. Full length MLL1 is insoluble when overexpressed, therefore the C-terminal portion of the protein is typically used. This C-terminal portion contains the catalytic Set domain (28). WDR5, RbBP5, and Ash2L are reported to form a stable trimer in the absence of MLL1. When present, MLL1 can bind this trimeric complex (28). The results of our co-infection experiments are consistent with previously reported data. When CHD8 and the components of the trimeric complex were used, RbBP5, Ash2L, WDR5, and CHD8 were detected in the Flag IP. Surprisingly, we also detected CHD8 in experiments performed using CHD8 and the members of the trimeric complex in the presence of MLL-C. Together, these data suggest that CHD8 can form a complex with the trimer, WDR5, Ash2L, and RbBP5, in the presence and absence of MLL-C. However, it is possible that in our immunoprecipitations CHD8 is interacting with each protein individually and not as a complex. We believe that this is unlikely. In addition to the data demonstrating that RbBP5, WDR5, and Ash2L form a stable trimer that can interact with MLL-C (28), recent reports demonstrate that WDR5 binds to arginine 3765 of MLL1. This arginine is located within the Win

(WDR5 interaction) motif of MLL1, a previously unidentified motif. WDR5 uses the same binding pocket thought to be the site of histone H3 binding to bind to MLL1 (91, 92, 115). Given the existence of the stable trimer and the interaction between WDR5 and MLL, we believe it is unlikely that CHD8 is interacting with each protein individually and not as a complex.

Additional studies of the CHD8/WDR5/RbBP5/Ash2L complex were performed to determine if the complex is bridged through DNA. Neither ethidium bromide nor micrococcal nuclease treatment disrupted the complex. The result of this experiment demonstrates that the complex is not bridged by DNA. The interactions are direct.

Proteins within a given complex or complexes of a comparable size should elute in the same fraction off a Superose 6 size exclusion column. To see if this is true for the CHD8 complex, we subjected the fractions eluted from our Superose 6 size exclusion column to Western blot analysis. CHD8, WDR5, RbBP5, Ash2L, and MLL were all detected in the same fraction. However, this fraction was not the peak CHD8 containing fraction. This data suggests that while CHD8 forms a complex with these proteins, multiple CHD8 complexes may exist. The identification of numerous CHD8 associated proteins by MS/MS analysis of our affinity purified sample supports this data.

Other groups have reported that WDR5 is recruited to Hox loci and regulates Hox gene expression (51, 135). Since CHD8 exists in a WDR5 containing complex, we wanted to examine whether the same is true for CHD8.

In RNAi experiments targeting CHD8 in NT2/D1 cells, we observed that knockdown of CHD8 results in increased expression of the HoxA1-HoxA4 genes. CHD8 appears to negatively regulate expression of these genes. To determine whether this regulation is possibly due to the presence of CHD8 at the promoter region of HoxA genes, chromatin immunoprecipitation experiments were performed. Our results indicate that CHD8 is bound to the promoter region of multiple HoxA genes in both HeLa and NT2/D1 cells. In humans four Hox gene clusters exist, HoxA, HoxB, HoxC, and HoxD. Among these four gene clusters, the HoxA and HoxD clusters are reported to have the most significant affect on limb development. Deletion of genes within the HoxA or HoxD clusters results in abnormal limb development. However, abnormal development is not observed when genes within the HoxB or HoxC clusters are deleted (140). Through the regulation of HoxA genes, CHD8 may play a role in limb development.

TABLE 3.1: Oligonucleotide sequences.

Name	Sequence (5'→ 3')
601 forward	CGGGATCCTAATGACCAAGGAAAGCA
601 reverse	CTCGGAACACTATCCGACTGGCA
CHD8 shRNA 493 top	GCTGTTAAGGATAACAATCTTAGGGGTTTTGGC CTCTGACTGACTCCTAGAAGTTATCCTAAC
CHD8 shRNA 493 bottom	TCCTGTTAAGGATAACTTCTAGGAGTCAGTCAG AGGCCAAAACCCCTAAGATTGTTATCCTTAA
CHD8 shRNA 6410 top	GCTGTTGTTCTCCATCTTCATTTGGGTTTTGGC CTCTGACTGACTCAAAGAGATGGAGAACAAC
CHD8 shRNA 6410 bottom	TCCTGTTGTTCTCCATCTCTTTGAGTCAGTCAG AGGCCAAAACCCAAATGAAGATGGAGAACAA
H1 RT forward	ACTCCACTCCCATGTCCCTTG
H1 RT reverse	CCGTTCTCTGGGAACCTCACCT
hoxa1rt6F	TTC AAC AAG TAC CTG ACG CGC
hoxa1rt6R	TTCATTCGGCGGTTCTGGA
hoxa2rt1F	AAGTACCTTTGCAGACCCCGA
hoxa2rt1R	TTGTGCTTCATCCTCCGGTTC
hoxa3rt1F	GATGGCCAATCTGCTGAACCT
hoxa3rt1R	TTAGCATGCCCTTGCCCTTCT
HOXA4rtfor	GCTCTGTTTGTCTGAGCGCC
HOXA4rtrev	AATTGGAGGATCGCATCTTGG
HOX4.ChIP -431F	GGATCTGCGGTTGAGAAAATG
HOX4.ChIP -531R	AGGCTAACAGGCGAAAGGAAG
HOX3-3.ChIP -411F	TGCACACTAGCCCCAGAATATT
HOX3-3.ChIP -520R	CAGAGGCAGGTGAGCACTTACT
HOX2.ChIP -443R	AAGATTTTGGTTGGGAAGGG
HOX2.ChIP -343F	CAGACCGAGAGAGATCAGTTTTGA
hoxa1-ChIPc-rev-811	GCCCCCTCCAAGTCGAATTACA
hoxa1-ChIPc-for-722	TTCCAGGAGGGTCTTCGAAAC
hoxa1 ChIPa-for-166	GTCACCTAGACGGCGGAGC

hoxa1 ChIPa-rev-74	GCTGAGCCTCCTGCAAAAGTT
hoxa1 ChIPb-for-175	CGACTGCGCGTCACCTAGA
hoxa1 ChIPb-rev-62	TGTCAGCCAATGGCTGAGC
hoxa3 ChIPa-for-391	CCCCAAACCTGAGAGAGGC
hoxa3 ChIPa-rev-303	CCTCCATGTGAACTTTTCCAGC
hoxa3 ChIPb-for-209	TATTGCCTTTCTGATTTGGACAAC
hoxa3 ChIPb-rev-121	CCTGCAGAGGAACAGAAGGG
hoxa5 ChIPa-for-440	ACCTCCCCCAATCCTCTG
hoxa5 ChIPa-rev-351	TCCCTCGCAGTTCCATTAGG
hoxa5 ChIPb-for-177	CCTCCACCCAACCTCCCCTAT
hoxa5 ChIPb-rev-81	ACGACTTCGAATCACGTGCTT
hoxa7 ChIPa-for-474	AGTCTAAGTCCGGCCTGTCCG
hoxa7 ChIPa-rev-386	CTTGTGGGCAGGACTCAGCT
hoxa7 ChIPb-for-121	GATTCTTTGGCCGCATATTTG
hoxa7 ChIPb-rev-33	CAGCAGTCCTCACAGGTGGTC
hoxa9 ChIPa-for-200	TAGAGCGGCACGATCCCTT
hoxa9 ChIPa-rev-112	CCGCACGCTATTAATGGTCC
hoxa9 ChIPb-for-344	GCCTTCTTGATGGCGTGATT
hoxa9 ChIPb-rev-256	TGTCTCTGTACTCTCCCGTCTCC
hoxa11 ChIPa-for-261	AGTTACACCGGCGATTACGTG
hoxa11 ChIPa-rev-173	CCGGCTTCCTTTCTTTGTAGC
hoxa11 ChIPb-for-130	GGAAAAGGCCCGGACTAGC
hoxa11 ChIPb-rev-35	TGACGTGGAAATCTATCCCCA
hoxa13 ChIPa-for-476	TTCTGAGCTAGGCTGGTCCC
hoxa13 ChIPa-rev-386	TTGCGATCTGGAGCAGTGG
hoxa13 ChIPb-for-399	GCTCCAGATCGCAACCCA
hoxa13 ChIPb-rev-311	CCTTCCCTTCCTTTATCCCAGT

TABLE 3.2: MS/MS identified sequences.

Known Complex	Protein
SWI/SNF	BAF47 BAF53 BAF60a BAF60b BAF155 BAF170 BAF250 BAF270
NURD	HDAC1 HDAC2 MBD2 MBD3 MTA2 MTA3 p66 RbAP48
WDR5/MLL	ASH2L HCFC1 Rbbp5 WDR5
CoREST	CoREST HDAC1 HDAC2
Splicing/Processing	CPSF1 CPSF5 Puf60 SF3A1 SF3B1,2,3 Symplekin U2AF116 U2AF65 U5snRNP40 U5snRNP200 U5snRNP220
Other	HSP70 MED27 WDC146 YY1 ZO-1

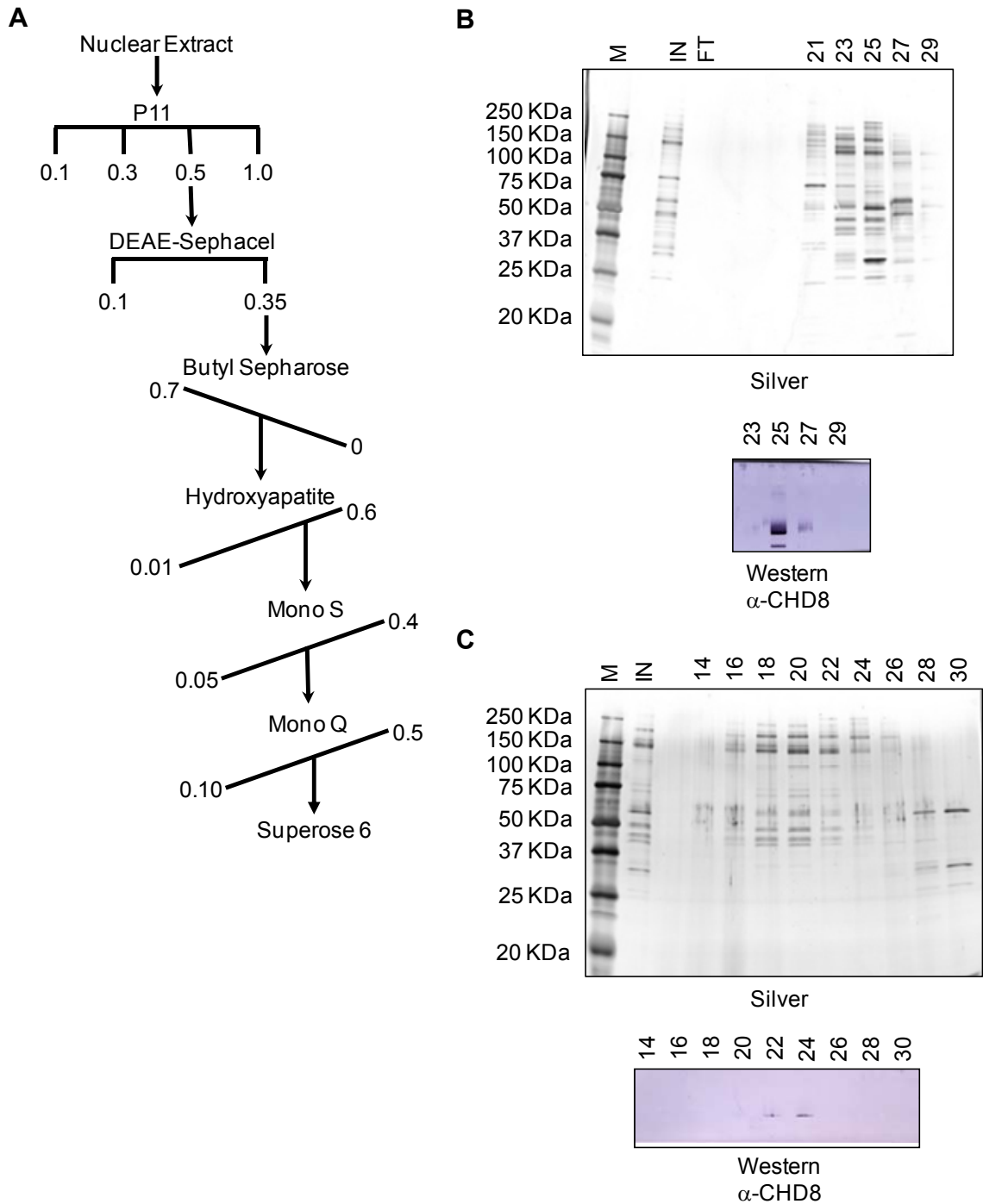


Figure 3.2: Conventional purification of CHD8. (A) Purification scheme. HeLa nuclear extract was fractionated by chromatography as described in Methods. The horizontal and diagonal lines indicate stepwise and gradient elution, respectively. Concentrations are given in molar. (B) Silver stain and Western blotting analysis. Select fractions from the MonoQ column were subjected to SDS-PAGE followed by Silver staining (Top) or Western blotting analysis using α -CHD8 antibodies (Bottom). The arrow indicates the peak CHD8 fraction that was further resolved on a Superose 6 column. (C) Silver stain and Western blotting analysis. Select fractions from the Superose 6 column were subjected to SDS-PAGE followed by Silver staining (Top) or Western blotting analysis using α -CHD8 antibodies (Bottom).

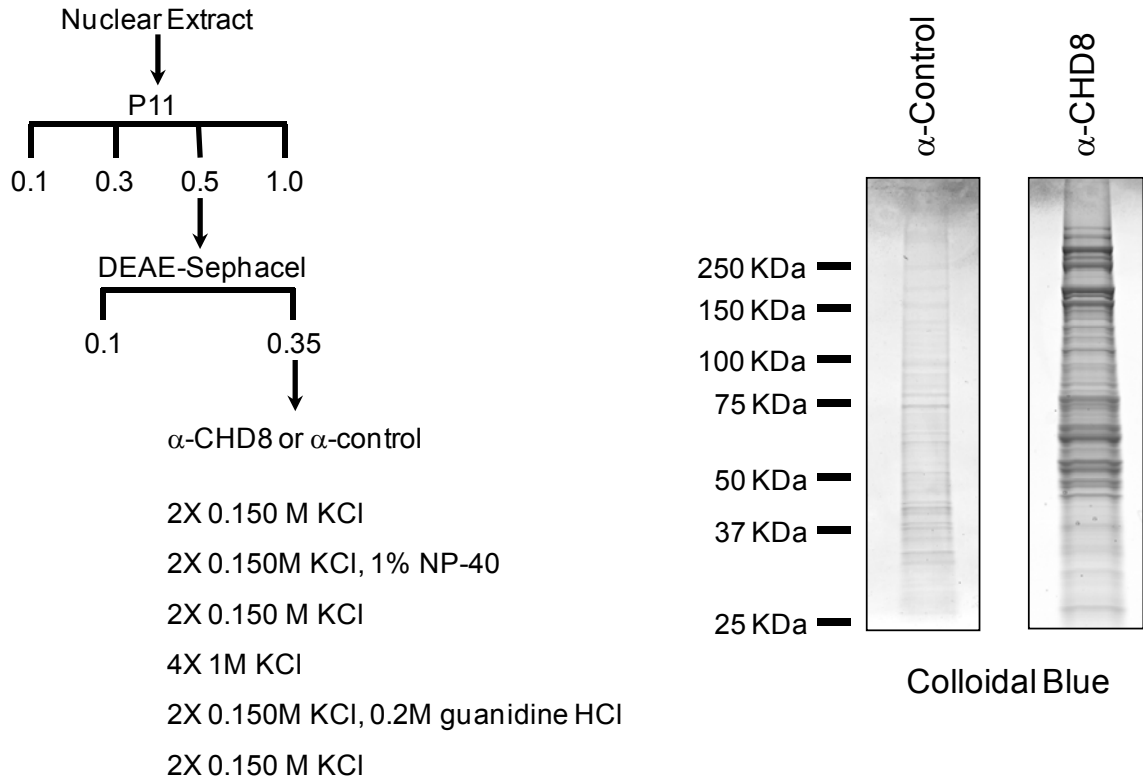


Figure 3.3: Affinity purification of CHD8. (A) Purification scheme. HeLa nuclear extract was fractionated by chromatography as described in Methods. The horizontal and diagonal lines indicate stepwise and gradient elution, respectively. Concentrations are given in molar. Also listed are the wash steps applied to the affinity columns. (B) Silver stain analysis. TCA precipitated material from the α -CHD8 or protein A purified normal rabbit IgG affinity columns were subjected to SDS-PAGE followed by Colloidal Blue staining. The arrow indicates the polypeptide identified as CHD8 by MS/MS analysis.

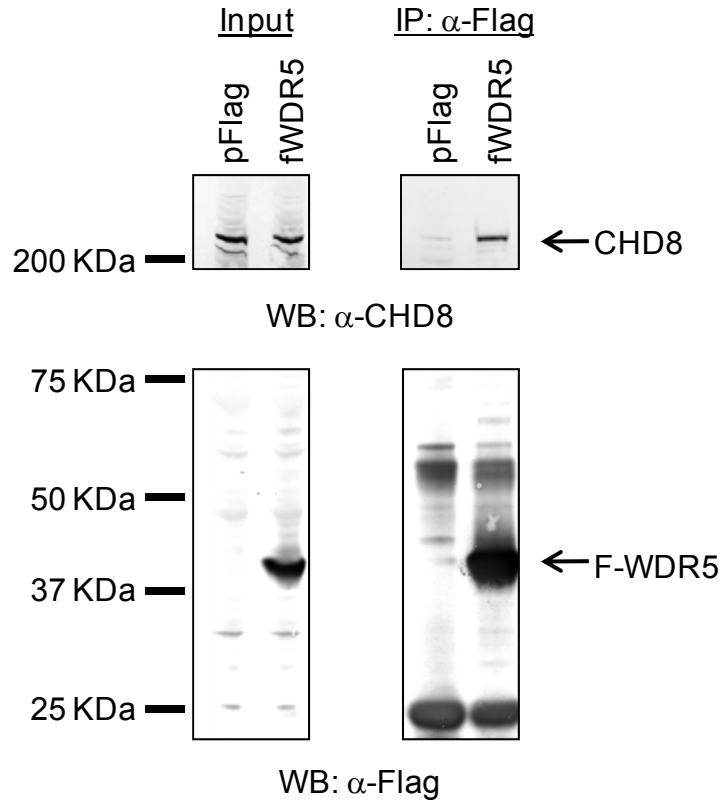


Figure 3.4: CHD8 interacts with WDR5 *in vivo*. 293 cells were transfected with Flag-WDR5 or the control vector. Immunoprecipitations (IP) were performed with anti-Flag M2 antibodies. After washing, purified samples were subjected to SDS-PAGE followed by Western blot analysis using the indicated antibodies.

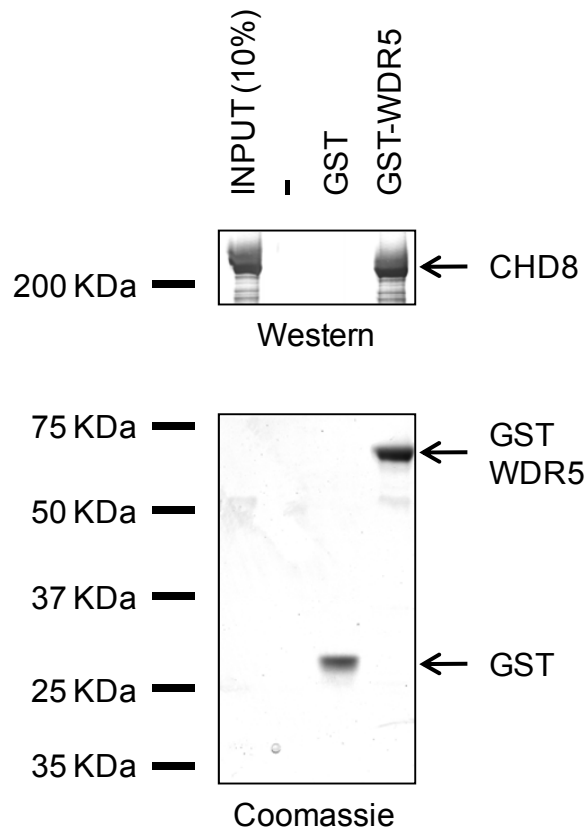


Figure 3.5: CHD8 interacts with WDR5 *in vitro*. Recombinant CHD8 was incubated with recombinant GST or GST-WDR5 as indicated at the top of the figure. After washing, glutathione-agarose-purified samples were subjected to SDS-PAGE. The top of the gel was subjected to Western blot analysis using α -CHD8 antibodies. The bottom of the gel was analyzed by Coomassie staining.

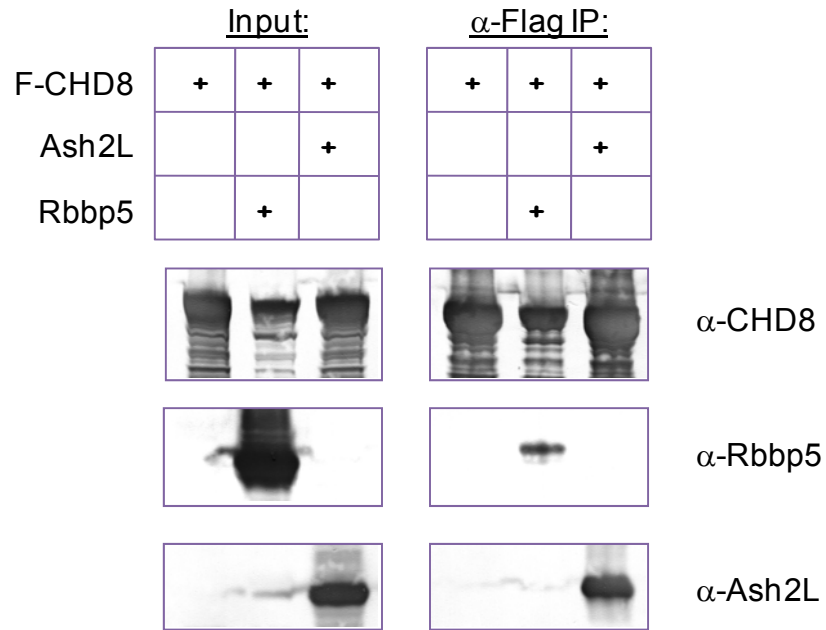


Figure 3.6: CHD8 directly interacts with RbBP5 and Ash2L. Cellular extracts were prepared from SF9 cells following co-infection with the indicated viruses. Immunoprecipitations were performed with anti-Flag-M2 antibodies. After washing, purified samples were subjected to SDS-PAGE followed by Western blotting analysis using the antibodies indicated to the right of the figure.

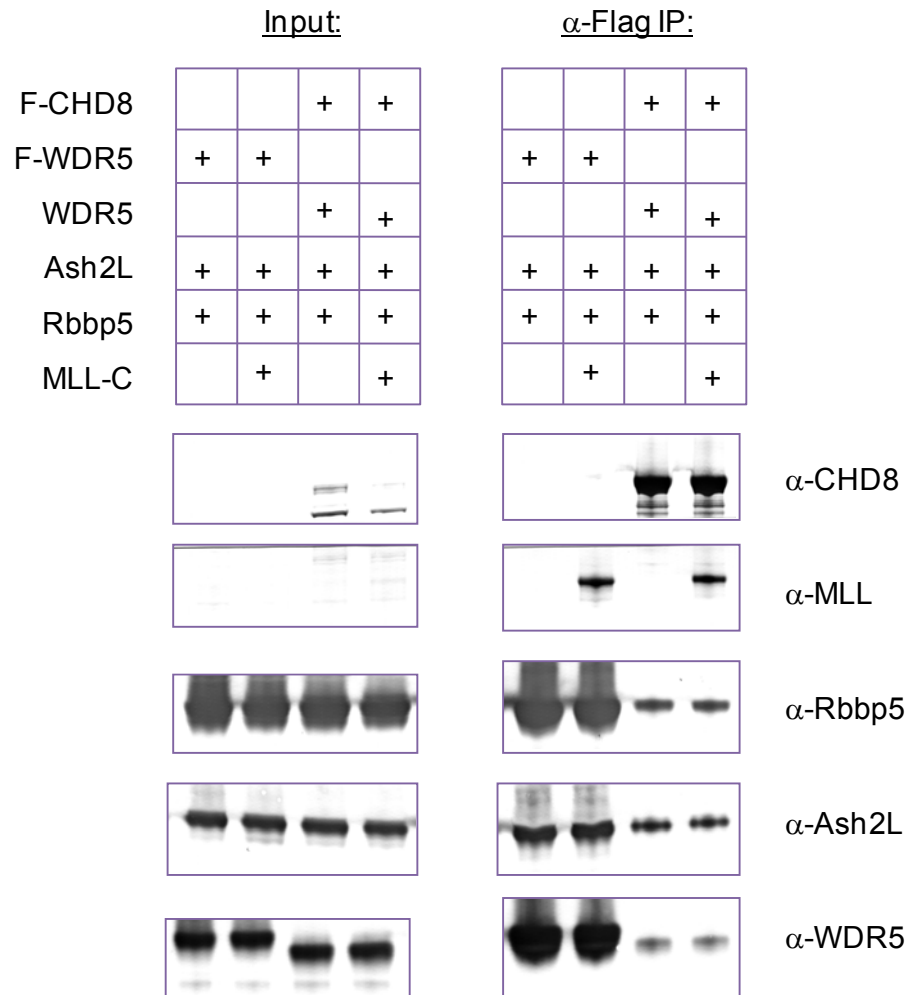


Figure 3.7: CHD8 directly interacts with the core WDR5/RbBP5/Ash2L complex. Cellular extracts were prepared from SF9 cells following co-infection with the indicated viruses. Immunoprecipitations were performed with anti-Flag-M2 antibodies. After washing, purified samples were subjected to SDS-PAGE followed by Western blotting analysis using the antibodies indicated to the right of the figure.

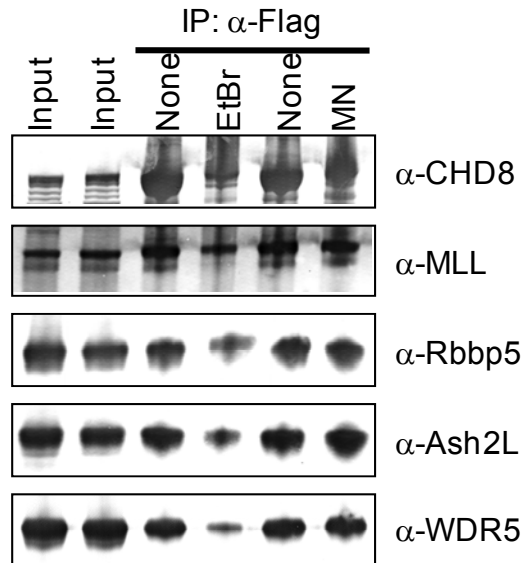


Figure 3.8: DNA does not mediate the interaction of CHD8 with the WDR5/RbBP5/Ash2L complex. Cellular extracts were prepared from SF9 cells following co-infection with CHD8, WDR5, RbBP5, Ash2L, and MLL-C viruses. Immunoprecipitations were performed with anti-Flag-M2 antibodies. After treatment with nothing (N), ethidium bromide (Eth), or micrococcal nuclease (MN) samples were washed. Purified samples were subjected to SDS-PAGE followed by Western blotting analysis using the antibodies indicated to the right of the figure.

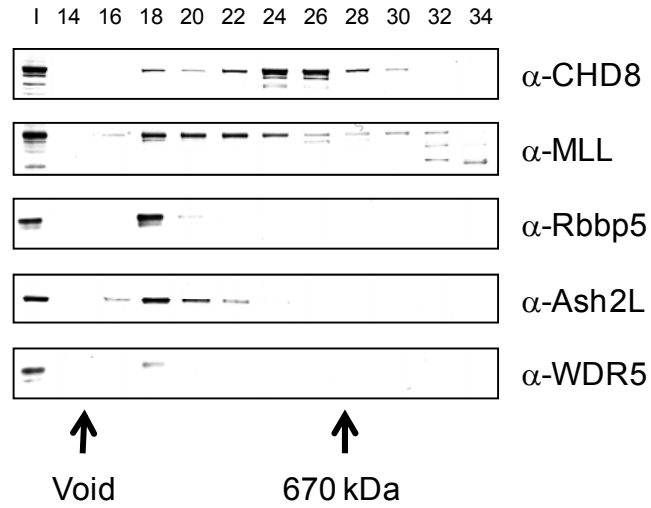


Figure 3.9: CHD8, WDR5, RbBP5, Ash2L, and MLL1 elute in the same fraction off a Superose 6 column. HeLa nuclear extract was fractionated by phosphocellulose (P11) chromatography utilizing stepwise elution with the 0.5 M KCl. The 0.5 M P11 fraction was further fractionated by DEAE-Sephacel chromatography and eluted stepwise with 0.35 M KCl. Samples were further resolved by chromatography on a Superose 6 HR 10/30 column. Western blotting was performed using antibodies indicated to the right of the figure. Arrows (bottom) indicate the elution position of thyroglobulin (670 kDa) and the void volume of the column (2 MDa).

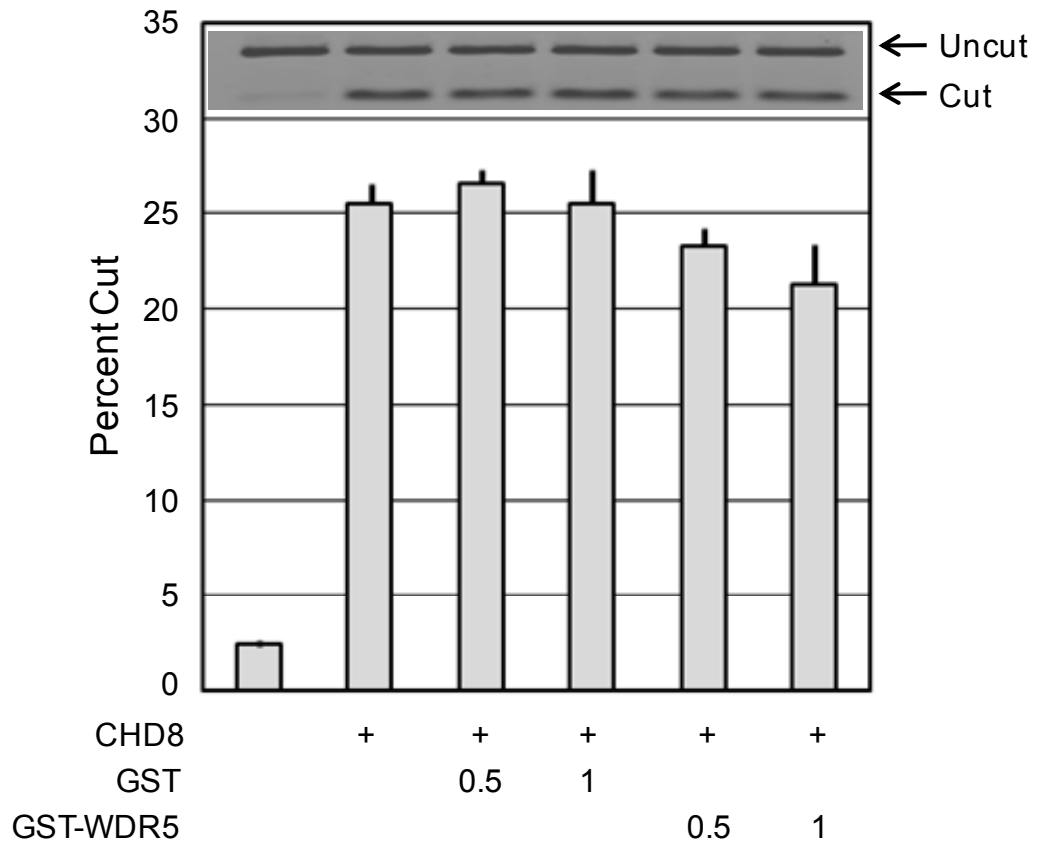


Figure 3.10: The remodeling activity of CHD8 is not stimulated by WDR5. Recombinant CHD8 was assayed for increased restriction enzyme accessibility on mononucleosomes. Reactions were performed with no additions, or with indicated concentrations of GST or GST-WDR5. Representative data is shown in the inset. The top band is the uncut template, and the bottom band is the resulting cut fragment.

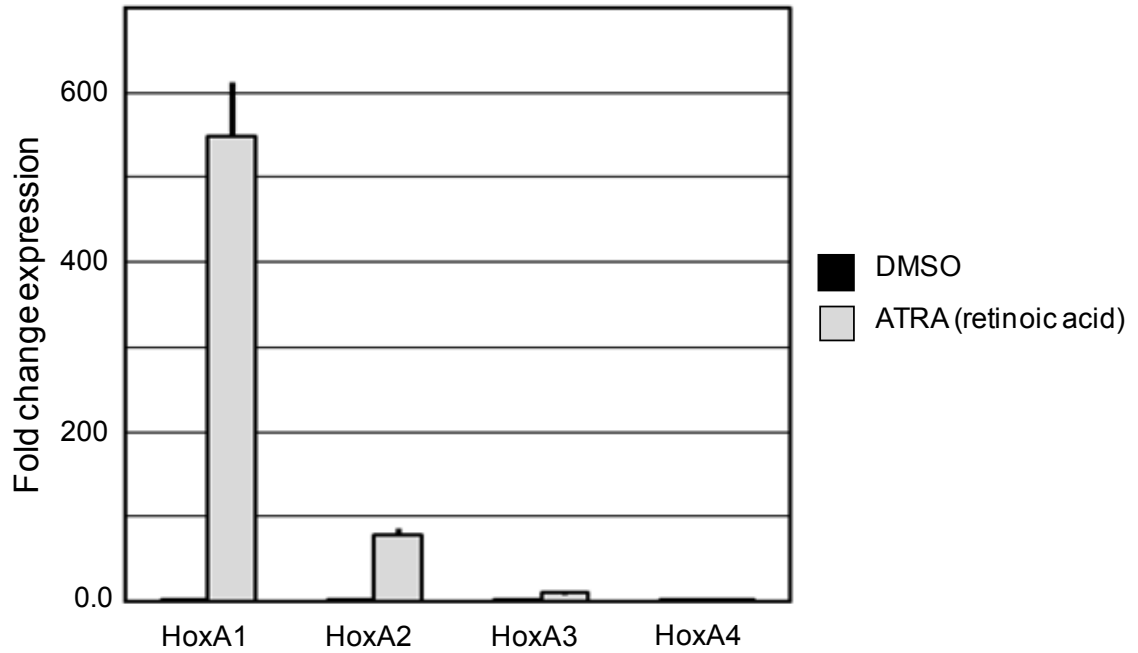


Figure 3.11: ATRA induces HoxA gene expression in NT2/D1 cells. Following treatment of NT2/D1 cells with ATRA or the DMSO vehicle, total RNA was harvested, and expression of the indicated genes was analyzed by real-time RT-PCR. For each treatment, threshold cycle values were normalized to the levels of polymerase III (Pol III)-transcribed H1 RNA. . Shown is the fold change relative to treatment with DMSO.

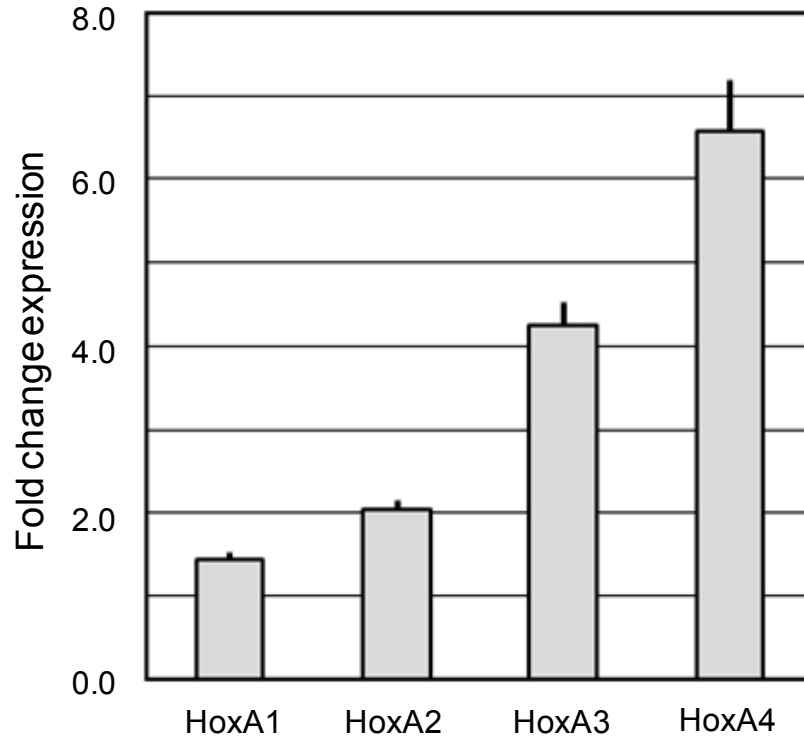


Figure 3.12: CHD8 regulates HoxA gene expression in NT2/D1 cells. NT2/D1 cells were transfected with a control shRNA or a CHD8 shRNA. Following selection of the transfected cells with puromycin, cells were treated with ATRA. Total RNA was then harvested and expression of the indicated genes was analyzed by real-time RT-PCR. For each treatment, threshold cycle values were normalized to the levels of polymerase III (Pol III)-transcribed H1 RNA. Shown is the fold change relative to the control shRNA treatment.

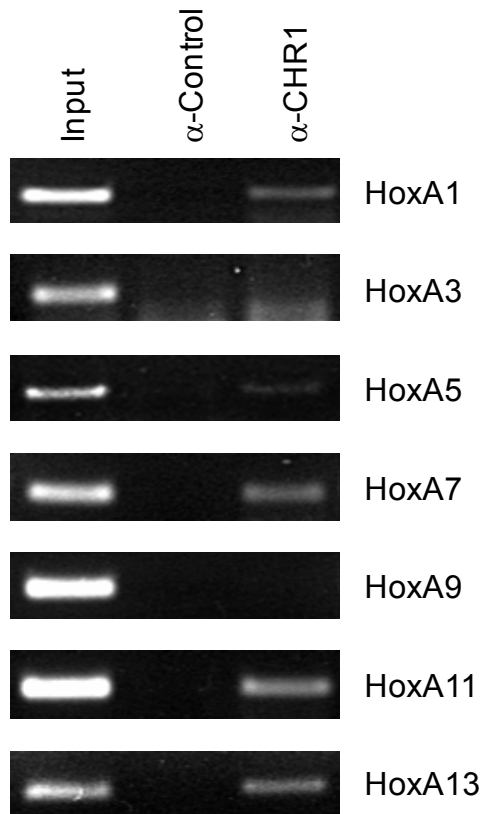


Figure 3.13: CHD8 is bound to the HoxA gene cluster in HeLa cells. Chromatin from HeLa cells was cross linked *in vivo* with formaldehyde. Cells were lysed, and chromatin immunoprecipitations were performed with α -CHD8 or protein A purified normal rabbit IgG. Immunoprecipitates were extensively washed and the cross linking was reversed. Bound DNA was detected by standard PCR using primers to the promoters of the indicated genes.

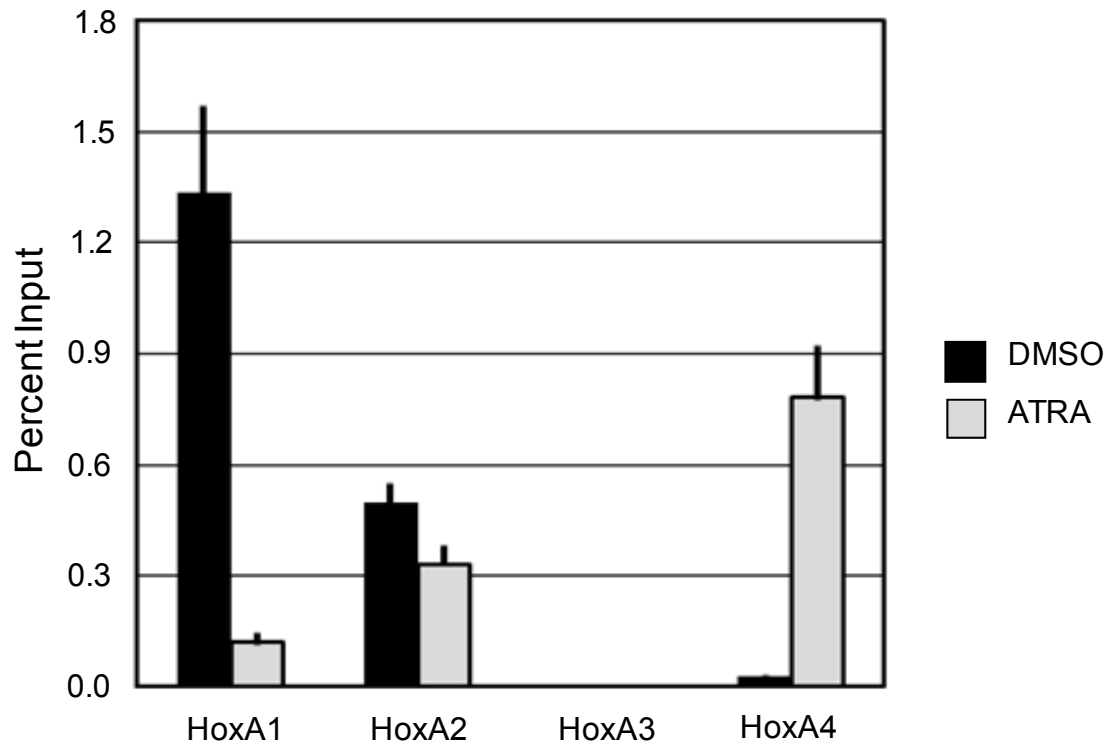


Figure 3.14: CHD8 is bound to the HoxA gene cluster in NT2/D1 cells. Chromatin from the NT2/D1 embryonal carcinoma cell line was cross linked *in vivo* with formaldehyde. Cells were lysed, and chromatin immunoprecipitations were performed with the indicated antibody. Immunoprecipitates were extensively washed and the cross linking was reversed. Bound DNA was detected by quantitative PCR with primer pairs to the promoter region of the gene indicated below. Control IgG precipitated samples in all experiments were less than 0.001% of input and therefore are not shown.

Chapter IV

The Double Chromodomains of CHD8 Recognize Both Modified and Unmodified H3/H4 Histones

Introduction

CHD8 Domain Structure

CHD8, a member of the CHD6-9 subfamily of CHD proteins, possesses multiple domains that are conserved within this subfamily of proteins (Figure 1.2). Within the N-terminal portion of the protein, there are double chromodomains (chromatin organization modifiers). A chromodomain is an ~50 amino acid sequence found in many proteins known to be involved in chromatin regulation (45, 77). Chromodomains have been shown to mediate chromatin interactions by targeting DNA, histones, and RNA (18, 77). The presence of the double chromodomains is a unique characteristic of all CHD proteins. Carboxy-terminal to the tandem chromodomains is the Snf2 helicase domain. This domain is also present in all CHD proteins. The Snf2 helicase domain received this name based on its similarity to the catalytic subunit (Snf2) of the Swi/Snf complex (45).

This domain is responsible for the binding and hydrolysis of ATP thereby providing the energy necessary to remodel nucleosomes. In the CHD6-9 subfamily, carboxy-terminal to the Snf2 helicase domain are two additional domains commonly found in other chromatin remodeling enzymes, the SANT and BRK domains. However, in the context of the CHD6-9 proteins, the function of these domains is unknown.

Chromodomain Function

The chromodomain (chromatin organization modifier) was first recognized as a sequence shared by the *Drosophila* proteins, HP1 and Polycomb, which are known to be involved in regulating chromatin structure (90). Early studies implicated chromodomains in heterochromatin formation, nucleosome binding, and the regulation of homeotic genes (45). Since their initial characterization, chromodomains have been identified in multiple organisms from protists to mammals (45). Some of the known chromodomain functions now include remodeling of chromatin structure (77), modified histone tail binding, RNA binding, targeting of complexes, and targeting to chromatin (18) Mutation studies performed in mouse and *Drosophila* lend additional information on the function of chromodomains present in the CHD proteins. In mouse, CHD1 chromodomain mutations result in nuclear redistribution. Deletion of the *Drosophila* CHD3/4 chromodomains results in weakened mobilization, nucleosome binding, and ATPase function (77). The chromodomains of these proteins are unique in that they exist in tandem.

Tandem Chromodomains

Proteins that contain chromodomains can be divided into three categories. The first category is composed of proteins that possess an N-terminal chromodomain followed by a chromo shadow domain. Examples of proteins within this category are Drosophila and Human HP1 (70). The second category is composed of proteins which possess a single chromodomain. Mammalian modifier 3 (70) and Drosophila Polycomb (90) belong to this category of chromodomain containing proteins. The third category is composed of proteins that possess double chromodomains. CHD proteins are the only known members of this category of chromodomain containing proteins (45, 77). While additional studies are needed to determine the significance of tandem chromodomains, recent studies of CHD1 suggest a possible function. The double chromodomains of CHD1 are reported to cooperate and form a recognition site for histone binding (38, 45).

CHD1 Chromodomains Bind Histones

Human CHD1, like the other CHD proteins, possesses tandem chromodomains N-terminal to a Snf2 helicase domain (45, 77). In an attempt to determine the function of the tandem chromodomains of human CHD1, Flanagan *et al.* performed fluorescence polarization assays using synthetic histone tail peptides to determine the chromodomains affinity for binding to various modifications. They determined that CHD1 preferentially binds to tri and monomethylated lysine 4 of histone H3 and not other modifications or unmodified

histones. Methylation of this lysine is typically associated with active chromatin. Additional studies demonstrated that the binding occurs through two aromatic residues within the tandem chromodomains. They also report that both chromodomains are required for binding. The two chromodomains cooperate to bind a single methylated histone tail (38). These studies provide insight into the function of double chromodomains and suggest that other CHD proteins may also bind histones in this fashion.

Hypothesis and Summary of Results

As previously stated, the chromodomains of CHD1 were found to bind a methylated lysine on the histone H3 tail (38). We hypothesized that the chromodomains of CHD8, like those of CHD1, also bind to a methylated lysine in histones. Here we demonstrate that the chromodomains of CHD8 bind purified HeLa core histones, with a high affinity for binding histones H3/H4. CHD8 chromodomains do not appear to have a preference for binding to a specific modification on histone H3 tails as they are able to bind histones containing H3 modified at lysines 4, 9, and 27. We demonstrate that CHD8 chromodomains also possess the ability to bind unmodified recombinant histone H3-H4 tetramers. Mutation of specific aromatic residues, which align with CHD1 chromodomain residues required for histone binding, does not disrupt CHD8 binding to histones. Pulldown experiments performed with histone H3 tails demonstrate that the chromodomains of CHD8 are unable to bind to the tail of histone H3. We also show that the chromodomains of CHD8 can bind to histone H3-H4 tetramers in which the tails are deleted. We demonstrate that the CHD8 chromodomains do

not bind to histone H3 directly through lysine 36 or 79. Together, these data support our hypothesis that the chromodomains of CHD8 bind histones, but also demonstrate that the CHD8 chromodomains do not bind to histone H3 or H4 tails, but bind to the histone core.

Materials and Methods

Purification of HeLa Core Histones

HeLa nuclear extracts were prepared from cells purchased from the National Cell Culture Center (Minneapolis, MN). Nuclear pellets were prepared using methods described by Dignam et al (27). Nuclear pellets isolated from HeLa cells were homogenized by douncing in a chilled buffer containing 20 mM Tris (pH 7.9), 25% glycerol, 0.42M NaCl, 1.5 mM MgCl₂, 0.2 mM EDTA, 0.5 mM PMSF, and 0.5 mM DTT. Purification of core histones was performed using hydroxyapatite chromatography methods described by Côté *et al.* (23) with minor changes. HAP buffer (50 mM NaPO₄ [pH 6.8], 1 mM BME, 0.5 mM PMSF) was prepared and chilled to 4°C. The DNA content of the homogenized nuclear pellet was estimated by diluting 1000 fold in 2 M NaCl in order to measure the OD₂₆₀ of the pellet. Approximately a 42 mg DNA equivalent of the homogenized pellet was added to 75 ml of HAP buffer with 0.6 M NaCl. This mixture was stirred gently at 4°C for 10 minutes. While stirring, 35 g of Hydroxyapatite Bio Gel HTP (BioRad) was added to the mixture. Additional HAP buffer containing 0.6 M NaCl was added to allow the mixture to be poured into a column. The column was washed overnight at 4°C with HAP buffer containing 0.6 M NaCl at a flow rate of

~1ml/min. Core histones were eluted with HAP buffer containing 2.5 M NaCl.

The peak fractions were identified by Bradford analysis. The peak fractions were pooled and concentrated using a Centriprep YM-10 concentrator (Amicon).

Production of Recombinant Proteins

The GST-Chromos expression construct was prepared by PCR amplifying the chromodomains of CHD8 using the following primers: CGG GAT CCG AGT GAA GAA GAT GCA GCC, CGG GAT CCT TAT GGG TGC CTT GAC TGA ATC CG. This PCR fragment was then cloned into a GST-expression vector, pGST-Parallel2 (107). The GST-Chromos mutant constructs were prepared using primers which introduced a tyrosine (Y) to leucine (L) mutation of one or two residues within the chromodomains of CHD8. The GST-Chromos (single) mutant was produced by PCR using CHD8 Y676L (AGA AGA ATT CTT TGT CAA GTA CAA GAA CTT AAG CTA TCT GCA TTG) and pGEX3p (CCG GGA GCT GCA TGT GTC AGA GG) with GST-Chromos as a template. The GST-Chromos (double) mutant was produced by PCR using CHD8 Y673L Y676L (AGA AGA ATT CTT TGT CAA GCT TAA GAA CTT AAG CTA TCT GCA TTG) and pGEX3p (CCG GGA GCT GCA TGT GTC AGA GG) with GST-Chromos as a template. The mutant PCR products were then digested with restriction enzymes and cloned into the wild type GST-Chromos vector.

Escherichia coli BL21 cells were used to express GST and GST-Chromos fusion proteins. After harvesting, cells were resuspended in buffer BC150 (150 mM KCl, 0.2 mM EDTA, 10 mM BME, 10% glycerol, 0.2 mM PMSF, 20 mM

Tris-HCl [pH 7.9]). Resuspended cells were lysed by passage twice through a French Pressure Cell, and lysates were centrifuged at 105,000 X g for 60 minutes at 4°C before collecting the supernatants. Samples were then subjected to sodium dodecyl sulfate-polyacrylamide gel electrophoresis (SDS-PAGE). The SDS-PAGE gels were Coomassie stained and used to determine the concentration of GST and GST fusion proteins in each cell lysate. GST-WDR5 was received as a kind gift from R.C. Trievel (24).

The pET-histone expression plasmids used to express recombinant histones H3 and H4 (tailed and tailless) were received as a kind gift from K. Luger (72, 73). Recombinant histone proteins were expressed, purified, and refolded using methods described by Luger *et al.* (73). The histone H3 C110A, K36C, and K79C mutant constructs mutant were a kind gift from M. Simon (112). K36C and K79C mutant constructs also contained the C110A mutation. These recombinant mutant histones were expressed, purified, and refolded into tetramers with recombinant histone H4 using methods described by Luger *et al.* (73). In the production of fluorescently labeled K36C and K79C histones, fluorescein-5-maleimide was used to label the recombinant mutant histone H3 proteins according to instructions supplied by the manufacturer (Thermo Scientific). After labeling, the mutant histone H3 proteins were refolded with recombinant histone H4 to form tetramers and purified using the Luger *et al.* protocol (73). The vector for the production of the H3 histone tail and the K4C, K9C, K27C, and K36C the H3 histone tail mutants were a kind gift from R.C. Trievel. These construct were prepared by cloning the H3 tail (1-40) or tail

mutants into the Champion pET SUMO Expression System, and were expressed and purified as recommended by the manufacturer (Invitrogen).

GST Pulldown Assays

BC150 plus 0.2% NP40 and BC350 (350 mM KCl, 0.2 mM EDTA, 10 mM BME, 10% glycerol, 0.2 mM PMSF, 20 mM Tris-HCl [pH 7.9]) were prepared and chilled to 4°C. Glutathione agarose beads (Sigma) were washed one time with cold PBS and one time with cold BC150 plus 0.2% NP40 prior to use in the assays. Beads were resuspended in BC150 plus 0.2% NP40 to produce a 50% slurry before dividing into 40 µl aliquots. Extracts that contained equal concentrations of GST, GST-Chromo (wt or mutant), or GST-WDR5 were added to each tube of beads. BC150 plus 0.2% NP40 was added to bring volumes up to 500 µl before rotating overnight at 4°C. After the overnight incubation, glutathione agarose beads were centrifuged at 1,000 X *g* for 2 minutes at 4°C. Beads were washed twice by rotating for 10 minutes per wash with 1ml of BC150 plus 0.2% NP40. After washing, 14 µg of the indicated histones were added to beads resuspended in total volume of 500 µl of BC150 plus 0.2% NP40. Pulldowns were then rotated overnight at 4°C. Samples were centrifuged at 1,000 X *g* for 2 minutes at 4°C to pellet the beads. Pulldowns were washed twice with BC150 plus 0.2%, once with BC350, and once with BC150 plus 0.2%. Each wash was performed using 1ml of buffer with rotation at 4°C for 10 minutes. Proteins bound to the recovered beads were eluted by adding 40 µl of 2X SDS loading buffer and heating to 70°C for ~5 minutes. Samples were resolved on a 15% Tris-glycine SDS-PAGE gel with a 5% stacker. Gels were subjected to

Western blot analysis, Coomassie staining, or imaging using a Typhoon Trio+ Imager (GE Healthcare).

Western Blot Analysis

Samples from the GST pulldown experiments were loaded on a 15% Tris-glycine SDS-PAGE gel with a 5% stacker. Proteins were wet transferred onto Immobilon-P Transfer Membrane (Millipore) using a BioRad transfer system. After blocking, membranes were incubated ~1 hour with a 1:2000 dilution in TTBS of α -trimethyl-H3K4 (07-473), α -trimethyl-H3K9 (07-422), or α -trimethyl-H3K27 (07-449) antibodies (Upstate). After three 5 minute washes with TTBS, membranes were incubated ~1 hour with α -rabbit IgG (Fc) AP conjugate (S373B) secondary antibody (Promega) diluted 1:12,500 in TTBS. Membranes were again washed 3 X 5 minutes with TTBS. Proteins were detected using the NBT/BCIP detection system (Roche).

Results

The Chromodomains of CHD8 Bind HeLa Core Histones

CHD8, like the other members of the CHD family of proteins, has double chromodomains N-terminal to a Snf2 helicase domain. Chromodomains within other proteins have been shown to bind both DNA and histone tails. The double chromodomains of human CHD1 have been reported to interact with lysine 4-methylated histone H3 tails (H3K4me), a hallmark of active chromatin (38). Given that other chromodomain containing proteins interact with histone tails, we wanted to examine whether the chromodomains of CHD8 also bind histone tails.

As a first step, we wanted to determine if the chromodomains of CHD8 can bind histones.

Recombinant GST and GST fusion proteins were prepared for use in the *in vitro* study of the potential interaction between histones and the chromodomains of human CHD8. *E. coli* BL21 cells were used to express GST or the GST-Chromos fusion protein. In this fusion protein, GST was fused to the double chromodomains of CHD8. Cleared lysates from cells expressing GST and the GST-Chromos fusion protein were incubated with glutathione agarose beads. After washing, the samples were incubated with core histones purified from HeLa cells. Washed samples were then eluted and subjected to SDS-PAGE followed by Coomassie staining. Our results demonstrate that the chromodomains of CHD8 do in fact interact with core histones (Figure 4.1, lane 5). The chromodomains appear to have a higher affinity for histones H3 and H4 (Figure 4.1, lane 5). The control GST did not pulldown the core histones, indicating that the interaction seen between GST-Chromos and the core histones is not merely due to an interaction between core histones and GST (Figure 4.1, lane 3).

The Chromodomains of CHD8 Do Not Appear to Have a Higher Affinity for Binding to Specific Modifications on the Tails of Histone H3

The chromodomains of multiple proteins have been reported to exhibit a preference for binding to specific modifications on histone tails. Fischle et al. reported that the chromodomains of Polycomb (Pc) have a high affinity for

binding methylated lysine 27 on histone H3 tails, while Heterochromatin Protein 1 (HP1) has an affinity for binding methylated lysine 9 (37). CHD1, a family member of CHD8, was reported to have a high affinity for binding to methylated lysine 4 on the tail of histone H3 (38). After determining that the chromodomains of CHD8 bind histones, we wanted to examine whether they have a higher affinity for specific histone modifications.

GST pulldown experiments were performed as described above. GST or the GST-Chromos fusion protein bound to glutathione agarose was incubated with purified HeLa core histones and samples were subjected to SDS-PAGE followed by Western blot analysis. Membranes were probed with primary antibodies targeting modifications on histone H3 tails known to interact with the chromodomains of other proteins. Bands corresponding to histone H3 were detected when membranes were probed with α -trimethyl H3 lysine 27, α -trimethyl H3 lysine 9, and α -trimethyl H3 lysine 4 antibodies (Figure 4.2). Our results demonstrate that the chromodomains of CHD8 have the ability to associate with core histones composed of H3 methylated on lysines 4, 9, and 27 of the H3 tail. The chromodomains do not appear to discriminate between the modifications studied here when binding to core histones.

The Chromodomains of CHD8 Bind Recombinant H3-H4 Tetramers

While the chromodomains of human CHD1 have been reported to interact with lysine 4 methylated histone H3 tails, they do not interact with unmodified H3 tails (38). Our data obtained from GST pulldown assays utilizing purified HeLa

core histones suggests that the CHD8 chromodomains have the ability to bind modified histones. Since the core histones used in our assays were purified from human cells, it is likely that the histones within the octamers were modified. To gain additional information about the binding specificity of the CHD8 chromodomains, we examined whether the double chromodomains have the ability to bind unmodified histones.

Since our previous experiments indicated that the chromodomains of CHD8 have a higher affinity for binding histones H3 and H4, we prepared recombinant histone H3 and H4 proteins. The recombinant proteins were expressed and purified by chromatography before being refolded into histone H3-H4 tetramers. GST pulldown experiments were prepared as previously described. GST or the GST-Chromos fusion protein bound to glutathione agarose beads was incubated with and without purified HeLa core histones or recombinant histone H3-H4 tetramers. As in our previous experiments, GST-Chromos pulls down purified HeLa core histones (Figure 4.3, lane 7). When incubated with recombinant histone H3-H4 tetramers, GST-Chromos also pull down histones H3 and H4 (Figure 4.3, lane 8). The control GST did not pulldown the core histones or recombinant H3-H4 tetramers (Figure 4.3, lanes 4 & 5). Since the recombinant histones were unmodified, our results indicate that, unlike CHD1, the chromodomains of CHD8 have the ability to bind unmodified and possibly modified histones H3 and H4.

Mutation of Aromatic Residues in the Putative Binding Domain of CHD8 Chromos Does Not Affect Binding

Two aromatic residues within the chromodomains of human CHD1 have been reported to be responsible for the recognition of methylated lysines in histone H3 (38). Other chromodomain containing proteins, such as HP1, have been shown to use a three residue aromatic cage to recognize methylated histone H3 tails (54). With evidence demonstrating that aromatic residues in the chromodomains of other proteins are responsible for binding to histones, we wanted to examine whether aromatic residues in the chromodomain of CHD8 are also responsible for binding to histones.

We compared the amino acid sequence of human CHD8 with that of the other CHD6-9 subfamily members and CHD1. Sequence analysis identified multiple aromatic residues within the chromodomains of CHD8 that are conserved among these five proteins. The aromatic tyrosines (Y) at positions 672 and 675 within the chromodomains of CHD8 were particularly interesting due to their alignment with the aromatic tryptophan (W) residues in CHD1 (Figure 4.4, yellow). These two tryptophans within the chromodomains of CHD1 have been reported to be required for binding to methylated K4 on the histone H3 tail (38). To examine whether tyrosines 672 and 675 are required for the binding of CHD8 chromodomains to histones H3 and H4, we produced tyrosine to leucine (L) mutations at these two positions by PCR. Two mutant GST-Chromos fusion proteins were prepared. The single mutant had amino acid 675 mutated from Y to L. The double mutant had two Y to L mutations, one at tyrosine 672 and

another at tyrosine 675. We performed GST pulldown assays as described above. GST, GST-Chromos (single), and GST-Chromos (double) bound to glutathione agarose beads were incubated with purified HeLa core histones and recombinant histone H3-H4 tetramers. Our results indicate that mutation of one or both aromatic tyrosine residues within the chromodomains of CHD8 does not disrupt binding to histones H3 and H4 (Figure 4.5). These two aromatic residues, Y672 and Y675, within the chromodomains of CHD8 are not required for binding to histones H3 and H4.

CHD8 Does Not Bind H3 Peptide Tails

Our experiments described thus far demonstrated that the chromodomains of CHD8 can bind unmodified histone H3-H4 tetramers. Our GST pulldown experiments using purified HeLa core histones and western blot analysis using modification specific antibodies suggested that the chromodomains of CHD8 might also bind modified histones. To further define the interaction between CHD8 chromodomains and histones, we asked whether the chromodomains of CHD8 bind to the tails of histones or to the core amino acids.

To begin to answer this question, we prepared several recombinant fusion proteins which had SUMO fused to wt and mutant histone H3 tails. The mutant histone tail fusion proteins had lysine (K) to cysteine (C) mutations in lysines 4, 9, 27, or 36. These lysines can be methylated and have been shown to interact with the chromodomains of other proteins (37, 38, 58). We performed GST

pulldown experiments using methods previously described. GST or GST-Chromos bound to glutathione agarose was incubated with wt or mutant H3 tail fusion proteins. The GST-Chromos fusion protein did not interact with wt or mutant histone H3 tail fusion proteins (Figure 4.6). Our results indicate that the chromodomains of CHD8 do not bind to the tail of unmodified histone H3.

CHD8 Chromodomains Bind Tailless Histones H3 and H4

In order to further investigate whether the chromodomains of CHD8 bind to the core or tails of histones, we prepared histone H3-H4 tetramers using different combinations of full length recombinant H3 or H4 and recombinant histone H3 or H4 in which the tails were deleted (Δ). GST pulldown experiments were performed as previously described. GST or GST-Chromos bound to glutathione agarose beads were incubated with recombinant H3-H4, Δ H3- Δ H4, Δ H3-H4, or H3- Δ H4 tetramers. In this experiment, the GST-Chromos fusion protein interacted with all four recombinant histone tetramers while GST alone did not (Figure 4.7). Our results demonstrate that the chromodomains of CHD8 can bind to tailless histone H3-H4 tetramers. This evidence indicates that the chromodomains of CHD8 bind to the core of unmodified histone H3 and/or H4.

CHD8 Binds H3-H4 Tetramers Containing Mutations in Histone H3

Our previous experiments demonstrated that the chromodomains of CHD8 bind to unmodified recombinant histone H3-H4 tetramers. In order to pinpoint the residues within the histones that CHD8 binds to, we designed an assay which would use fluorescein to label residues within the amino acid sequence of each

histone to determine whether binding occurs at or near that specific site.

Fluorescein-5-maleimide can bind to sulfhydryl groups on cysteines. If we mutate a specific histone residue to a cysteine and then treat with fluorescein, we would be able to determine whether the presence of a bulky fluorescein group at that position affects binding of the chromodomains. Within the amino acid sequence of *Xenopus* histone H3 one cysteine already exists at position 110. This cysteine would have to be mutated in order to avoid double fluorescein labeling in our assays.

The first part of this assay required the production of mutant histone proteins in which specific residues were mutated to cysteines. Recombinant histone H3 with a cysteine (C) to alanine (A) mutation at residue 110 was prepared and used to form H3 (C110A)-H4 tetramers. We prepared H3 (K36C)-H4 tetramers using recombinant histone H3 with the C110A mutation and a lysine to cysteine mutation at residue 36, a residue known to interact with the chromodomain of other proteins (58). GST pulldown assays were performed as previously described. GST or the GST-Chromos fusion protein bound to glutathione agarose beads was incubated with wt H3-H4, H3 (K36C)-H4, or H3 (C110A)-H4 tetramers. The GST-Chromos fusion protein was able to interact with both the wt and mutant H3-H4 tetramers (Figure 4.8). Our results demonstrate that mutation of histone H3 residues 36 and 110 does not disrupt binding of the CHD8 chromodomains to histone H3-H4 tetramers. Therefore, these residues are not required for binding of the CHD8 chromodomains to histone H3-H4 tetramers.

Binding of the CHD8 Chromodomains to H3-H4 Tetramers is Not Disrupted by the Presence of a Fluorescein Labeled Residue

Fluorescein is a large molecule. Therefore, labeling of a specific histone residue with fluorescein would disrupt interaction with a histone binding protein if the labeled cysteine is in or near the binding pocket. After preparing histone H3 with mutations of specific amino acid residues to cysteines, fluorescein-5-maleimide was used to label the sulfhydryl groups of the recombinant histone proteins. The histone H3 (K36C) protein was fluorescein labeled and used to produce fluor H3 (K36C)-H4 tetramers. GST pulldown assays were performed as previously described. GST or the GST-Chromos fusion protein bound to glutathione agarose was incubated with wt H3-H4 or fluor H3 (K36C)-H4 tetramers. The GST-Chromos fusion protein was able to interact with fluorescein labeled H3 (K36C)-H4 tetramers as indicated by the fluorescent band corresponding to H3 detected in this pulldown (Figure 4.9).

Recombinant histone H3 with the C110A mutation and a lysine to cysteine mutation at residue 79 was also fluorescein labeled and used to form H3-H4 tetramers. GST pulldown experiments were performed as described above. GST or GST-Chromos bound to glutathione agarose was incubated with H3 (C110A)-H4 or H3 (K79C)-H4 tetramers. The chromodomains were able to bind the fluor H3 (K79C)-H4 tetramers as indicated by the fluorescent band corresponding to histone H3 (Figure 4.10). Together our results demonstrate that the presence of fluorescein labeled groups at residues 36 or 79 does not interrupt binding of the chromodomains to histone H3. Since fluorescein is a

large molecule, our results suggest that the chromodomains are also not binding near residues 36 or 79.

Discussion

CHD8 contains multiple domains that are conserved among the members of the CHD6-9 subfamily. The double chromodomains, located N-terminal to the Snf2 helicase domain, are particularly interesting due to previous reports demonstrating that the chromodomains of other proteins bind to modified histone tails. The chromodomains of polycomb (Pc) and heterochromatin protein 1 (HP1) bind histone H3 tails methylated at lysines 27 and 9 respectively, modifications typically associated with heterochromatin and repression (37). The chromodomains of CHD1, a member of the CHD family of proteins, were reported to bind histone H3 lysine 4 methylated tails, a modification typically associated with active chromatin and activation (38). We hypothesized that CHD8, like CHD1, binds to histones via double chromodomains. Given the association between histone modifications, activation, and repression, investigating possible binding of the CHD8 double chromodomains to histones could provide information related to the function of CHD8.

In order to determine whether the chromodomains of CHD8 bind to histones, we performed GST pulldown experiments with purified HeLa core histones and a fusion protein in which GST was fused to the double chromodomains of CHD8. The data obtained from our pulldown experiments indicated that the double chromodomains of CHD8 do in fact bind core histones

(Figure 4.1). In our pulldown assay the chromodomains seemed to have a higher affinity for binding to histone H3 and H4 and not H2A or H2B. Since the core histones used in this initial experiment were purified from HeLa cells, one would assume that these histones would be modified. We wanted to examine whether the CHD8 chromodomains, like those of proteins such as CHD1 (38), have an affinity for binding to a specific histone modification. We first looked at three histone tail modifications known to interact with the chromodomains of other proteins. Western blot analysis of samples taken from our pulldown assay with HeLa core histones indicated that the chromodomains of CHD8 can bind to core histones containing histone H3 trimethylated on lysines 4, 9, or 27

(Figure 4.2). The chromodomains did not seem to have a preference for binding to core histones with one of these modifications as compared to the others.

It is possible, although we think unlikely, that the core histones bound to the CHD8 chromodomains in our initial GST pulldown assay were unmodified. In order to test whether the chromodomains of CHD8 can bind to unmodified histones, we prepared recombinant histones H3 and H4. We prepared histone H3-H4 tetramers since the chromodomains exhibited an affinity for histones H3 and H4 in our experiments using purified HeLa core histones. Our results from the GST pulldown experiments using recombinant H3-H4 demonstrate that the chromodomains can indeed bind unmodified histones (Figure 4.3). The fact that CHD8 chromodomains can bind unmodified H3-H4 tetramers does not eliminate the possibility that the chromodomains can also bind modified histones. Our initial GST pulldown experiments using HeLa core histones in addition to western

blot analysis provide evidence in favor of this possibility. It is likely that CHD8 binds modified as well as unmodified histones.

After determining that the chromodomains of CHD8 can bind unmodified and possibly modified histones, we questioned whether CHD8 chromodomains bind to histone tails or the cores. We designed several experiments to provide answers to this question. In preparations for assays which would be performed using fluorescein, we prepared recombinant histone H3 with a C110A mutation. With C110 being the only cysteine in the H3 sequence, we were able to design assays in which various H3 residues could be mutated to cysteine and labeled with fluorescein-5-maleimide. Any interaction at or near the labeled residue would in theory be disrupted by the presence of a bulky fluorescein group. Residues 36 and 79, in the tail and core of histone H3 respectively, are known to be methylated. Fluorescein labeling of H3 residues 36 or 79 did not disrupt binding of the CHD8 chromodomains to H3-H4 tetramers (Figure 4.9 and 4.10). Our data demonstrated that residues 36 and 79 are not in the binding pocket where the chromodomain-histone interaction occurs.

To gain additional information about which region of the histone CHD8 chromodomains bind to, we prepared several recombinant proteins with SUMO fused to histone H3 tails. Each tail contained K to C mutations in residues known to interact with the chromodomains of other proteins. In GST pulldown assays, CHD8 chromodomains did not interact with the wt histone H3 tail or H3 tails containing a mutation at residue 4, 9, 27, or 36 (Figure 4.6). The results of this experiment suggested that CHD8 chromodomains bind to either histone H4

and/or the core of histone H3. To gain more clarity we performed GST pulldown experiments with H3-H4 tetramers composed of different combinations of tailed and tailless versions of each histone protein. CHD8 chromodomains were able to interact with tetramers even when both the H3 and H4 tail was deleted (Figure 4.7). This demonstrates that the chromodomains interact with the core and not the tail of unmodified histones.

After demonstrating that CHD8 chromodomains do indeed bind histones, we sought to define the residues within the chromodomains of CHD8 that are required for this interaction. Sequence alignment of the CHD8 chromos with CHD1, 6, 7, and 9 identified two aromatic residues as the same position as the residues required the interaction between CHD1 and methylated H3K4 (38). Mutation of these two aromatic residues, 672 and 675, within the chromodomains of CHD8 did not disrupt the interaction between the chromodomains and histones (Figure 4.4 and 4.5). We have yet to identify the residues that are required for binding, however analysis of our alignment identified several aromatic residues that are conserved between these five CHD proteins (Figure 4.4, pink). These putative binding sites could be tested in the future using the same method.

After performing our initial GST pulldown experiments which demonstrate that CHD8 chromodomains bind to the core of histone H3-H4 tetramers, another group reported data related to binding of CHD8 to histones. Yuan *et al.* reported that CHD8 binds to unmodified, dimethylated, and trimethylated K4 peptides (139). Given that lysine 4 is located within the tail region of histone H3, this

report conflicts with our data. It is important to note that the Yuan *et al.* study used CHD8 containing samples from an affinity purification performed with a GST-hStaf column. Therefore, their experiments could be affected by the presence of other complex components that interact with hstaf. Our studies, conducted with recombinant CHD8 and not a complex, examined and identified a direct interaction between CHD8 chromodomains and histones. However, it is possible that CHD8 chromodomains bind to the core of unmodified histones and to the tails and/or core of modified histones. This is a scenario we intend to study in the future.

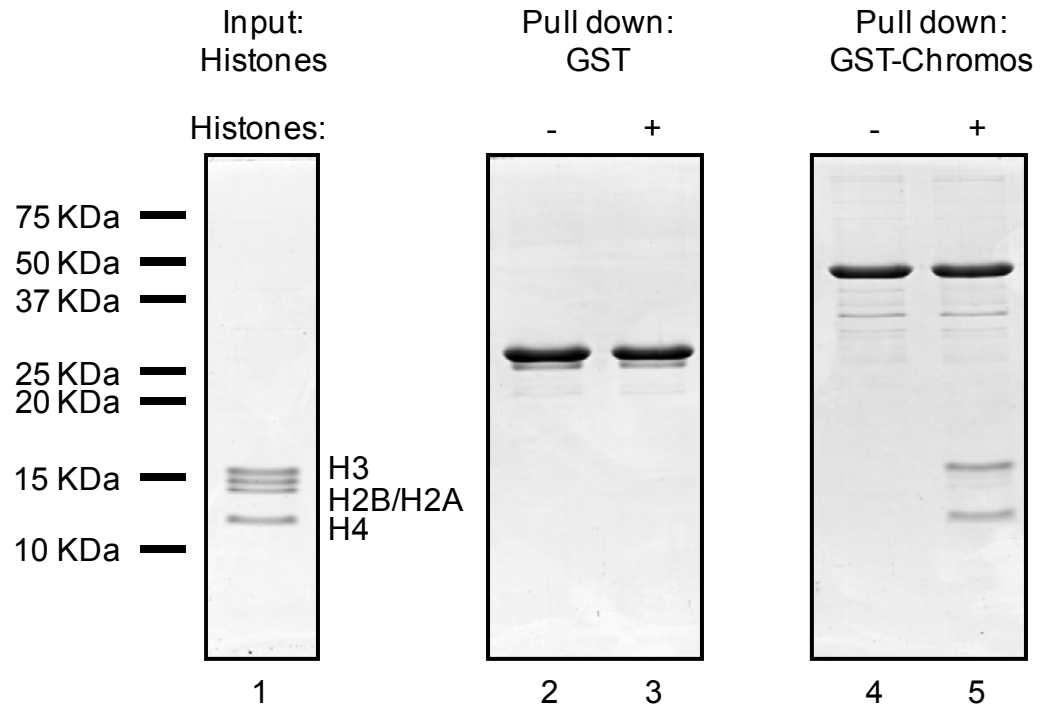
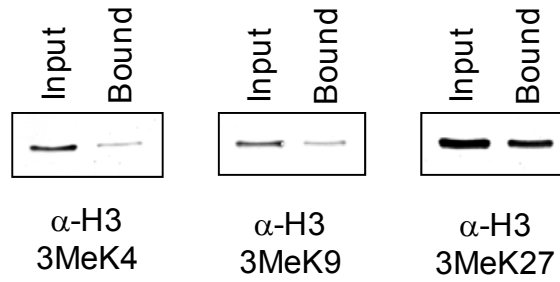


Figure 4.1. CHD8 chromodomains bind H3/H4 tetramers. Purified HeLa core histones (Input) were incubated with recombinant GST or GST-Chromos as indicated at the top of the figure. After washing, glutathione-agarose-purified samples were subjected to SDS-PAGE. Gels were analyzed by Coomassie staining.



Western

Figure 4.2. Western blot analysis of histones bound to GST-Chromos. Purified HeLa core histones (Input) were incubated with recombinant GST-Chromos as in Figure 4.1. After washing, glutathione-agarose-purified samples were subjected to SDS-PAGE and Western blot analysis with the antibodies indicated at the bottom of the figure.

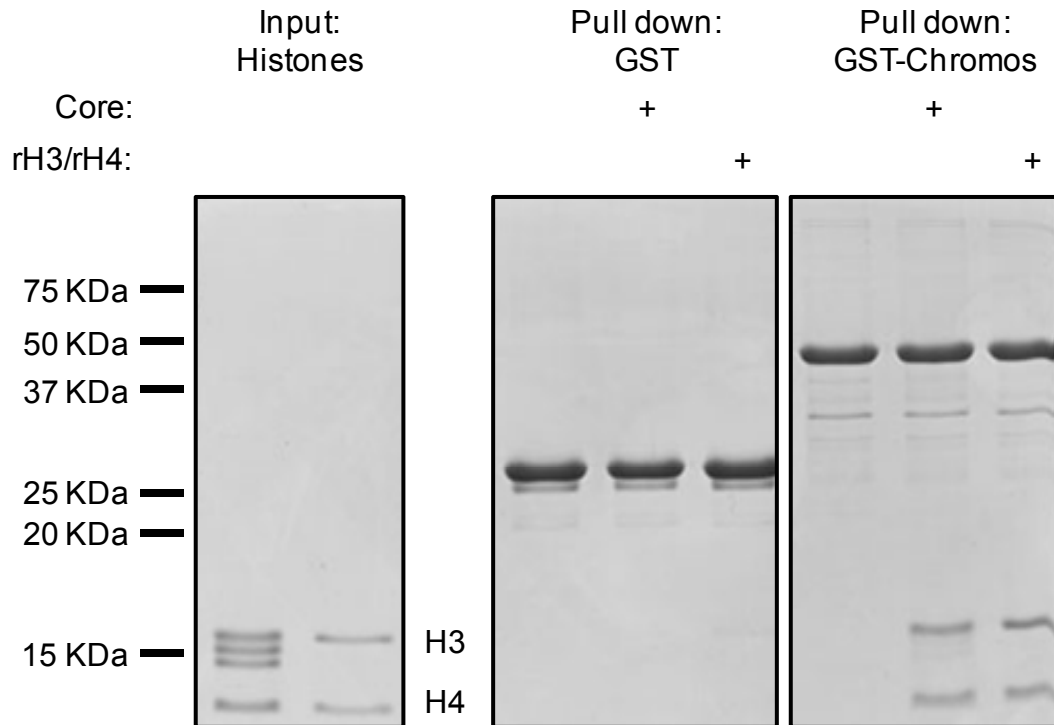


Figure 4.3: CHD8 chromodomains bind recombinant H3/H4 tetramers. Purified recombinant H3/H4 tetramers or HeLa core histones were incubated with recombinant GST or GST-Chromos as indicated at the top of the figure. After washing, glutathione-agarose-purified samples were subjected to SDS-PAGE. Gels were analyzed by Coomassie staining.

```

CHD8      -----GSSEEDAAIVDKVLSMRIVKKELPSGQYTEAEFFVVKYKNYSY
chd9      -----SEEDAAIVDKILSSRTVKKEISPGVMIDTEEFFVVKYKNYSY
chd6      -----ASTLAWQAEEPPEDDANIIEKILASKTVQEVHPGEPFDLELFYVKYRNFSY
chd7      ----DSPSNTSQSEQQESVDAEGPVVEKIMSSRSVKKQKESGEEVEIEEFFVVKYKNFSY
CHD1      EEEFETIERFMDCRIGRKGATGATTTIYAVEADGDPNAGFEKNKEPGEIQYLKWKGWSH
          :   :   :   :   :   :   :   :   :   :   :   :   :   :   :   :
          :   :   :   :   :   :   :   :   :   :   :   :   :   :   :   :

CHD8      LHCEWATISQLEK-DKRIHQKIKRFFKTKMAQMRHFFHE-----DEEPFNPDYVE
chd9      LHCEWATEEQLLK-DKRIQQKIKRFFKLRQAQRAHFFADM-----EEEPFNPDYVE
chd6      LHCKWATMEELEK-DPRIAQKIKRFRNKQAQMKHIFTEP-----DEDLFNPDYVE
chd7      LHCQWASIEDLEK-DKRIQQKIKRFFKAKQGQNK-FLSEI-----EDELFPNDYVE
CHD1      IHNTWETEETLKQONVRGMKKLDNFKKKDQETKRWLKNASPEDVEYYNCQOELTDDLHKQ
          :*  *  :  .  *  :  :  *  :  *  :  :  :  :  :  :  :  :  :  :  :  :  :  :
          :  :  :  :  :  :  :  :  :  :  :  :  :  :  :  :  :  :  :  :  :  :

CHD8      VDRILDESHSIDKDNQEPVIYYLVKWCSLPYEDSTWELKEDVDEGKIREFKRIQSRH---
chd9      VDRVLEVSFCEDKDTGEPVIYYLVKWCSLPYEDSTWELKEDVDLAKIEEFEQLQASR---
chd6      VDRILEVAHTKDAETGEEVTHYLVKWCSLPYEESTWELEEDVDPKVKEFESLQVLPEIK
chd7      VDRIMDFARSTD-DRGEPVTHYLVKWCSLPYEDSTWERRQDIDQAKIEEFEKLMSREP--
CHD1      YQIVERIIAHSNQKSAAGYPDYCKWQGLPYSECSWEDGALISKKFQACIDEYFSRKK--
          :  :  :  :  :  :  :  :  :  :  :  :  :  :  :  :  :  :  :  :  :  :

CHD8      -----
chd9      -----
chd6      HVERPASDS
chd7      ETER-----
CHD1      -----

```

Figure 4.4: Clustalw alignment of CHD1 and CHD6-9 chromodomains. The histone binding region of CHD1 was aligned with the CHD6-9 subfamily members using the Clustalw program. Residues within the sequence of CHD8 that were mutated in our studies, 672 and 675 are shown in yellow. These residues within the CHD8 sequence align with the residues responsible for histone binding by CHD1 (yellow). Additional conserved aromatic residues which could potentially be mutated in order to identify the histone binding sites within CHD8 are shown in pink. (Stars=identical residues, two dots=strong conservation, one dot=weak conservation)

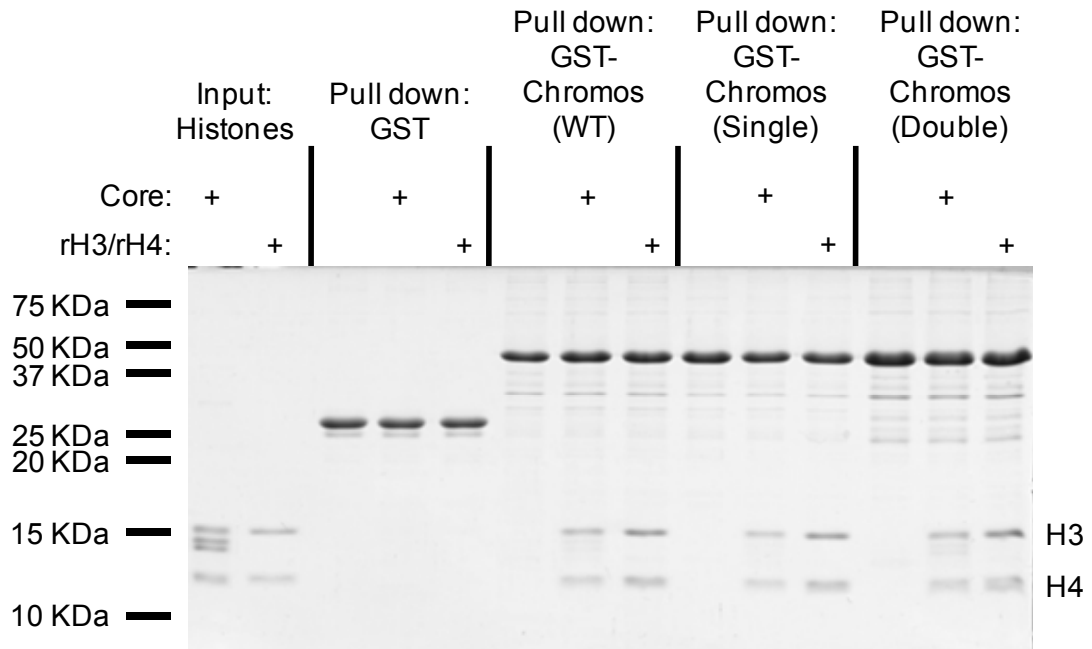


Figure 4.5: Mutation of conserved aromatic residues in the CHD8 chromodomains does not alter binding to core histones or recombinant H3/H4 tetramers. Purified recombinant H3/H4 tetramers or HeLa core histones were incubated with recombinant GST or GST-Chromos with the indicated mutations as outlined at the top of the figure. After washing, glutathione-agarose-purified samples were subjected to SDS-PAGE. Gels were analyzed by Coomassie staining.

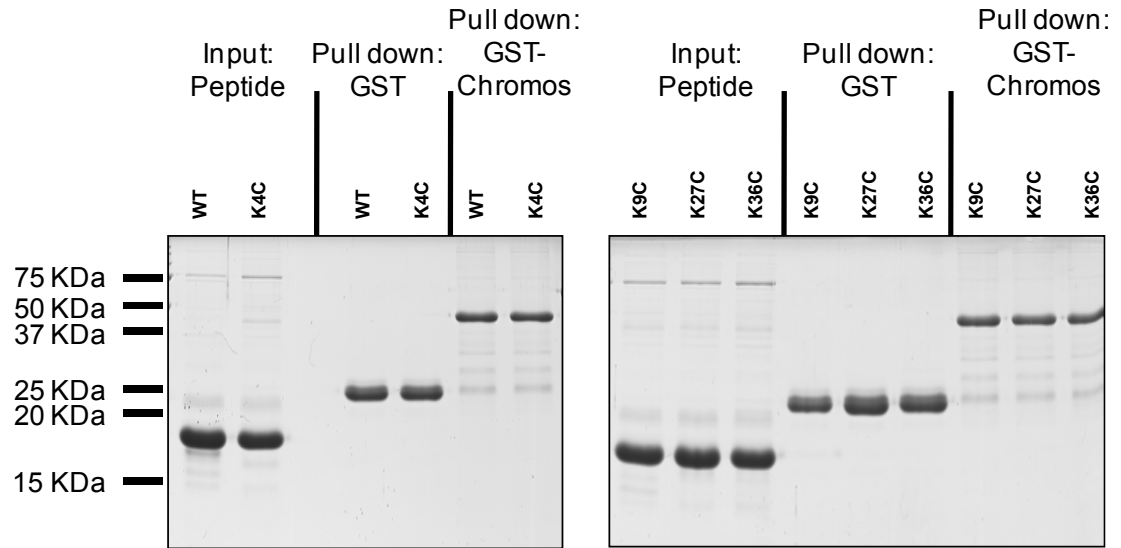


Figure 4.6: CHD8 chromodomains do not bind wild type or mutant H3 tails. Purified recombinant sumo-fused wild type or mutant H3 histone tails were incubated with recombinant GST or GST-Chromos indicated at the top of the figure. After washing, glutathione-agarose-purified samples were subjected to SDS-PAGE. Gels were analyzed by Coomassie staining.

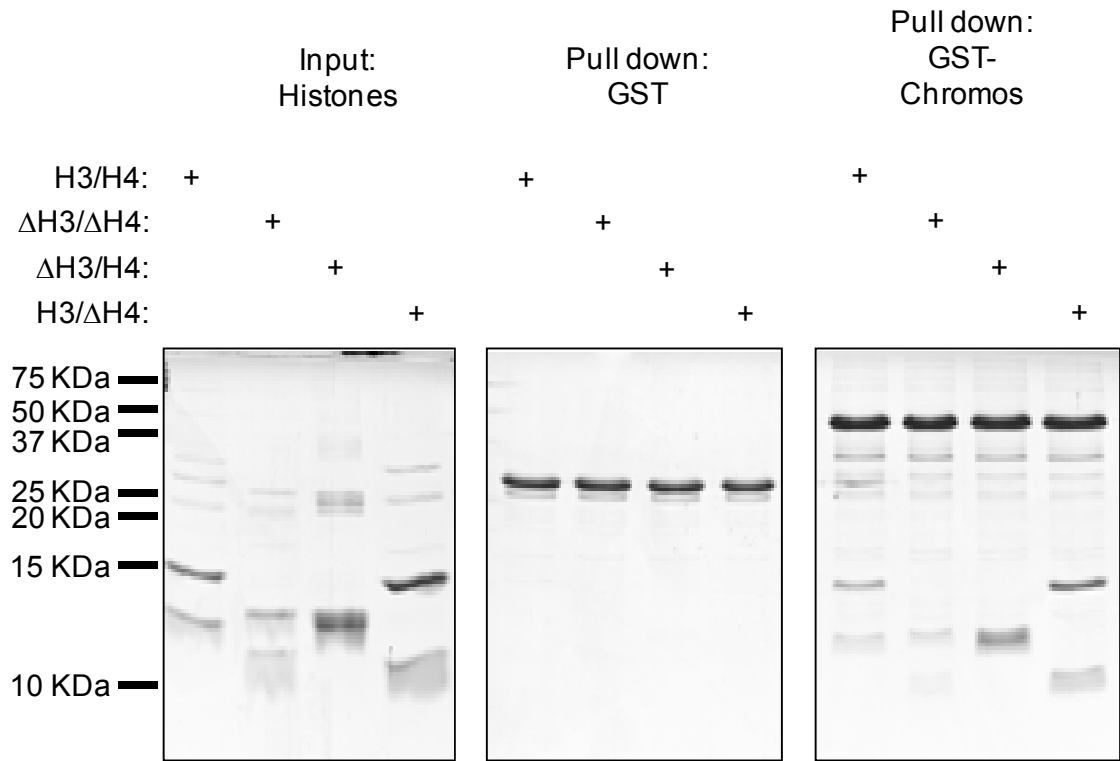


Figure 4.7: CHD8 chromodomains bind both recombinant H3/H4 tetramers and tailless H3/H4 tetramers. Purified recombinant H3/H4 tetramers or tailless H3/H4 tetramers (Input) were incubated with recombinant GST or GST-Chromos as indicated at the top of the figure. After washing, glutathione-agarose-purified samples were subjected to SDS-PAGE. Gels were analyzed by Coomassie staining.

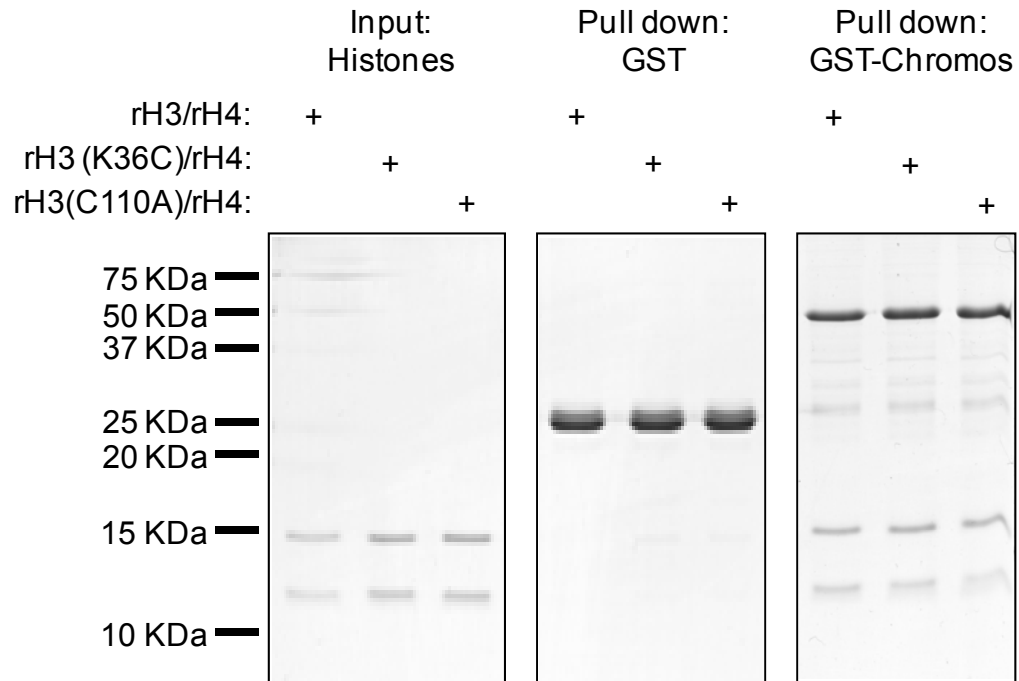


Figure 4.8: CHD8 chromodomains bind recombinant H3 (K36C/C110A)/H4 tetramers.

Purified recombinant H3(K36C/C110A)/H4 tetramers or wild type recombinant H3/H4 tetramers were incubated with recombinant GST or GST-Chromos as indicated at the top of the figure. After washing, glutathione-agarose-purified samples were subjected to SDS-PAGE. Gels were analyzed by Coomassie staining.

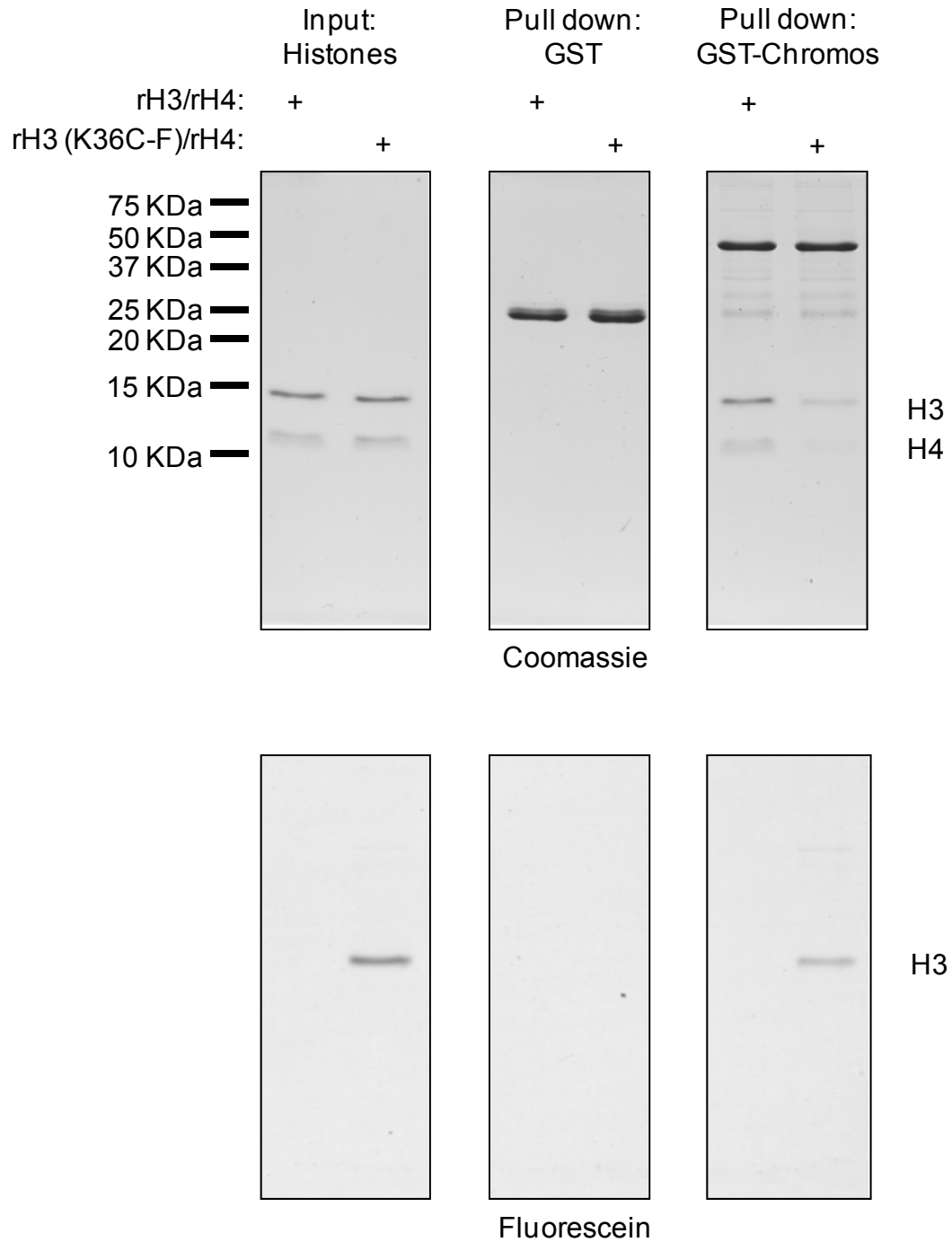


Figure 4.9: CHD8 chromodomains bind recombinant H3/H4 tetramers fluorescein labeled at K36. Purified recombinant H3/H4 tetramers fluorescein labeled at K36 or wild type recombinant H3/H4 tetramers were incubated with recombinant GST or GST-Chromos as indicated at the top of the figure. After washing, glutathione-agarose-purified samples were subjected to SDS-PAGE. Gels were analyzed by Coomassie staining (Top) or fluorescent imaging with a Typhoon Trio+ Imager (Bottom).

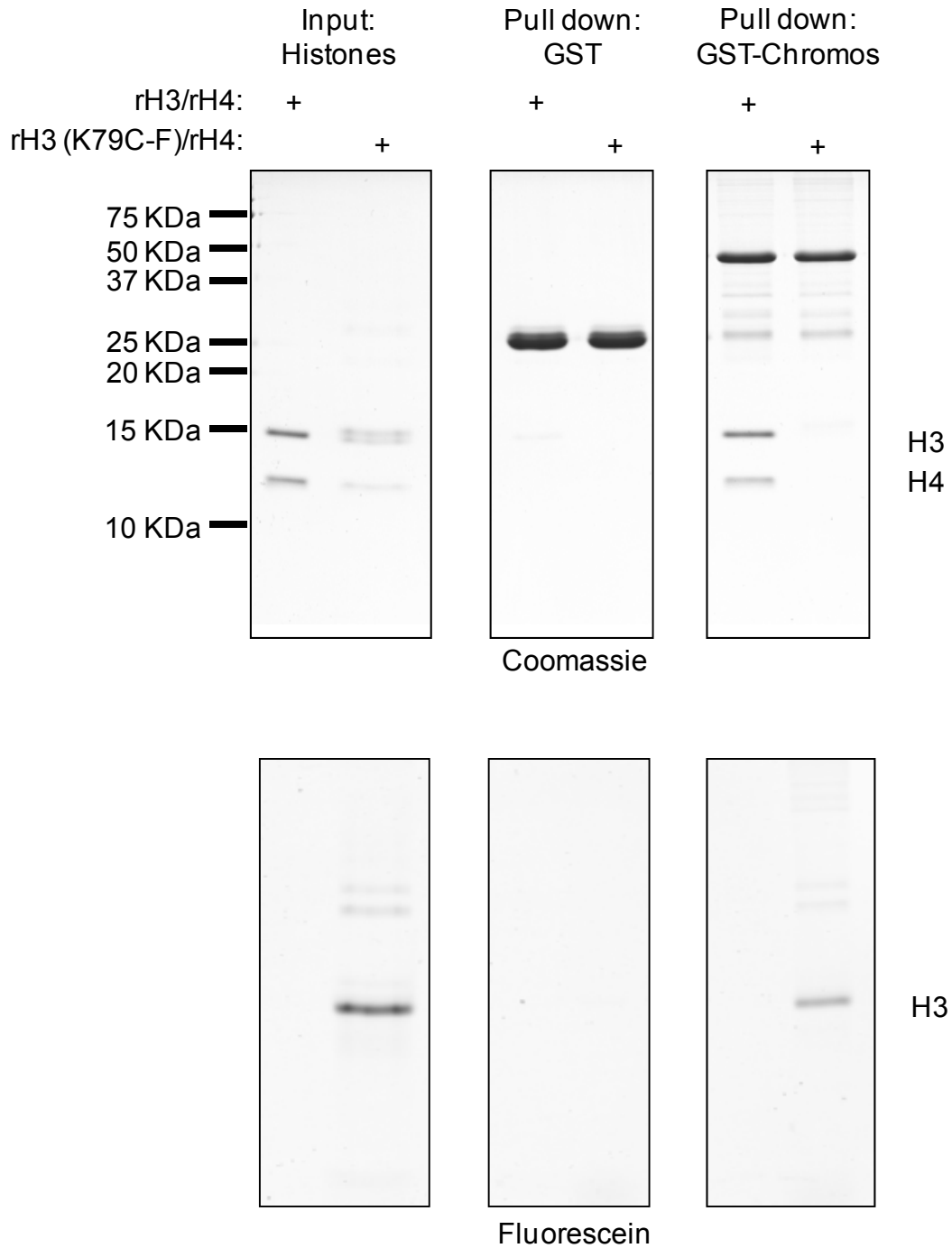


Figure 4.10: CHD8 chromodomains bind recombinant H3/H4 tetramers fluorescein labeled at K79. Purified recombinant H3/H4 tetramers fluorescein labeled at K79 or wild type recombinant H3/H4 tetramers were incubated with recombinant GST or GST-Chromos as indicated at the top of the figure. After washing, glutathione-agarose-purified samples were subjected to SDS-PAGE. Gels were analyzed by Coomassie staining (Top) or fluorescent imaging with a Typhoon Trio+ Imager (Bottom).

Chapter V

Conclusion

The highly condensed nature of chromatin structure presents a significant barrier to cellular processes that use DNA as substrate. Therefore, enzymes that alter chromatin structure can have a significant impact on these cellular processes such as transcription, replication, repair, and recombination. Remodeling enzymes not only affect normal cellular processes, but can also affect disease states such as cancer. Therefore, the study of enzymes that can alter chromatin structure is crucial for understanding human health. When embarking on this study, we sought to further define the function of CHD8, a member of the CHD6-9 subfamily of CHD proteins. While the CHD1-2 and CHD3-4 subfamilies were well studied, little information was known about the CHD6-9 subfamily. To gain additional information on CHD8 we tested two major hypotheses; 1) CHD8 is an ATP-dependent chromatin remodeling enzyme and 2) CHD8 exists in a multi-subunit complex with other proteins required for the function of CHD8. Our findings support both hypotheses and suggest that CHD8 plays a role in both cancer and development.

In Chapter II, we performed experiments to test the hypothesis that CHD8 is an ATP-dependent chromatin remodeling enzyme. Members of the CHD family of proteins possess a conserved Snf2 helicase domain, a domain present in all ATP-dependent chromatin remodeling enzymes. While members of the CHD1-2 and CHD3-4 subfamilies have previously been reported to be ATP-dependent chromatin remodelers, this activity has not been observed for a member of the CHD6-9 subfamily. However, both CHD6 and CHD9 were reported to possess nucleosome or DNA stimulated ATPase activity (75, 109), an indicator of potential chromatin remodeling activity. Our studies demonstrate that CHD8 also possesses ATPase activity, and this activity requires the Snf2 helicase domain. To directly test for remodeling activity, we performed restriction enzyme accessibility assays. Our results clearly demonstrate that CHD8 is an ATP-dependent chromatin remodeling enzyme. When nucleosome sliding assays were performed using CHD8, we observed sliding of nucleosomes when both CHD8 and ATP were present. This result indicates that CHD8 can remodel chromatin by moving histone octamers to new locations along DNA. Our data is the first evidence of chromatin remodeling activity for a member of the CHD6-9 subfamily. Given the high level of similarity between the Snf2 helicase domains within this subfamily and the fact that ATPase activity has been documented for other subfamily members, our results suggest that the other members of this subfamily also possess chromatin remodeling activity.

In Chapter II we also test the hypothesis that β -catenin interacts with human CHD8 and regulates transcription of β -catenin responsive genes. An

N-terminal fragment of CHD8 in rat, termed Duplin, was previously shown to bind β -catenin and inhibit TCF-dependent transcription (103). However, there is no evidence of this truncated form of CHD8 in human cells. β -catenin has been reported to interact with multiple proteins involved in opening the chromatin structure; however, an *in vitro* study of β -catenin mediated transcription demonstrated the requirement of p300 and an unknown chromatin remodeling enzyme (125). The interaction of Duplin with β -catenin, and the requirement of an unknown chromatin remodeling factor in β -catenin mediated transcription suggest that CHD8 could possibly be this unidentified remodeler. We demonstrate that human CHD8 interacts with β -catenin both *in vitro* and *in vivo*. This interaction occurs through the armadillo repeats of β -catenin. We also ChIP CHD8 to the 5' promoter region of several β -catenin responsive genes. By targeting CHD8 for depletion in human HCT116 and Drosophila S2 cells, we demonstrate that knockdown of CHD8 results in increase expression of β -catenin responsive genes. These results demonstrate that CHD8 negatively regulates the transcription of these β -catenin responsive genes.

Together, the data presented in Chapter II support our initial hypothesis that CHD8 is an ATP-dependent chromatin remodeling enzyme. Our data also suggest a model in which CHD8 regulates the transcription of β -catenin responsive genes by remodeling chromatin in the 5' promoter region of these genes. The most likely explanation is that CHD8 remodels the chromatin into a closed state, and therefore represses transcription. CHD8 may also repress

transcription of β -catenin responsive genes by recruiting other proteins to the promoter region which function as transcriptional co-repressors.

In Chapter III, we test the hypothesis that CHD8 exists in a multi-subunit complex with other proteins that may be required for the function of CHD8. In order to estimate the size of the potential CHD8 complex, we performed a partial purification of HeLa nuclear extract using P11, DEAE, and Superose 6 chromatography. The elution profile from the Superose 6 size exclusion column is consistent with an ~900kDa CHD8 containing complex. We performed both a conventional and affinity purification to identify the individual complex components. MS/MS analysis of the affinity purified sample identified CHD8 and multiple other factors known to be involved in altering chromatin structure. Among these proteins were the core components of the MLL methyltransferase complex; WDR5, RbBP5, and Ash2L. We initially focused on confirming the interaction between CHD8 and WDR5, as CHD8 was identified in a previous study of a MLL histone methyltransferase complex purified via an affinity-tagged WDR5 (29). We demonstrate that CHD8 interacts with WDR5 both *in vitro* and *in vivo*, confirming this association. Our co-infection experiments demonstrated that CHD8 also forms a complex with RbBP5, Ash2L, and WDR5 and suggest that this complex may also include MLL. Western blot analysis of fractions from the Superose 6 size exclusion column demonstrate that CHD8, WDR5, RbBP5, Ash2L, and MLL1 elute in the same fraction as would be expected for components of a complex. However, since this fraction is not the peak CHD8 containing fraction, our analysis indicates that the bulk of CHD8 exists outside of

this complex. Together, our results demonstrate that CHD8 exists in a complex with WDR5, RbBP5, and Ash2L that may also contain MLL. Our results also suggest that multiple CHD8 complexes exist. These data support our initial hypothesis that CHD8 is a component of a multi-subunit complex and opens the door for future studies which would confirm the existence of additional CHD8 containing complexes.

In Chapter III, we also hypothesized that CHD8 may be involved in the regulation of Hox gene expression. As WDR5 was previously shown to regulate Hox gene expression (135), and we demonstrate that CHD8 directly interacts and forms a complex with WDR5, we wanted to determine whether CHD8 could also regulate Hox gene expression. Supporting this hypothesis, we demonstrate using ChIP assays that CHD8 binds to the promoter region of several HoxA genes in both NT2/D1 and HeLa cells. By using RNAi targeting CHD8 in induced NT2/D1 cells, we demonstrate that depletion of CHD8 results in increased expression of HoxA1-HoxA4. Our results indicate that CHD8 negatively regulates the expression of these genes, similar to the results from the β -catenin responsive genes.

When comparing the results from our Hox gene induction, RNAi experiments, and ChIP assays, we made several interesting observations. We noticed that the increased expression observed when CHD8 is depleted inversely correlates with the level of Hox gene expression induced by ATRA. In other words, the higher the expression observed when a given HoxA gene is induced, the lower the increase in expression observed when CHD8 is depleted. We see

the smallest increase in Hox gene expression for the gene that had the highest expression when induced (compare Figure 3.11 with 3.12). This seems to suggest that CHD8 has a greater effect on Hox genes which are expressed at lower levels. We also made a second interesting observation when examining our ChIP data. In the uninduced state, the highest level of CHD8 binding is observed for HoxA1 while lower levels are observed for HoxA2 and A4. Upon ATRA induction, we observe a significant decrease in the level of CHD8 binding to the HoxA1 promoter and an increase in binding to the HoxA2 and A4 promoters (Figure 3.14). This result seems to suggest that CHD8 is moving to the promoter region of genes that are being expressed at lower levels. This observation correlates with the previous observation that CHD8 has a greater effect on Hox genes that are expressed at lower levels. Upon Hox gene induction, the highest level of CHD8 binding is observed for the gene that has the lowest ATRA induced expression (compare Figure 3.11 with Figure 3.14).

Taken together, the results in Chapter III provide evidence in support of our initial hypothesis that CHD8 exists in a complex with other proteins that may be required for the function of CHD8. Our data also suggest a model in which CHD8 regulates the transcription of Hox genes by remodeling chromatin in the 5' promoter region of these genes. As with the β -catenin responsive genes, it is possible that CHD8 remodels the promoter regions into a closed state which prevents efficient transcription. It is again also possible that CHD8 represses transcription by recruiting co-repressors to these genes. It is interesting to speculate that the inverse correlation of Hox gene expression with the level of

CHD8 bound to the promoter serves as a possible mechanism for feedback regulation.

In Chapter IV, we test the hypothesis that the chromodomains of CHD8 function in the binding of methylated lysines in histones. As previously stated, the chromodomains of CHD1 were found to bind methylated lysine 4 on the histone H3 tail (38). We wanted to determine whether the chromodomains of CHD8 could also bind methylated lysines in histones. We demonstrate that the chromodomains of CHD8 bind purified HeLa core histones, with a high affinity for histones H3/H4. CHD8 chromodomains do not appear to have an obvious preference for binding to a specific modification on histone H3 tails, as they are able to bind histones containing H3 modified at lysines 4, 9, and 27. We demonstrate that CHD8 chromodomains also possess the ability to bind unmodified recombinant histone H3-H4 tetramers. Mutation of specific aromatic residues, which align with residues in the chromodomains of CHD1 required for histone binding, does not disrupt CHD8 binding to histones. Pulldown experiments performed with histone H3 tails demonstrate that the chromodomains of CHD8 are unable to bind to the N-terminal tail of histone H3. We also show that the chromodomains of CHD8 can bind to histone H3-H4 tetramers in which the tails are deleted. Finally we demonstrate that the CHD8 chromodomains do not bind to histone H3 directly through lysine 36 or 79. Together this data supports our hypothesis that the chromodomains of CHD8 bind histones, but not to the histone H3 or H4 tails as expected.

After analyzing the data presented in Chapter II, III, and IV, we are able to propose a model describing how CHD8 functions. CHD8 is an ATP-dependent remodeling enzyme which can associate with globular histone cores via the tandem chromodomains. This association with histones is limited to the promoter regions of its target genes. At these promoters, CHD8 remodels the chromatin and thereby negatively or positively regulates transcription of this given target gene. Although the molecular mechanism for determining negative or positive regulation is currently unclear, given our identification of multiple CHD8 interacting proteins it is tempting to speculate that the decision results from the association of CHD8 with different binding partners at a given promoter. Our western blot analysis of size exclusion purified HeLa nuclear extracts (Figure 3.9) supports the existence of these numerous complexes.

Our studies of HoxA genes and β -catenin responsive genes indicate that CHD8 negatively regulates these genes, as knockdown of CHD8 results in increased expression of these genes. While CHD8 negatively regulates these genes, our chromodomain data suggests that CHD8 may also positively regulate other genes. In Chapter IV, our Western blot analysis detected CHD8 bound to histone H3 methylated on lysines 4, 9, and 27 of the H3 tail. Methylated lysine 4 is typically associated with active genes while methylation of lysine 9 and 27 is associated with repressed genes. What mechanism would CHD8 use to both negatively and positively regulate genes? It is possible that CHD8 remodels the promoter region into an “open” or “closed” chromatin state and/or recruits factors that act as activators or repressors to the promoter region. Whether CHD8 is

involved in negatively or positively regulating a given target gene may partially depend on the composition of the given CHD8 complex which is associated with the target gene promoter.

The three main steps of the transcription cycle are initiation, promoter clearance, and elongation. During different steps of the cycle, the C-terminal domain (CTD) of Pol II becomes phosphorylated at various serine residues. In the initiation step, Pol II is recruited to the promoter and the CTD is unphosphorylated. During the early stages of elongation after the Pol II clears the promoter region, the CTD becomes phosphorylated at serine 5. As elongation proceeds, the CTD becomes phosphorylated at serine 2 in the late stages of elongation.

What about the difference in Kismet and CHD8? Studies performed by Kennison and Tamkun suggest that Kismet functions as an activator of homeotic gene expression (57). In contrast, our results demonstrate that knockdown of CHD8 results in increased expression of the human homeotic genes HoxA1-4. Our results therefore suggest that CHD8 negatively regulates Hox gene expression.

Further research by the Tamkun group suggests a model for Kismet's involvement in the transcription cycle (116). In their model, Kismet is recruited to promoter regions through interactions with activators or components of the general transcription machinery. Once at the promoter, Kismet recognizes H3K4 methylated nucleosomes via the chromodomains. Kismet then remodels the

nucleosomes allowing Pol II elongation to proceed. Their model also depicts CHD1 playing a role in the later steps of elongation, downstream of Kismet involvement (116).

Our data demonstrates that CHD8 negatively regulates the expression of both β -catenin responsive genes and Hox genes. Above we presented the following model describing how CHD8 functions. CHD8 is an ATP-dependent remodeling enzyme which can associate with globular histone cores via the tandem chromodomains. This association with histones is limited to the promoter regions of its target genes. At these promoters, CHD8 remodels the chromatin and thereby negatively or positively regulates transcription of this given target gene. Our data suggests that CHD8, like Kismet, may also play a role in promoter clearance. However, with respect to the β -catenin responsive genes and Hox genes studied here, it appears that CHD8 remodels the nucleosomes to produce a barrier to transcriptional elongation and thereby pausing Pol II and elongation.

In summary, the data presented in this thesis adds additional information to the field of chromatin remodeling. Through regulating the localization of β -catenin, the Wnt signaling pathway is intimately involved in development and tumorigenesis. The regulation of HoxA gene expression is also strongly tied to development and disease. The data we present here is further evidence of a connection between the modification of chromatin structure, and human development and disease states such as cancer. This suggests that CHD8 may be a future therapeutic target in the treatment of human diseases.

References

1. **Aberle, H., A. Bauer, J. Stappert, A. Kispert, and R. Kemler.** 1997. beta-catenin is a target for the ubiquitin-proteasome pathway. *EMBO J* **16**:3797-804.
2. **Alen, C., N. A. Kent, H. S. Jones, J. O'Sullivan, A. Aranda, and N. J. Proudfoot.** 2002. A role for chromatin remodeling in transcriptional termination by RNA polymerase II. *Mol Cell* **10**:1441-52.
3. **Bao, Y., and X. Shen.** 2007. INO80 subfamily of chromatin remodeling complexes. *Mutat Res* **618**:18-29.
4. **Barak, O., M. A. Lazzaro, W. S. Lane, D. W. Speicher, D. J. Picketts, and R. Shiekhattar.** 2003. Isolation of human NURF: a regulator of Engrailed gene expression. *EMBO J* **22**:6089-100.
5. **Barker, N., A. Hurlstone, H. Musisi, A. Miles, M. Bienz, and H. Clevers.** 2001. The chromatin remodelling factor Brg-1 interacts with beta-catenin to promote target gene activation. *EMBO J* **20**:4935-43.
6. **Barski, A., S. Cuddapah, K. Cui, T. Y. Roh, D. E. Schones, Z. Wang, G. Wei, I. Chepelev, and K. Zhao.** 2007. High-resolution profiling of histone methylations in the human genome. *Cell* **129**:823-37.
7. **Becker, P. B., and W. Horz.** 2002. ATP-dependent nucleosome remodeling. *Annu Rev Biochem* **71**:247-73.
8. **Behrens, J., J. P. von Kries, M. Kuhl, L. Bruhn, D. Wedlich, R. Grosschedl, and W. Birchmeier.** 1996. Functional interaction of beta-catenin with the transcription factor LEF-1. *Nature* **382**:638-42.
9. **Berger, S. L.** 2007. The complex language of chromatin regulation during transcription. *Nature* **447**:407-12.
10. **Berger, S. L.** 2002. Histone modifications in transcriptional regulation. *Curr Opin Genet Dev* **12**:142-8.
11. **Bernstein, B. E., M. Kamal, K. Lindblad-Toh, S. Bekiranov, D. K. Bailey, D. J. Huebert, S. McMahon, E. K. Karlsson, E. J. Kulbokas, 3rd, T. R. Gingeras, S. L. Schreiber, and E. S. Lander.** 2005. Genomic maps and comparative analysis of histone modifications in human and mouse. *Cell* **120**:169-81.
12. **Bochar, D. A., J. Savard, W. Wang, D. W. Lafleur, P. Moore, J. Cote, and R. Shiekhattar.** 2000. A family of chromatin remodeling factors related to Williams syndrome transcription factor. *Proc Natl Acad Sci U S A* **97**:1038-43.
13. **Bozhenok, L., P. A. Wade, and P. Varga-Weisz.** 2002. WSTF-ISWI chromatin remodeling complex targets heterochromatic replication foci. *EMBO J* **21**:2231-41.

14. **Bracken, A. P., D. Kleine-Kohlbrecher, N. Dietrich, D. Pasini, G. Gargiulo, C. Beekman, K. Theilgaard-Monch, S. Minucci, B. T. Porse, J. C. Marine, K. H. Hansen, and K. Helin.** 2007. The Polycomb group proteins bind throughout the INK4A-ARF locus and are disassociated in senescent cells. *Genes Dev* **21**:525-30.
15. **Brannon, M., J. D. Brown, R. Bates, D. Kimelman, and R. T. Moon.** 1999. XCtBP is a XTcf-3 co-repressor with roles throughout Xenopus development. *Development* **126**:3159-70.
16. **Brannon, M., M. Gomperts, L. Sumoy, R. T. Moon, and D. Kimelman.** 1997. A beta-catenin/XTcf-3 complex binds to the siamois promoter to regulate dorsal axis specification in Xenopus. *Genes Dev* **11**:2359-70.
17. **Brantjes, H., J. Roose, M. van De Wetering, and H. Clevers.** 2001. All Tcf HMG box transcription factors interact with Groucho-related co-repressors. *Nucleic Acids Res* **29**:1410-9.
18. **Brehm, A., K. R. Tufteland, R. Aasland, and P. B. Becker.** 2004. The many colours of chromodomains. *Bioessays* **26**:133-40.
19. **Bultman, S., T. Gebuhr, D. Yee, C. La Mantia, J. Nicholson, A. Gilliam, F. Randazzo, D. Metzger, P. Chambon, G. Crabtree, and T. Magnuson.** 2000. A Brg1 null mutation in the mouse reveals functional differences among mammalian SWI/SNF complexes. *Mol Cell* **6**:1287-95.
20. **Cadigan, K. M., and R. Nusse.** 1997. Wnt signaling: a common theme in animal development. *Genes Dev* **11**:3286-305.
21. **Chung, K. H., C. C. Hart, S. Al-Bassam, A. Avery, J. Taylor, P. D. Patel, A. B. Vojtek, and D. L. Turner.** 2006. Polycistronic RNA polymerase II expression vectors for RNA interference based on BIC/miR-155. *Nucleic Acids Res* **34**:e53.
22. **Corona, D. F., G. Langst, C. R. Clapier, E. J. Bonte, S. Ferrari, J. W. Tamkun, and P. B. Becker.** 1999. ISWI is an ATP-dependent nucleosome remodeling factor. *Mol Cell* **3**:239-45.
23. **Côté, J., Utley, R. T., and Workman, J. L.** 1995. Basic Analysis of Transcription Factor Binding to Nucleosomes. *Methods Mol. Genet.* **6**:108-129.
24. **Couture, J. F., E. Collazo, and R. C. Trievel.** 2006. Molecular recognition of histone H3 by the WD40 protein WDR5. *Nat Struct Mol Biol* **13**:698-703.
25. **Decristofaro, M. F., B. L. Betz, C. J. Rorie, D. N. Reisman, W. Wang, and B. E. Weissman.** 2001. Characterization of SWI/SNF protein expression in human breast cancer cell lines and other malignancies. *J Cell Physiol* **186**:136-45.
26. **Deschamps, J.** 2007. Ancestral and recently recruited global control of the Hox genes in development. *Curr Opin Genet Dev* **17**:422-7.
27. **Dignam, J. D., R. M. Lebovitz, and R. G. Roeder.** 1983. Accurate transcription initiation by RNA polymerase II in a soluble extract from isolated mammalian nuclei. *Nucleic Acids Res* **11**:1475-89.
28. **Dou, Y., T. A. Milne, A. J. Ruthenburg, S. Lee, J. W. Lee, G. L. Verdine, C. D. Allis, and R. G. Roeder.** 2006. Regulation of MLL1 H3K4

- methyltransferase activity by its core components. *Nat Struct Mol Biol* **13**:713-9.
29. **Dou, Y., T. A. Milne, A. J. Tackett, E. R. Smith, A. Fukuda, J. Wysocka, C. D. Allis, B. T. Chait, J. L. Hess, and R. G. Roeder.** 2005. Physical association and coordinate function of the H3 K4 methyltransferase MLL1 and the H4 K16 acetyltransferase MOF. *Cell* **121**:873-85.
 30. **Ebbert, R., A. Birkmann, and H. J. Schuller.** 1999. The product of the SNF2/SWI2 paralogue INO80 of *Saccharomyces cerevisiae* required for efficient expression of various yeast structural genes is part of a high-molecular-weight protein complex. *Mol Microbiol* **32**:741-51.
 31. **Eberharter, A., and P. B. Becker.** 2004. ATP-dependent nucleosome remodelling: factors and functions. *J Cell Sci* **117**:3707-11.
 32. **Eberharter, A., G. Langst, and P. B. Becker.** 2004. A nucleosome sliding assay for chromatin remodeling factors. *Methods Enzymol* **377**:344-53.
 33. **Eisen, J. A., K. S. Sweder, and P. C. Hanawalt.** 1995. Evolution of the SNF2 family of proteins: subfamilies with distinct sequences and functions. *Nucleic Acids Res* **23**:2715-23.
 34. **Elfring, L. K., R. Deuring, C. M. McCallum, C. L. Peterson, and J. W. Tamkun.** 1994. Identification and characterization of *Drosophila* relatives of the yeast transcriptional activator SNF2/SWI2. *Mol Cell Biol* **14**:2225-34.
 35. **Ferreira, H., A. Flaus, and T. Owen-Hughes.** 2007. Histone modifications influence the action of Snf2 family remodelling enzymes by different mechanisms. *J Mol Biol* **374**:563-79.
 36. **Fischle, W., Y. Wang, and C. D. Allis.** 2003. Histone and chromatin cross-talk. *Curr Opin Cell Biol* **15**:172-83.
 37. **Fischle, W., Y. Wang, S. A. Jacobs, Y. Kim, C. D. Allis, and S. Khorasanizadeh.** 2003. Molecular basis for the discrimination of repressive methyl-lysine marks in histone H3 by Polycomb and HP1 chromodomains. *Genes Dev* **17**:1870-81.
 38. **Flanagan, J. F., L. Z. Mi, M. Chruszcz, M. Cymborowski, K. L. Clines, Y. Kim, W. Minor, F. Rastinejad, and S. Khorasanizadeh.** 2005. Double chromodomains cooperate to recognize the methylated histone H3 tail. *Nature* **438**:1181-5.
 39. **Flaus, A., D. M. Martin, G. J. Barton, and T. Owen-Hughes.** 2006. Identification of multiple distinct Snf2 subfamilies with conserved structural motifs. *Nucleic Acids Res* **34**:2887-905.
 40. **Gangaraju, V. K., and B. Bartholomew.** 2007. Mechanisms of ATP dependent chromatin remodeling. *Mutat Res* **618**:3-17.
 41. **Groden, J., A. Thliveris, W. Samowitz, M. Carlson, L. Gelbert, H. Albertsen, G. Joslyn, J. Stevens, L. Spirio, M. Robertson, and et al.** 1991. Identification and characterization of the familial adenomatous polyposis coli gene. *Cell* **66**:589-600.
 42. **Gunduz, E., M. Gunduz, M. Ouchida, H. Nagatsuka, L. Beder, H. Tsujigiwa, K. Fukushima, K. Nishizaki, K. Shimizu, and N. Nagai.**

2005. Genetic and epigenetic alterations of BRG1 promote oral cancer development. *Int J Oncol* **26**:201-10.
43. **Guschin, D., T. M. Geiman, N. Kikyo, D. J. Tremethick, A. P. Wolffe, and P. A. Wade.** 2000. Multiple ISWI ATPase complexes from xenopus laevis. Functional conservation of an ACF/CHRAC homolog. *J Biol Chem* **275**:35248-55.
 44. **Hakimi, M. A., D. A. Bochar, J. A. Schmiesing, Y. Dong, O. G. Barak, D. W. Speicher, K. Yokomori, and R. Shiekhattar.** 2002. A chromatin remodelling complex that loads cohesin onto human chromosomes. *Nature* **418**:994-8.
 45. **Hall, J. A., and P. T. Georgel.** 2007. CHD proteins: a diverse family with strong ties. *Biochem Cell Biol* **85**:463-76.
 46. **Harlow, E., and D. Lane.** 1988. *Antibodies: a laboratory manual.*
 47. **Hecht, A., K. Vleminckx, M. P. Stemmler, F. van Roy, and R. Kemler.** 2000. The p300/CBP acetyltransferases function as transcriptional coactivators of beta-catenin in vertebrates. *EMBO J* **19**:1839-50.
 48. <http://www.stanford.edu/~rnusse/pathway/targetcomp.html>, posting date. [Online.]
 49. **Huber, A. H., W. J. Nelson, and W. I. Weis.** 1997. Three-dimensional structure of the armadillo repeat region of beta-catenin. *Cell* **90**:871-82.
 50. **Hueber, S. D., and I. Lohmann.** 2008. Shaping segments: Hox gene function in the genomic age. *Bioessays* **30**:965-79.
 51. **Hyllus, D., C. Stein, K. Schnabel, E. Schiltz, A. Imhof, Y. Dou, J. Hsieh, and U. M. Bauer.** 2007. PRMT6-mediated methylation of R2 in histone H3 antagonizes H3 K4 trimethylation. *Genes Dev* **21**:3369-80.
 52. **Ikeda, S., S. Kishida, H. Yamamoto, H. Murai, S. Koyama, and A. Kikuchi.** 1998. Axin, a negative regulator of the Wnt signaling pathway, forms a complex with GSK-3beta and beta-catenin and promotes GSK-3beta-dependent phosphorylation of beta-catenin. *EMBO J* **17**:1371-84.
 53. **Ito, T., M. Bulger, M. J. Pazin, R. Kobayashi, and J. T. Kadonaga.** 1997. ACF, an ISWI-containing and ATP-utilizing chromatin assembly and remodeling factor. *Cell* **90**:145-55.
 54. **Jacobs, S. A., and S. Khorasanizadeh.** 2002. Structure of HP1 chromodomain bound to a lysine 9-methylated histone H3 tail. *Science* **295**:2080-3.
 55. **Jenuwein, T., and C. D. Allis.** 2001. Translating the histone code. *Science* **293**:1074-80.
 56. **Jiang, J., and G. Struhl.** 1998. Regulation of the Hedgehog and Wingless signalling pathways by the F-box/WD40-repeat protein Slimb. *Nature* **391**:493-6.
 57. **Kennison, J. A., and J. W. Tamkun.** 1988. Dosage-dependent modifiers of polycomb and antennapedia mutations in *Drosophila*. *Proc Natl Acad Sci U S A* **85**:8136-40.
 58. **Keogh, M. C., S. K. Kurdistani, S. A. Morris, S. H. Ahn, V. Podolny, S. R. Collins, M. Schuldiner, K. Chin, T. Punna, N. J. Thompson, C. Boone, A. Emili, J. S. Weissman, T. R. Hughes, B. D. Strahl, M.**

- Grunstein, J. F. Greenblatt, S. Buratowski, and N. J. Krogan.** 2005. Cotranscriptional set2 methylation of histone H3 lysine 36 recruits a repressive Rpd3 complex. *Cell* **123**:593-605.
59. **Khavari, P. A., C. L. Peterson, J. W. Tamkun, D. B. Mendel, and G. R. Crabtree.** 1993. BRG1 contains a conserved domain of the SWI2/SNF2 family necessary for normal mitotic growth and transcription. *Nature* **366**:170-4.
60. **Kim, T. H., L. O. Barrera, M. Zheng, C. Qu, M. A. Singer, T. A. Richmond, Y. Wu, R. D. Green, and B. Ren.** 2005. A high-resolution map of active promoters in the human genome. *Nature* **436**:876-80.
61. **Korinek, V., N. Barker, P. J. Morin, D. van Wichen, R. de Weger, K. W. Kinzler, B. Vogelstein, and H. Clevers.** 1997. Constitutive transcriptional activation by a beta-catenin-Tcf complex in APC^{-/-} colon carcinoma. *Science* **275**:1784-7.
62. **Kornberg, R. D., and Y. Lorch.** 1999. Twenty-five years of the nucleosome, fundamental particle of the eukaryote chromosome. *Cell* **98**:285-94.
63. **Kouzarides, T.** 2002. Histone methylation in transcriptional control. *Curr Opin Genet Dev* **12**:198-209.
64. **Krogan, N. J., M. Kim, S. H. Ahn, G. Zhong, M. S. Kobor, G. Cagney, A. Emili, A. Shilatifard, S. Buratowski, and J. F. Greenblatt.** 2002. RNA polymerase II elongation factors of *Saccharomyces cerevisiae*: a targeted proteomics approach. *Mol Cell Biol* **22**:6979-92.
65. **Lai, J. S., and W. Herr.** 1992. Ethidium bromide provides a simple tool for identifying genuine DNA-independent protein associations. *Proc Natl Acad Sci U S A* **89**:6958-62.
66. **Langst, G., and P. B. Becker.** 2004. Nucleosome remodeling: one mechanism, many phenomena? *Biochim Biophys Acta* **1677**:58-63.
67. **LeRoy, G., A. Loyola, W. S. Lane, and D. Reinberg.** 2000. Purification and characterization of a human factor that assembles and remodels chromatin. *J Biol Chem* **275**:14787-90.
68. **LeRoy, G., G. Orphanides, W. S. Lane, and D. Reinberg.** 1998. Requirement of RSF and FACT for transcription of chromatin templates in vitro. *Science* **282**:1900-4.
69. **Li, B., M. Carey, and J. L. Workman.** 2007. The role of chromatin during transcription. *Cell* **128**:707-19.
70. **Lomberk, G., L. Wallrath, and R. Urrutia.** 2006. The Heterochromatin Protein 1 family. *Genome Biol* **7**:228.
71. **Lowary, P. T., and J. Widom.** 1998. New DNA sequence rules for high affinity binding to histone octamer and sequence-directed nucleosome positioning. *J Mol Biol* **276**:19-42.
72. **Luger, K., T. J. Rechsteiner, A. J. Flaus, M. M. Waye, and T. J. Richmond.** 1997. Characterization of nucleosome core particles containing histone proteins made in bacteria. *J Mol Biol* **272**:301-11.

73. **Luger, K., T. J. Rechsteiner, and T. J. Richmond.** 1999. Preparation of nucleosome core particle from recombinant histones. *Methods Enzymol* **304**:3-19.
74. **Lusser, A., and J. T. Kadonaga.** 2003. Chromatin remodeling by ATP-dependent molecular machines. *Bioessays* **25**:1192-200.
75. **Lutz, T., R. Stoger, and A. Nieto.** 2006. CHD6 is a DNA-dependent ATPase and localizes at nuclear sites of mRNA synthesis. *FEBS Lett* **580**:5851-7.
76. **MacCallum, D. E., A. Losada, R. Kobayashi, and T. Hirano.** 2002. ISWI remodeling complexes in *Xenopus* egg extracts: identification as major chromosomal components that are regulated by INCENP-aurora B. *Mol Biol Cell* **13**:25-39.
77. **Marfella, C. G., and A. N. Imbalzano.** 2007. The Chd family of chromatin remodelers. *Mutat Res* **618**:30-40.
78. **Marikawa, Y., and R. P. Elinson.** 1998. beta-TrCP is a negative regulator of Wnt/beta-catenin signaling pathway and dorsal axis formation in *Xenopus* embryos. *Mech Dev* **77**:75-80.
79. **McConnell, A. D., M. E. Gelbart, and T. Tsukiyama.** 2004. Histone fold protein Dls1p is required for Isw2-dependent chromatin remodeling in vivo. *Mol Cell Biol* **24**:2605-13.
80. **Mikaelian, I., and A. Sergeant.** 1992. A general and fast method to generate multiple site directed mutations. *Nucleic Acids Res* **20**:376.
81. **Milne, T. A., S. D. Briggs, H. W. Brock, M. E. Martin, D. Gibbs, C. D. Allis, and J. L. Hess.** 2002. MLL targets SET domain methyltransferase activity to Hox gene promoters. *Mol Cell* **10**:1107-17.
82. **Miyagishi, M., R. Fujii, M. Hatta, E. Yoshida, N. Araya, A. Nagafuchi, S. Ishihara, T. Nakajima, and A. Fukamizu.** 2000. Regulation of Lef-mediated transcription and p53-dependent pathway by associating beta-catenin with CBP/p300. *J Biol Chem* **275**:35170-5.
83. **Molenaar, M., M. van de Wetering, M. Oosterwegel, J. Peterson-Maduro, S. Godsave, V. Korinek, J. Roose, O. Destree, and H. Clevers.** 1996. XTcf-3 transcription factor mediates beta-catenin-induced axis formation in *Xenopus* embryos. *Cell* **86**:391-9.
84. **Morin, P. J., A. B. Sparks, V. Korinek, N. Barker, H. Clevers, B. Vogelstein, and K. W. Kinzler.** 1997. Activation of beta-catenin-Tcf signaling in colon cancer by mutations in beta-catenin or APC. *Science* **275**:1787-90.
85. **Mosimann, C., G. Hausmann, and K. Basler.** 2006. Parafibromin/Hyrax activates Wnt/Wg target gene transcription by direct association with beta-catenin/Armadillo. *Cell* **125**:327-41.
86. **Narlikar, G. J., H. Y. Fan, and R. E. Kingston.** 2002. Cooperation between complexes that regulate chromatin structure and transcription. *Cell* **108**:475-87.
87. **Nishisho, I., Y. Nakamura, Y. Miyoshi, Y. Miki, H. Ando, A. Horii, K. Koyama, J. Utsunomiya, S. Baba, and P. Hedge.** 1991. Mutations of

- chromosome 5q21 genes in FAP and colorectal cancer patients. *Science* **253**:665-9.
88. **Orford, K., C. Crockett, J. P. Jensen, A. M. Weissman, and S. W. Byers.** 1997. Serine phosphorylation-regulated ubiquitination and degradation of beta-catenin. *J Biol Chem* **272**:24735-8.
 89. **Osley, M. A., T. Tsukuda, and J. A. Nickoloff.** 2007. ATP-dependent chromatin remodeling factors and DNA damage repair. *Mutat Res* **618**:65-80.
 90. **Paro, R., and D. S. Hogness.** 1991. The Polycomb protein shares a homologous domain with a heterochromatin-associated protein of *Drosophila*. *Proc Natl Acad Sci U S A* **88**:263-7.
 91. **Patel, A., V. Dharmarajan, and M. S. Cosgrove.** 2008. Structure of WDR5 Bound to Mixed Lineage Leukemia Protein-1 Peptide. *J Biol Chem* **283**:32158-61.
 92. **Patel, A., V. E. Vought, V. Dharmarajan, and M. S. Cosgrove.** 2008. A Conserved Arginine-containing Motif Crucial for the Assembly and Enzymatic Activity of the Mixed Lineage Leukemia Protein-1 Core Complex. *J Biol Chem* **283**:32162-75.
 93. **Peifer, M., S. Berg, and A. B. Reynolds.** 1994. A repeating amino acid motif shared by proteins with diverse cellular roles. *Cell* **76**:789-91.
 94. **Pfaffl, M. W.** 2001. A new mathematical model for relative quantification in real-time RT-PCR. *Nucleic Acids Res* **29**:e45.
 95. **Poot, R. A., G. Dellaire, B. B. Hulsmann, M. A. Grimaldi, D. F. Corona, P. B. Becker, W. A. Bickmore, and P. D. Varga-Weisz.** 2000. HuCHRAC, a human ISWI chromatin remodelling complex contains hACF1 and two novel histone-fold proteins. *EMBO J* **19**:3377-87.
 96. **Racki, L. R., and G. J. Narlikar.** 2008. ATP-dependent chromatin remodeling enzymes: two heads are not better, just different. *Curr Opin Genet Dev* **18**:137-44.
 97. **Reisman, D. N., J. Sciarrotta, W. Wang, W. K. Funkhouser, and B. E. Weissman.** 2003. Loss of BRG1/BRM in human lung cancer cell lines and primary lung cancers: correlation with poor prognosis. *Cancer Res* **63**:560-6.
 98. **Reisman, D. N., M. W. Strobeck, B. L. Betz, J. Sciarrotta, W. Funkhouser, Jr., C. Murchardt, M. Yaniv, L. S. Sherman, E. S. Knudsen, and B. E. Weissman.** 2002. Concomitant down-regulation of BRM and BRG1 in human tumor cell lines: differential effects on RB-mediated growth arrest vs CD44 expression. *Oncogene* **21**:1196-207.
 99. **Rippe, K., A. Schrader, P. Riede, R. Strohner, E. Lehmann, and G. Langst.** 2007. DNA sequence- and conformation-directed positioning of nucleosomes by chromatin-remodeling complexes. *Proc Natl Acad Sci U S A* **104**:15635-40.
 100. **Roberts, C. W., S. A. Galusha, M. E. McMenamin, C. D. Fletcher, and S. H. Orkin.** 2000. Haploinsufficiency of Snf5 (integrator 1) predisposes to malignant rhabdoid tumors in mice. *Proc Natl Acad Sci U S A* **97**:13796-800.

101. **Roberts, C. W., M. M. Leroux, M. D. Fleming, and S. H. Orkin.** 2002. Highly penetrant, rapid tumorigenesis through conditional inversion of the tumor suppressor gene Snf5. *Cancer Cell* **2**:415-25.
102. **Roose, J., M. Molenaar, J. Peterson, J. Hurenkamp, H. Brantjes, P. Moerer, M. van de Wetering, O. Destree, and H. Clevers.** 1998. The *Xenopus* Wnt effector XTcf-3 interacts with Groucho-related transcriptional repressors. *Nature* **395**:608-12.
103. **Sakamoto, I., S. Kishida, A. Fukui, M. Kishida, H. Yamamoto, S. Hino, T. Michiue, S. Takada, M. Asashima, and A. Kikuchi.** 2000. A novel beta-catenin-binding protein inhibits beta-catenin-dependent Tcf activation and axis formation. *J Biol Chem* **275**:32871-8.
104. **Santos-Rosa, H., R. Schneider, A. J. Bannister, J. Sherriff, B. E. Bernstein, N. C. Emre, S. L. Schreiber, J. Mellor, and T. Kouzarides.** 2002. Active genes are tri-methylated at K4 of histone H3. *Nature* **419**:407-11.
105. **Sevenet, N., A. Lellouch-Tubiana, D. Schofield, K. Hoang-Xuan, M. Gessler, D. Birnbaum, C. Jeanpierre, A. Jouvret, and O. Delattre.** 1999. Spectrum of hSNF5/INI1 somatic mutations in human cancer and genotype-phenotype correlations. *Hum Mol Genet* **8**:2359-68.
106. **Sevenet, N., E. Sheridan, D. Amram, P. Schneider, R. Handgretinger, and O. Delattre.** 1999. Constitutional mutations of the hSNF5/INI1 gene predispose to a variety of cancers. *Am J Hum Genet* **65**:1342-8.
107. **Sheffield, P., S. Garrard, and Z. Derewenda.** 1999. Overcoming expression and purification problems of RhoGDI using a family of "parallel" expression vectors. *Protein Expr Purif* **15**:34-9.
108. **Shen, X., G. Mizuguchi, A. Hamiche, and C. Wu.** 2000. A chromatin remodelling complex involved in transcription and DNA processing. *Nature* **406**:541-4.
109. **Shur, I., and D. Benayahu.** 2005. Characterization and functional analysis of CReMM, a novel chromodomain helicase DNA-binding protein. *J Mol Biol* **352**:646-55.
110. **Sif, S.** 2004. ATP-dependent nucleosome remodeling complexes: enzymes tailored to deal with chromatin. *J Cell Biochem* **91**:1087-98.
111. **Simic, R., D. L. Lindstrom, H. G. Tran, K. L. Roinick, P. J. Costa, A. D. Johnson, G. A. Hartzog, and K. M. Arndt.** 2003. Chromatin remodeling protein Chd1 interacts with transcription elongation factors and localizes to transcribed genes. *EMBO J* **22**:1846-56.
112. **Simon, M. D., F. Chu, L. R. Racki, C. C. de la Cruz, A. L. Burlingame, B. Panning, G. J. Narlikar, and K. M. Shokat.** 2007. The site-specific installation of methyl-lysine analogs into recombinant histones. *Cell* **128**:1003-12.
113. **Smith, C. L., and C. L. Peterson.** 2005. ATP-dependent chromatin remodeling. *Curr Top Dev Biol* **65**:115-48.
114. **Smith, C. L., and C. L. Peterson.** 2005. A conserved Swi2/Snf2 ATPase motif couples ATP hydrolysis to chromatin remodeling. *Mol Cell Biol* **25**:5880-92.

115. **Song, J. J., and R. E. Kingston.** 2008. WDR5 interacts with mixed-lineage Leukemia (MLL) protein via the histone H3 binding pocket. *J Biol Chem.*
116. **Srinivasan, S., J. A. Armstrong, R. Deuring, I. K. Dahlsveen, H. McNeill, and J. W. Tamkun.** 2005. The *Drosophila* trithorax group protein Kismet facilitates an early step in transcriptional elongation by RNA Polymerase II. *Development* **132**:1623-35.
117. **Stein, L. D.** 2004. Human genome: end of the beginning. *Nature* **431**:915-6.
118. **Steward, M. M., J. S. Lee, A. O'Donovan, M. Wyatt, B. E. Bernstein, and A. Shilatifard.** 2006. Molecular regulation of H3K4 trimethylation by ASH2L, a shared subunit of MLL complexes. *Nat Struct Mol Biol* **13**:852-4.
119. **Strohner, R., A. Nemeth, P. Jansa, U. Hofmann-Rohrer, R. Santoro, G. Langst, and I. Grummt.** 2001. NoRC--a novel member of mammalian ISWI-containing chromatin remodeling machines. *EMBO J* **20**:4892-900.
120. **Sun, Y., F. T. Kolligs, M. O. Hottiger, R. Mosavin, E. R. Fearon, and G. J. Nabel.** 2000. Regulation of beta -catenin transformation by the p300 transcriptional coactivator. *Proc Natl Acad Sci U S A* **97**:12613-8.
121. **Tong, J. K., C. A. Hassig, G. R. Schnitzler, R. E. Kingston, and S. L. Schreiber.** 1998. Chromatin deacetylation by an ATP-dependent nucleosome remodelling complex. *Nature* **395**:917-21.
122. **Tsukiyama, T., C. Daniel, J. Tamkun, and C. Wu.** 1995. ISWI, a member of the SWI2/SNF2 ATPase family, encodes the 140 kDa subunit of the nucleosome remodeling factor. *Cell* **83**:1021-6.
123. **Tsukiyama, T., J. Palmer, C. C. Landel, J. Shiloach, and C. Wu.** 1999. Characterization of the imitation switch subfamily of ATP-dependent chromatin-remodeling factors in *Saccharomyces cerevisiae*. *Genes Dev* **13**:686-97.
124. **Tsukiyama, T., and C. Wu.** 1995. Purification and properties of an ATP-dependent nucleosome remodeling factor. *Cell* **83**:1011-20.
125. **Tutter, A. V., C. J. Fryer, and K. A. Jones.** 2001. Chromatin-specific regulation of LEF-1-beta-catenin transcription activation and inhibition in vitro. *Genes Dev* **15**:3342-54.
126. **Varga-Weisz, P. D., M. Wilm, E. Bonte, K. Dumas, M. Mann, and P. B. Becker.** 1997. Chromatin-remodelling factor CHRAC contains the ATPases ISWI and topoisomerase II. *Nature* **388**:598-602.
127. **Vary, J. C., Jr., V. K. Gangaraju, J. Qin, C. C. Landel, C. Kooperberg, B. Bartholomew, and T. Tsukiyama.** 2003. Yeast Isw1p forms two separable complexes in vivo. *Mol Cell Biol* **23**:80-91.
128. **Versteeg, I., N. Sevenet, J. Lange, M. F. Rousseau-Merck, P. Ambros, R. Handgretinger, A. Aurias, and O. Delattre.** 1998. Truncating mutations of hSNF5/INI1 in aggressive paediatric cancer. *Nature* **394**:203-6.
129. **Wade, P. A., P. L. Jones, D. Vermaak, and A. P. Wolffe.** 1998. A multiple subunit Mi-2 histone deacetylase from *Xenopus laevis*

- cofractionates with an associated Snf2 superfamily ATPase. *Curr Biol* **8**:843-6.
130. **Walker, J. E., M. Saraste, M. J. Runswick, and N. J. Gay.** 1982. Distantly related sequences in the alpha- and beta-subunits of ATP synthase, myosin, kinases and other ATP-requiring enzymes and a common nucleotide binding fold. *EMBO J* **1**:945-51.
 131. **Wang, G. G., C. D. Allis, and P. Chi.** 2007. Chromatin remodeling and cancer, Part I: Covalent histone modifications. *Trends Mol Med* **13**:363-72.
 132. **Wang, G. G., C. D. Allis, and P. Chi.** 2007. Chromatin remodeling and cancer, Part II: ATP-dependent chromatin remodeling. *Trends Mol Med* **13**:373-80.
 133. **Worby, C. A., and J. E. Dixon.** 2004. RNA interference in cultured *Drosophila* cells. *Curr Protoc Mol Biol* **Chapter 26**:Unit 26 5.
 134. **Workman, J. L.** 2006. Nucleosome displacement in transcription. *Genes Dev* **20**:2009-17.
 135. **Wysocka, J., T. Swigut, T. A. Milne, Y. Dou, X. Zhang, A. L. Burlingame, R. G. Roeder, A. H. Brivanlou, and C. D. Allis.** 2005. WDR5 associates with histone H3 methylated at K4 and is essential for H3 K4 methylation and vertebrate development. *Cell* **121**:859-72.
 136. **Xue, Y., J. Wong, G. T. Moreno, M. K. Young, J. Cote, and W. Wang.** 1998. NURD, a novel complex with both ATP-dependent chromatin-remodeling and histone deacetylase activities. *Mol Cell* **2**:851-61.
 137. **Yasui, D., M. Miyano, S. Cai, P. Varga-Weisz, and T. Kohwi-Shigematsu.** 2002. SATB1 targets chromatin remodelling to regulate genes over long distances. *Nature* **419**:641-5.
 138. **Yost, C., M. Torres, J. R. Miller, E. Huang, D. Kimelman, and R. T. Moon.** 1996. The axis-inducing activity, stability, and subcellular distribution of beta-catenin is regulated in *Xenopus* embryos by glycogen synthase kinase 3. *Genes Dev* **10**:1443-54.
 139. **Yuan, C. C., X. Zhao, L. Florens, S. K. Swanson, M. P. Washburn, and N. Hernandez.** 2007. CHD8 associates with human Staf and contributes to efficient U6 RNA polymerase III transcription. *Mol Cell Biol* **27**:8729-38.
 140. **Zakany, J., and D. Duboule.** 2007. The role of Hox genes during vertebrate limb development. *Curr Opin Genet Dev* **17**:359-66.
 141. **Zhang, Y., G. LeRoy, H. P. Seelig, W. S. Lane, and D. Reinberg.** 1998. The dermatomyositis-specific autoantigen Mi2 is a component of a complex containing histone deacetylase and nucleosome remodeling activities. *Cell* **95**:279-89.
 142. **Zhang, Y., and D. Reinberg.** 2001. Transcription regulation by histone methylation: interplay between different covalent modifications of the core histone tails. *Genes Dev* **15**:2343-60.